PBPK Model equations

The following equations describe the transport of labeled (indexed with *) and unlabeled peptide via blood flow, extravasation, binding, internalization, degradation and release, excretion and radioactive decay. The peptide was injected as a 51±8 min infusion for pre-therapeutic measurements.

Compared to the recently published model (1), more organs (including the red marrow) are explicitly, i.e. closer to physiological reality, modelled. A less empirical and more physiological model usually allows more accurate extrapolation from different condition (here different peptide amounts) and can be easier adapted for other peptides. The variables are defined in Table A.

Bound and internalized peptide:

Liver, spleen, tumor, kidney, red marrow (RM), GI, muscle, prostate/uterus, adrenals and rest.

Constraint for total sst2 receptors $R_{0,i}$

$$R_{0,\,i} = R_i + RP_i + RP_i^* \tag{1}$$

Internalized peptide

$$\begin{aligned} \frac{d}{dt} P_{\text{intern i}} &= \lambda_{\text{int},i} \cdot RP_i - \lambda_{release,i} \cdot P_{\text{intern } i} + \lambda_{phy} \cdot P^*_{\text{intern } i} \\ \frac{d}{dt} P^*_{\text{intern } i} &= \lambda_{\text{int},i} \cdot RP^*_{\,i} - \lambda_{release,i} \cdot P^*_{\text{intern } i} - \lambda_{phy} \cdot P^*_{\text{intern } i} \end{aligned} \tag{2}$$

Bound peptide on cell surface

$$\frac{d}{dt}RP_i = k_{on} \cdot P_{i,\text{int}} \cdot \frac{R_i}{V_{i,\text{int}}} - (k_{off} + \lambda_{\text{int},i}) \cdot RP_i + \lambda_{phy} \cdot RP_i^*$$
$$\frac{d}{dt}RP_i^* = k_{on} \cdot P_{i,\text{int}}^* \cdot \frac{R_i}{V_{i,\text{int}}} - (k_{off} + \lambda_{\text{int},i}) \cdot RP_i^* - \lambda_{phy} \cdot RP_i^* \quad (3)$$

Free peptide, vascular:

Transcapillary extravasation is described by the permeability surface area product (PS_i) and the vascular ($V_{i,v}$) and interstitial volumes ($V_{i,\text{int}}$) of the pertaining tissue. Convection from the vascular to the interstitial space is neglected as ^{90}Y-DOTATATE represents a rather small molecule (2).

All tissues except kidneys and lungs

$$\frac{d}{dt}P_{i,v} = PS_i\left(\frac{P_{i,\text{int}}}{V_{i,\text{int}}} - \frac{P_{i,v}}{V_{i,v}}\right) + F_i\left(\frac{P_{ART}}{V_{ART}} - \frac{P_{i,v}}{V_{i,v}}\right) + \lambda_{phy} \cdot P_{i,v}^*$$
$$\frac{d}{dt}P_{i,v}^* = PS_i\left(\frac{P_{i,\text{int}}^*}{V_{i,\text{int}}} - \frac{P_{i,v}^*}{V_{i,v}}\right) + F_i\left(\frac{P_{ART}^*}{V_{ART}} - \frac{P_{i,v}^*}{V_{i,v}}\right) - \lambda_{phy} \cdot P_{i,v}^* \quad (4)$$

For brain PS = 0

Lungs

$$\frac{d}{dt}P_{LU,v} = PS_{LU}\left(\frac{P_{LU,\text{int}}}{V_{LU,\text{int}}} - \frac{P_{LU,v}}{V_{LU,v}}\right) + F\left(\frac{P_{VEN}}{V_{VEN}} - \frac{P_{LU,v}}{V_{LU,v}}\right) + \lambda_{phy} \cdot P_{LU,v}^*$$
$$\frac{d}{dt}P_{LU,v}^* = PS_{LU}\left(\frac{P_{LU,\text{int}}^*}{V_{LU,\text{int}}} - \frac{P_{LU,v}^*}{V_{LU,v}}\right) + F\left(\frac{P_{VEN}}{V_{VEN}} - \frac{P_{LU,v}^*}{V_{LU,v}}\right) - \lambda_{phy} \cdot P_{LU,v}^* \quad (5)$$

Kidneys

$$\frac{d}{dt}P_{K,v} = -\frac{P_{K,v}}{V_{K,v}} \cdot (F_{fil} + F_K) + \frac{F_K}{V_{ART}} \cdot P_{\mathrm{ART}} + \frac{P_{\mathrm{intra,K}}}{V_{\mathrm{intra,K}}} \cdot (F_{fil} - F_{ex}) + \lambda_{phy} \cdot P^*_{K,v}$$
$$\frac{d}{dt}P^*_{K,v} = -\frac{P^*_{K,v}}{V_{K,v}} \cdot (F_{fil} + F_K) + \frac{F_K}{V_{ART}} \cdot P^*_{\mathrm{ART}} + \frac{P^*_{\mathrm{intra,K}}}{V_{\mathrm{intra,K}}} \cdot (F_{fil} - F_{ex}) - \lambda_{phy} \cdot P^*_{K,v} \quad (6)$$

Veins

$$\frac{d}{dt}P_{VEN} = -k_{\mathrm{Pr}} \cdot P_{VEN} + \sum \frac{F_i}{V_i} P_{i,\mathrm{v}} - \frac{F_M}{V_M} P_{M,\mathrm{v}} - \frac{F_{GI}}{V_{GI}} P_{\mathrm{GI,v}} + \frac{F_M + F_{GI}}{V_L} P_{L,\mathrm{v}} + \lambda_{phy} \cdot P^*_{\mathrm{VEN}}$$
$$\frac{d}{dt}P^*_{VEN} = -k_{\mathrm{Pr}} \cdot P^*_{VEN} + \sum \frac{F_i}{V_i} P^*_{i,\mathrm{v}} - \frac{F_M}{V_M} P^*_{M,\mathrm{v}} - \frac{F_{GI}}{V_{GI}} P^*_{\mathrm{GI,v}} + \frac{F_M + F_{GI}}{V_L} P^*_{L,\mathrm{v}} - \lambda_{phy} \cdot P^*_{\mathrm{VEN}} \quad (7)$$

Arteries

$$\frac{d}{dt}P_{\mathrm{ART}} = -\sum \frac{F_i}{V_{ART}} \cdot P_{i,\mathrm{v}} + \frac{F}{V_{LU,v}} \cdot P_{\mathrm{LU,v}} + \lambda_{phy} \cdot P^*_{ART}$$
$$\frac{d}{dt}P^*_{ART} = -\sum \frac{F_i}{V_{ART}} \cdot P_{i,\mathrm{v}} + \frac{F}{V_{LU,v}} \cdot P_{\mathrm{LU,v}} - \lambda_{phy} \cdot P^*_{ART} \quad (8)$$

Free peptide, interstitial spaces:

Kidneys:

$$\frac{d}{dt}P_{K,\mathrm{int}} = -k_{on} \cdot P_{K,\mathrm{int}} \cdot \frac{R_K}{V_{K,\mathrm{int}}} + k_{off} \cdot RP_K + F_{fil}\left(\frac{P_{K,v}}{V_{K,v}} - \frac{P_{K,\mathrm{int}}}{V_{K,\mathrm{int}}}\right) + \lambda_{phy} \cdot P^*_{K,\mathrm{int}}$$
$$\frac{d}{dt}P^*_{K,\mathrm{int}} = -k_{on} \cdot P^*_{K,\mathrm{int}} \cdot \frac{R_K}{V_{K,\mathrm{int}}} + k_{off} \cdot RP^*_K + F_{fil}\left(\frac{P^*_{K,v}}{V_{K,v}} - \frac{P^*_{K,\mathrm{int}}}{V_{K,\mathrm{int}}}\right) - \lambda_{phy} \cdot P^*_{K,\mathrm{int}} \quad (9)$$

Skin, adipose tissue, heart, bone, lungs and brain (PS = 0):

$$\frac{d}{dt}P_{i,\text{int}} = PS_i\left(\frac{P_{i,v}}{V_{i,v}} - \frac{P_{i,\text{int}}}{V_{i,\text{int}}}\right) + \lambda_{phy}\cdot P^*_{i,\text{int}}$$
$$\frac{d}{dt}P^*_{i,\text{int}} = PS_i\left(\frac{P^*_{i,v}}{V_{i,v}} - \frac{P^*_{i,\text{int}}}{V_{i,\text{int}}}\right) - \lambda_{phy}\cdot P^*_{i,\text{int}} \quad (10)$$

Liver, spleen, tumor, RM, GI, muscle, prostate/uterus, adrenals, rest:

$$\frac{d}{dt}P_{i,\text{int}} = -k_{on}\cdot P_{i,\text{int}}\cdot\frac{R_i}{V_{i,\text{int}}} + k_{off}\cdot RP_i + PS_i\left(\frac{P_{i,v}}{V_{i,v}} - \frac{P_{i,\text{int}}}{V_{i,\text{int}}}\right) + \lambda_{phy}\cdot P^*_{i,\text{int}}$$
$$\frac{d}{dt}P^*_{i,\text{int}} = -k_{on}\cdot P^*_{i,\text{int}}\cdot\frac{R_i}{V_{i,\text{int}}} + k_{off}\cdot RP_i^* + PS_i\left(\frac{P^*_{i,v}}{V_{i,v}} - \frac{P^*_{i,\text{int}}}{V_{i,\text{int}}}\right) - \lambda_{phy}\cdot P^*_{i,\text{int}} \quad (11)$$

Further equations:

Peptide in kidney cells (unspecific)

$$\frac{d}{dt}P_{\text{intra,K}} = \frac{P_{\text{int,K}}}{V_{\text{int},K}}\cdot(F_{fil} - F_{ex}) - \frac{P_{\text{intra,K}}}{V_{\text{intra,K}}}\cdot(F_{fil} - F_{ex}) + \lambda_{phy}\cdot P^*_{\text{intra,K}}$$
$$\frac{d}{dt}P^*_{\text{intra,K}} = \frac{P^*_{\text{int,K}}}{V_{\text{int},K}}\cdot(F_{fil} - F_{ex}) - \frac{P^*_{\text{intra,K}}}{V_{\text{intra,K}}}\cdot(F_{fil} - F_{ex}) - \lambda_{phy}\cdot P^*_{\text{intra,K}} \quad (12)$$

Bound to protein

$$\frac{d}{dt}PPR = k_{PR}\cdot P_{VEN} + \lambda_{phy}\cdot PPR^*$$
$$\frac{d}{dt}PPR^* = k_{PR}\cdot P^*_{VEN} - \lambda_{phy}\cdot PPR^* \quad (13)$$

SUPPLEMENTAL TABLE 1 Parameter definition

Variable		Value	Unit	Source
k_{on}	association rate	k_{off} / K_D	$l \cdot nmol^{-1} \cdot min^{-1}$	
k_{off}	dissociation rate	0.04	min^{-1}	(3)[a]
K_D	dissociation constant	0.4	$nmol \cdot l^{-1}$	(1)
λ_{phy}	physical decay ^{111}In ^{90}Y	$1.72 \cdot 10^{-4}$ and $1.80 \cdot 10^{-4}$	min^{-1}	
BW	body weight	individually measured	kg	
H	hematocrit	individually measured	unity	
F	flow total serum	$V_P \cdot 1.23/min$[b]	$l \cdot min^{-1}$	(4)
V_P	volume of total body serum	male $2.8 \cdot (1- H) \cdot BSA$ female $2.4 \cdot (1- H) \cdot BSA$	l	(5)
Tumor				
$V_{TU,total}$	total volume of tumor 1 and 2	measured	l	
$V_{TU, int}$	interstitial space of tumor	$v_{tu,int} \cdot V_{Tu\ total}$	l	
$V_{TU, v}$	interstitial space of tumor	$v_{tu,v} \cdot V_{Tu\ total}$	l	
$v_{TU,int}$	interstitial space fraction of total tumor	0.3 for NET 0.23 for meningioma	unity	derived from (6) menin. (7)
$v_{TU,v}$	vascular fraction of total tumor	0.1 for NET 0.11 for meningioma	unity	NET (8) menin. (7)
F_{TU}	serum flow tumor	$f_{tu} \cdot (1-H) \cdot V_{total,Tu}$	$l \cdot min^{-1}$	
f_{TU}	serum flow density tumor	$1.0 \cdot (1-H)$ for NET metastasis $0.9 \cdot (1-H)$ for meningioma	$ml \cdot min^{-1} \cdot g^{-1}$	NET (8) menin. (9)
PS_{TU}	permeability surface area product	$k_{TU} \cdot V_{Tu,\ total}$	$ml \cdot min^{-1}$	
k_{TU}	permeability surface area product per unit mass (scaled for molecule size of DOTATATE)	0.2 NET metastasis 0.31 meningioma	$ml \cdot min^{-1} \cdot g^{-1}$	NET (8) menin. (7)
$[R_{TU,0}]$	sst2 receptor density tumour	fitted	$nmol \cdot l^{-1}$	
$R_{TU,0}$	sst2 receptor number tumour	$[R_{TU,0}] \cdot V_{Tu,total}$	nmol	
$\lambda_{TU,int}$		0.001 (preliminary fits, Sup. D)	min^{-1}	
$\lambda_{TU,release}$		fitted	min^{-1}	
Measured organs				
$V_{L,total}$	volume total liver	individually measured	l	
$V_{S,total}$	volume total spleen	individually measured	l	
$V_{K,total}$	volume total kidney	individually measured	l	
$V_{i,v}$	Vascular (serum) volume organ liver, spleen, kidney	$V_{i,total} \cdot v_{i,v}$	l	
$V_{i,int}$	interstitial volume liver, spleen, kidneys	$V_{i,total} \cdot v_{i,int}$	l	
$V_{K,\ intra}$	volume intracellular kidney	$(V_{K,total} - V_{K,int} - V_{K,v}) \cdot 2/3$[c]	l	
$v_{L,v}$	vascular (serum) fraction liver	0.085	unity	(10)
$v_{S,v}$	vascular (serum) fraction spleen	0.12	unity	(10)
$v_{K,v}$	vascular (serum) fraction kidneys	0.055	unity	(10)
$v_{L,int}$	interstitial fraction liver	0.2	unity	(10)
$v_{S,int}$	interstitial fraction spleen	0.2	unity	(10)
$v_{K,int}$	interstitial fraction kidney	0.15	unity	(10)
F_L	serum flow liver arterial	$0.065 \cdot F$	$l \cdot min^{-1}$	(4)
F_S	serum flow spleen	$0.03 \cdot F$	$l \cdot min^{-1}$	(4)
F_K	serum flow kidneys	$0.19 \cdot F$	$l \cdot min^{-1}$	(4)
φ	ratio of sieving coefficients	$\Theta_{DOTATATE}$ / $\theta_{Cr\text{-}51\text{-}EDTA=}$ 0.66	unity	(11)
F_{fil}	filtration	$GFR_{measured} \cdot \varphi$[d]	$l \cdot min^{-1}$	
F_{ex}	excretion	$F_{fil} \cdot f_{ex}$	$l \cdot min^{-1}$	
f_{ex}	excretion/filtration	0.98	unity	(1)
k_L	permeability surface area product per unit mass for liver	$k_{MUS} \cdot 100$	$ml \cdot min^{-1} \cdot g^{-1}$	(12)
k_S	permeability surface area product per unit mass for spleen	k_L (due to similar capillary structure)	$ml \cdot min^{-1} \cdot g^{-1}$	
$[R_{L,0}]$	receptor density liver	fitted	$nmol \cdot l^{-1}$	
$[R_{S,0}]$	receptor density spleen	fitted	$nmol \cdot l^{-1}$	
$[R_{K,0}]$	receptor density kidneys	fitted	$nmol \cdot l^{-1}$	
$\lambda_{L,int}$	internalization rate sst2 liver	$\lambda_{K,int}$	min^{-1}	(13)

$\lambda_{S,int}$	internalization rate sst2 spleen	$\lambda_{K,int}$	min^{-1}	(13)
$\lambda_{K,int}$	internalization rate sst2 kidneys	$\Lambda_{TU,int} \cdot 1.7^{e}$	min^{-1}	(13)
$\lambda_{L,release}$	release rate liver	$\lambda_{NT,release}$	min^{-1}	(1, 14)
$\lambda_{S,release}$	release rate spleen	$\lambda_{NT,release}$	min^{-1}	(1)
$\lambda_{K,release}$	release rate kidneys	$\lambda_{NT,release}$	min^{-1}	(1)
Other organs				
$V_{PRO,total}$ $V_{UT,total}$	volume total prostate volume total uterus	0.016·BW/71 0.080·BW/71	l	(15) (15)
$V_{LU,total}$	volume total lungs	1·BW/71	l	(15)
$V_{AD,total}$	volume total adrenals	0.014·BW/71	l	(15)
$V_{MUS,total}$	volume total muscles	30.078·BW/71	l	(15)
$V_{GI,total}$	volume total GI + pancreas	(0.385+0.548+0.104+0.15)·BW/71	l	(15)
$V_{SKIN,total}$	volume total skin	3.408·BW/71	l	(15)
$V_{ADI,total}$	volume total adipose tissue	13.465·BW/71	l	
$V_{RM,total}$	volume total red marrow	1.1·BW/71	l	(15)
$V_{BONE,total}$	volume total bone without red marrow	10.165·BW/71 - $V_{RM,total}$	l	(15)
$V_{HRT,total}$	volume total heart	0.341·BW/71	l	(15)
$V_{BR,total}$	volume total brain	1.45·BW/71	l	(15)
V_{BW}	volume of total body based on BW	1 ml ≙ 1 g	l	
$V_{REST,total}$	volume of rest body i = all organs except tumor	$V_{BW} - \sum_i V_{i,total}$	l	
$V_{PRO,v}$ $V_{UT,v}$	vascular fraction prostate/uterus	0.04 · (1-H) · $V_{PRO,total}$ 0.07 · (1-H) · $V_{UT,total}$	l	(16) (17)
$V_{LU,v}$	vascular (serum) volume lungs	0.105 · V_P	l	(4)
$V_{AD,v}$	vascular (serum) volume adrenals	0.03 · (1-H) · $V_{AD,total}$	l	(15)
$V_{MUS,v}$	vascular (serum) volume muscles	0.14 · V_P	l	(4)
$V_{GI,v}$	vascular (serum) volume GI+ pancreas	0.076 · V_P	l	(4)
$V_{SKIN,v}$	vascular(serum) volume skin	0.03 · V_P	l	(4)
$V_{ADI,v}$	vascular(serum) volume adipose tissue	0.05 · V_P	l	(4)
$V_{RM,v}$	vascular(serum) volume red marrow	0.04 · V_P	l	(4)
$V_{BONE,v}$	vascular volume bone without red marrow	0.07 · V_P - V_{RM}	l	(4)
$V_{HRT,v}$	vascular (serum) volume heart	0.01 · V_P	l	(4)
$V_{BR,v}$	vascular(serum) volume brain	0.012 · V_P	l	(4)
$V_{REST,v}$	serum volume rest i = all organs except tumor	$V_P - \sum_i V_{i,v}$	l	
V_{ART}	arterial serum plus ½ serum content of heart	0.06 · V_P + 0.045 · V_P	l	(4)
V_{VENES}	venous serum plus ½ serum content of heart	0.18 · V_P + 0.045 · V_P	l	(4)
$V_{PRO,int}$ $V_{UT,int}$	interstitial volume prostate/uterus	0.25 · $V_{PRO,total}$ 0.5 · $V_{UT,total}$	l	(16) (18)
$V_{LU,int}$	interstitial volume lungs	$V_{LU,v} \cdot \alpha_{LU}$	l	
$V_{AD,int}$	interstitial volume adrenals (the value for salivary gland is used)	0.24 · $V_{AD,total}$	l	(19)
$V_{MUS,int}$	interstitial volume muscles	$V_{MUS,v} \cdot \alpha_{MUS}$	l	
$V_{GI,int}$	interstitial volume GI+ pancreas	$V_{GI,v} \cdot \alpha_{GI}$	l	
$V_{SKIN,int}$	interstitial volume skin	$V_{SKIN,v} \cdot \alpha_{SKIN}$	l	
$V_{ADI,int}$	interstitial volume adipose tissue	$V_{ADI,v} \cdot \alpha_{ADI}$	l	
$V_{RM,int}$	interstitial volume red marrow	$V_{RM,v} \cdot \alpha_{RM}$	l	
$V_{BONE,int}$	interstitial volume bone without red marrow	$V_{BONE,v} \cdot \alpha_{BONE}$	l	
$V_{HRT,int}$	interstitial volume heart	$V_{HRT,v} \cdot \alpha_{HRT}$	l	
$V_{REST,int}$	volume of rest body	$V_{REST,v} \cdot \alpha_{REST}$	l	
α_{MUS}	ratio of interstitial to vascular volume average man	$V_{MUS,int}/V_{MUS,v}$ = 5.9	unity	(10)
α_{GI}	ratio of interstitial to vascular volume	$V_{GI,int}/V_{GI,v}$ = 8.8	unity	(10)

	average man			
α_{SKIN}	ratio of interstitial to vascular volume average man	$V_{SKIN,int}/ V_{SKIN,v}$ = 8.9	unity	(10)
α_{ADI}	ratio of interstitial to vascular volume average man	$V_{ADI,int}/ V_{ADI,v}$ = 15. 5	unity	(10)
α_{RM}	ratio of interstitial to vascular volume average man	$V_{RM,int}/ V_{RM,v}$ = 3.7	unity	(10)
α_{HRT}	ratio of interstitial to vascular volume average man	$V_{HRT,int}/ V_{HRT,v}$ = 3.7	unity	(10)
α_{LU}	ratio of interstitial to vascular volume average man	$V_{LU,int}/ V_{LU,v}$ = 5.5	unity	(10)
α_{BONE}	ratio of interstitial to vascular volume average man	$V_{BONE,int}/ V_{BONE,v}$ = 9.3	unity	(10)
α_{REST}	ratio of interstitial to vascular volume average man	$V_{REST,int}/ V_{REST,v}$ = 3.7	unity	(10)
f_{PRO}		0.18	$ml \cdot min^{-1} \cdot g^{-1}$	(16)
f_{UT}		1	$ml \cdot min^{-1} \cdot g^{-1}$	(18)
f_{AD}		6	$ml \cdot min^{-1} \cdot g^{-1}$	(15)
F_{PRO} F_{UT}	Total serum flow to prostate/uterus	$f_{PRO} \cdot (1\text{-}H) \cdot V_{PRO,total}$ $f_{UT} \cdot (1\text{-}H) \cdot V_{UT,total}$	$ml \cdot min^{-1}$	
F_{LU}	Total serum flow lungs	F	$ml \cdot min^{-1}$	(4)
F_{AD}	Total serum flow to adrenals	$f_{AD} \cdot (1\text{-}H) \cdot V_{AD,total}$	$ml \cdot min^{-1}$	
F_{MUS}	Total serum flow to muscle	0.17·F	$ml \cdot min^{-1}$	(4)
F_{GI}	Total serum flow to GI+ pancreas	0.16·F	$ml \cdot min^{-1}$	(4)
F_{SKIN}	Total serum flow to skin	0.05·F	$ml \cdot min^{-1}$	(4)
F_{ADI}	Total serum flow to adipose	0.05·F	$ml \cdot min^{-1}$	(4)
F_{RM}	Total serum flow to red marrow (RM)	0.03·F	$ml \cdot min^{-1}$	(4)
F_{BONE}	Total serum flow to bone (without RM)	0.05·F	$ml \cdot min^{-1}$	(4)
F_{HRT}	Total serum flow to heart	0.04·F	$ml \cdot min^{-1}$	(4)
F_{BR}	Total serum flow to brain	0.12·F	$ml \cdot min^{-1}$	(4)
F_{REST}	i = all organs except tumor	$F - \sum_i F_i$	$ml \cdot min^{-1}$	
F_{TOTAL}		$F + F_{TU,1} + F_{TU,2} + F_{TU,REST}$	$ml \cdot min^{-1}$	
PS_i	permeability surface area product	$k_i \cdot V_{i\ total}$	$ml \cdot min^{-1}$	
k_{PRO} k_{UT}	permeability surface area product per unit mass (scaled for molecule size of DOTATATE) for prostate/uterus	0.1 0.2	$ml \cdot min^{-1} \cdot g^{-1}$	(16) (18)
k_{LU}	permeability surface area product per unit mass for lungs	k_{MUS} ·100	$ml \cdot min^{-1} \cdot g^{-1}$	(12)
k_{AD}	permeability surface area product per unit mass for adrenals	k_{MUS} ·100(assumed to be very high as for salivary glands)	$ml \cdot min^{-1} \cdot g^{-1}$	(20)
k_{MUS}	permeability surface area product per unit mass for muscle	0.02	$ml \cdot min^{-1} \cdot g^{-1}$	(12)
k_{GI}	permeability surface area product per unit mass for GI and pancreas	0.02 (assumed to similar to muscle)	$ml \cdot min^{-1} \cdot g^{-1}$	
k_{SKIN}	permeability surface area product per unit mass for skin	0.02 (assumed to similar to muscle)	$ml \cdot min^{-1} \cdot g^{-1}$	
k_{ADI}	permeability surface area product per unit mass for adipose	0.02 (assumed to similar to muscle)	$ml \cdot min^{-1} \cdot g^{-1}$	
k_{RM}	permeability surface area product per unit mass for red marrow	k_L(assumed to similar to liver)	$ml \cdot min^{-1} \cdot g^{-1}$	
k_{HRT}	permeability surface area product per unit mass for heart	0.02 (assumed to similar to muscle)	$ml \cdot min^{-1} \cdot g^{-1}$	
k_{BONE}	permeability surface area product per unit mass for bone	0.02 (assumed to similar to muscle)	$ml \cdot min^{-1} \cdot g^{-1}$	

k_{REST}	permeability surface area product per unit mass for rest	0.02 (assumed to similar to muscle)	$ml \cdot min^{-1} \cdot g^{-1}$	
$[R_{PRO,0}]$ $[R_{UT,0}]$	receptor density prostate based on sst2 density ratios calculated from (21)	$[R_{K,0}] \cdot 0.26$ $[R_{K,0}] \cdot 0.092$	$nmol \cdot l^{-1}$	(21)
$[R_{AD,0}]$	receptor density adrenals based on sst2 density ratios calculated from (21)	$[R_{K,0}] \cdot 1.65$	$nmol \cdot l^{-1}$	(21)
$[R_{MUS,0}]$	receptor density muscle based on sst2 density ratios calculated from (21)	$[R_{K,0}] \cdot 0.0056$	$nmol \cdot l^{-1}$	(21)
$[R_{GI,0}]$	receptor density GI + pancreas based on sst2 density ratios calculated from (21)	$[R_{K,0}] \cdot 0.16$	$nmol \cdot l^{-1}$	(21)
$[R_{RM,0}]$	receptor density RM based on sst2 density ratios calculated from (21)	$[R_{K,0}] \cdot 0.028$	$nmol \cdot l^{-1}$	(21)
$[R_{REST,0}]$	receptor density rest based on sst2 density ratios calculated from (21)	fitted	$nmol \cdot l^{-1}$	
$\lambda_{NT,int}$	internalization rate for sst2 normal tissue	$\lambda_{K,int}$	min^{-1}	(22)
$\lambda_{NT,release}$	degradation and release from sst2 cells normal tissue	fitted	min^{-1}	(1)
R	receptors free		nmol	
$R_{i,0}$	receptors total number of organ i	$[R_{i,0}] \cdot V_{i,total}$	nmol	
$[R_{i,0}]$	receptor density of organ i		$nmol \cdot l^{-1}$	
RP_i	peptide bound		nmol	
PPR	peptide bound to serum protein		nmol	
k_{PR}	binding rate peptide to serum	fitted	min^{-1}	
P_{intern}	peptide internalized		nmol	
$P_{i,v}$	peptide free vascular		nmol	
$P_{i,int}$	peptide free interstitial		nmol	
$P_{K,intra}$	peptide interacellular kidneys		nmol	

[a]In house Biacore measurements (23) of PSMA specific peptides yielded typical values of 0.04 1/min. Ferl et al report similar values [1].

[b]For the average normal adult (blood) F = 6500 ml/min and V = 5300 ml. Therefore, a factor of 1.23 was assigned to account for the changes in total serum flow due to volume changes.

[c]It is assumed that 2/3 of the total intracellular volume of the kidney is represented by the proximal tubular cells

[d] Scaling of GFR due to different molecular sizes

[e]The internalization of ^{111}In-DOTATATE was not directly measured for kidney cells (13). However, in reference (13) the kidney and tumor cell values for other ^{111}In-labeled ligands are reported. The mean value of the kidney to tumor ratio for these actually measured internalization rates was calculated. This average value of 1.7 was used as the ratio of kidney to the tumor ^{111}In-DOTATATE internalization rate.

.

2D imaging corrections:

Background correction, self-attenuation and scatter corrections were performed according to MIRD pamphlet 16 (24) for conjugative view counting. For organ activity estimation, a ROI was placed in an area with no overlapping activity of other organs and then scaled according to the total organ size. The background ROI was placed in the abdomen. For liver metastasis, the liver or abdomen were considered background depending on the size of the lesion.

For red marrow, time activity data could not be directly delineated. The herein used PBPK model allowed including information such as receptor density (according to Boy et al.) in the red marrow. It further allowed simultaneously fitting all parameters to all data (serum, whole body and all organs plus tumor). The time-integrated activity coefficient was estimated by integrating all compartments describing the red marrow including red marrow serum, interstitial space, bound and internalized peptide. For red marrow absorbed dose estimation, see equation 21, below.

Absorbed dose (D) and biologically effective dose (BED):

To calculate the absorbed dose and the BED of the kidneys, tumor, spleen and liver, the following equations and parameter values (Table B) were used:

$$\dot{D}_i(t) = A_i(t) \cdot S_{i \leftarrow i} = A_{inj} \cdot a_i(t) \cdot S_{i \leftarrow i} \tag{14}$$

$$D_i(T) = \int_0^T \dot{D}_i(t)dt = A_{inj} \cdot \tilde{a}_i(T) \cdot S_{i \leftarrow i} \tag{15}$$

The BED (25) is defined as

$$BED_i = D_i \cdot (1 + \frac{G_i}{\alpha_i / \beta_i} \cdot D_i) \tag{16}$$

The factor G_i (Lea–Catcheside factor) (25) is defined as

$$G_i(T) = \frac{2}{D_i^2} \cdot \int_0^T \dot{D}_i(t)dt \cdot \int_0^t \dot{D}_i(\omega) \cdot e^{-\mu_i(t-\omega)} d\omega \tag{17}$$

Thus, after inserting Eq. (17) in (16) one obtains

$$BED_i = D_i + \frac{2 \cdot \int_0^T \dot{D}_i(t)dt \cdot \int_0^t \dot{D}_i(\omega) \cdot e^{-\mu_i(t-\omega)} d\omega}{\alpha_i / \beta_i} \tag{18}$$

The activity to administer yielding a fixed kidney $BED_{K,\,fixed}$ is calculated according to

$$BED_{K,\,fixed} = A_{inj,BED_{K,fixed}} \cdot \tilde{a}_K(T) \cdot S_{K \leftarrow K} + \frac{2 \cdot A_{inj,BED_{K,fixed}}^2 \int_0^T a_K(t) \cdot S_{K \leftarrow K} dt \cdot \int_0^t a_K(\omega) \cdot S_{K \leftarrow K} \cdot e^{-\mu_K(t-\omega)} d\omega}{\alpha_K / \beta_K} \tag{19}$$

Solving Eq (19) for the administered activity yields

$$A_{inj,BED_{K,fixed}} = \frac{-\tilde{a}_K(T)\cdot S_{K\leftarrow K} \pm \sqrt{(\tilde{a}_K(T)\cdot S_{K\leftarrow K})^2 + \dfrac{8\cdot\int_0^T a_K(t)\cdot S_{K\leftarrow K}dt\cdot\int_0^t a_K(\omega)\cdot S_{K\leftarrow K}\cdot e^{-\mu_K(t-\omega)}d\omega\cdot BED_{K,fixed}}{\alpha_K/\beta_K}}}{\dfrac{4\cdot\int_0^T a_K(t)\cdot S_{K\leftarrow K}dt\cdot\int_0^t a_K(\omega)\cdot S_{K\leftarrow K}\cdot e^{-\mu_K(t-\omega)}d\omega}{\alpha_K/\beta_K}}$$

$$A_{inj,BED_{K,fixed}} = \frac{-\tilde{a}_K(T) \pm \sqrt{\tilde{a}_K(T)^2 + \dfrac{8\cdot\int_0^T a_K(t)\cdot dt\cdot\int_0^t a_K(\omega)\cdot e^{-\mu_K(t-\omega)}d\omega\cdot BED_{K,fixed}}{\alpha_K/\beta_K}}}{\dfrac{4\cdot S_{K\leftarrow K}\cdot\int_0^T a_K(t)\cdot dt\cdot\int_0^t a_K(\omega)\cdot e^{-\mu_K(t-\omega)}d\omega}{\alpha_K/\beta_K}} \qquad (20)$$

To calculate the BED of the red marrow, equation (21) was used instead of Eq. (14):

$$\dot{D}_{RM} = A_{RM}(t)\cdot S_{RM\leftarrow RM} + A_{REM}(t)\cdot S_{RM\leftarrow REM} \qquad (21)$$

SUPPLEMENTAL TABLE 2

Variable		Value	Unit	Source
$S_{K\leftarrow K}$	dose factor kidney to kidney phantom (are scaled using the actual organ mass)	$2.93\cdot10^{-5}$ male $3.18\cdot10^{-5}$ female	$Gy\cdot min^{-1}\cdot MBq^{-1}$	(26)
$S_{S\leftarrow S}$	dose factor kidney to kidney phantom (are scaled using the actual organ mass)	$4.76\cdot10^{-5}$ male $5.80\cdot10^{-5}$ female	$Gy\cdot min^{-1}\cdot MBq^{-1}$	(26)
$S_{L\leftarrow L}$	dose factor kidney to kidney phantom (are scaled using the actual organ mass)	$4.70\cdot10^{-6}$ male $6.42\cdot10^{-6}$ female	$Gy\cdot min^{-1}\cdot MBq^{-1}$	(26)
$S_{TU\leftarrow TU}$	dose factor tumor to tumor phantom	Table C	$Gy\cdot min^{-1}\cdot MBq^{-1}$	(27)
$S_{RM\leftarrow RM}$	dose factor red marrow to red marrow phantom (are scaled using BW)	$3.52\cdot10^{-6}$ male $3.14\cdot10^{-6}$ female	$Gy\cdot min^{-1}\cdot MBq^{-1}$	(26)
$S_{RM\leftarrow REM}$	dose factor remainder to red marrow corrected according to Hindorf et al.	$8.46\cdot10^{-8}$ male $1.03\cdot10^{-7}$ female	$Gy\cdot min^{-1}\cdot MBq^{-1}$	(26) (28)
α/β_K	radiobiological parameters kidneys	2.5	Gy	(29)
μ_K	repair rate kidney	ln(2)/60/2.8	min^{-1}	(29)
α/β_S	radiobiological parameters spleen	α/β_K	Gy	
μ_S	repair rate spleen	μ_K	min^{-1}	(29)
α/β_L	radiobiological parameters liver	α/β_K	Gy	
μ_L	repair rate liver	μ_K	min^{-1}	
α/β_{TU}	radiobiological parameters tumor	10	Gy	(30)
μ_{TU}	repair rate tumor	ln(2)/60/1	min^{-1}	(30)
α/β_{RM}	radiobiological parameters red marrow	15	Gy	(31)
μ_{RM}	repair rate red marrow	ln(2)/60/1.5	min^{-1}	(31)
A_i	activity of organ i		MBq	
A_{REM}	activity of remainder	$A_{Total} - A_{TU} - A_L - A_S - A_K - A_{RM}$	MBq	
A_{inj}	injected activity		MBq	
$A_{inj,\ BED\ K,fixed}$	activity to inject for BED_K = 20 Gy		MBq	
$\tilde{a}_i$	time-integrated activity coefficient of organ i		h	
a_i	fraction of administered activity of organ i		unity	
D_i	absorbed dose to organ i		Gy	
$\dot{D}_i$	absorbed dose rate to organ i		$Gy\cdot min^{-1}$	
T	Integration time	30000	min	
G_i	Lea–Catcheside factor of organ i		unity	(30)
BED_i	biologically effective dose to organ i		Gy	(30)

SUPPLEMENTAL TABLE 3

Volume [ml]	Tumor dose factors [Gy·min^{-1}·MBq^{-1}]
0.5	$1.27 \cdot 10^{-2}$
2	$3.64 \cdot 10^{-3}$
2.8	$2.50 \cdot 10^{-3}$
3	$2.40 \cdot 10^{-3}$
4	$1.90 \cdot 10^{-3}$
20	$4.08 \cdot 10^{-4}$
23	$3.50 \cdot 10^{-4}$
30	$2.80 \cdot 10^{-4}$
87	$9.00 \cdot 10^{-5}$
111	$8.00 \cdot 10^{-5}$
116	$7.80 \cdot 10^{-5}$
2522	$3.50 \cdot 10^{-6}$

References

1. Kletting P, Muller B, Erentok B, Schmaljohann J, Behrendt FF, Reske SN, et al. Differences in predicted and actually absorbed doses in peptide receptor radionuclide therapy. Med Phys. 2012;39(9):5708-17. Epub 2012/09/11.
2. Rippe B, Haraldsson B. Fluid and protein fluxes across small and large pores in the microvasculature. Application of two-pore equations. acta Physiol Scand. 1987;131(3):411-28.
3. Ferl GZ, Dumont RA, Hildebrandt IJ, Armijo A, Haubner R, Reischl G, et al. Derivation of a Compartmental Model for Quantifying 64Cu-DOTA-RGD Kinetics in Tumor-Bearing Mice. J Nucl Med. 2009;50(2):250–8.
4. Leggett RW, Williams LR. A proposed blood circulation model for reference man. Health Phys. 1995;69(2):187-201.
5. Buchmann I, Kull T, Glatting G, Bunjes D, Hale G, Kotzerke J, et al. A comparison of the biodistribution and biokinetics of 99mTc-anti-CD66 mAb BW 250/183 and 99mTc-anti-CD45 mAb YTH 24.5 with regard to suitability for myeloablative radioimmunotherapy. Eur J Nucl Med Mol Imaging. 2003;30(5):667-73.
6. Jain RK. Transport of molecules in the tumor interstitium: a review. Cancer Res. 1987;47(12):3039-51.
7. Ludemann L, Grieger W, Wurm R, Wust P, Zimmer C. Quantitative measurement of leakage volume and permeability in gliomas, meningiomas and brain metastases with dynamic contrast-enhanced MRI. Magn Reson Imaging. 2005;23(8):833-41. Epub 2005/11/09.
8. Guyennon A, Mihaila M, Palma J, Lombard-Bohas C, Chayvialle JA, Pilleul F. Perfusion characterization of liver metastases from endocrine tumors: Computed tomography perfusion. World journal of radiology. 2010;2(11):449-54. Epub 2010/12/24.
9. Kimura H, Takeuchi H, Koshimoto Y, Arishima H, Uematsu H, Kawamura Y, et al. Perfusion imaging of meningioma by using continuous arterial spin-labeling: comparison with dynamic susceptibility-weighted contrast-enhanced MR images and histopathologic features. AJNR Am J Neuroradiol. 2006;27(1):85-93. Epub 2006/01/19.

10. Shah DK, Betts AM. Towards a platform PBPK model to characterize the plasma and tissue disposition of monoclonal antibodies in preclinical species and human. J Pharmacokinet Pharmacodyn. 2012;39(1):67-86. Epub 2011/12/07.
11. Schmidt MM, Wittrup KD. A modeling analysis of the effects of molecular size and binding affinity on tumor targeting. Mol Cancer Ther. 2009;8(10):2861-71.
12. Groothuis DR. The blood-brain and blood-tumor barriers: a review of strategies for increasing drug delivery. Neuro-oncology. 2000;2(1):45-59. Epub 2001/04/17.
13. Antunes P, Ginj M, Zhang H, Waser B, Baum RP, Reubi JC, et al. Are radiogallium-labelled DOTA-conjugated somatostatin analogues superior to those labelled with other radiometals? Eur J Nucl Med Mol Imaging. 2007;34(7):982-93.
14. Velikyan I, Sundin A, Eriksson B, Lundqvist H, Sorensen J, Bergstrom M, et al. In vivo binding of [68Ga]-DOTATOC to somatostatin receptors in neuroendocrine tumours--impact of peptide mass. Nucl Med Biol. 2010;37(3):265-75.
15. Snyder WS, Cook MJ, Nasset ES, Karhausen RS, Howells GP. Report of the Task Group on Reference Man. ICRP publication 23. Oxford: Elsevier; 1975.
16. Buckley DL, Roberts C, Parker GJ, Logue JP, Hutchinson CE. Prostate cancer: evaluation of vascular characteristics with dynamic contrast-enhanced T1-weighted MR imaging--initial experience. Radiology. 2004;233(3):709-15. Epub 2004/10/23.
17. Lotgering FK, Gilbert RD, Longo LD. Exercise responses in pregnant sheep: oxygen consumption, uterine blood flow, and blood volume. Journal of applied physiology: respiratory, environmental and exercise physiology. 1983;55(3):834-41. Epub 1983/09/01.
18. McRae AC, Heap RB. Uterine vascular permeability, blood flow and extracellular fluid space during implantation in rats. Journal of reproduction and fertility. 1988;82(2):617-25. Epub 1988/03/01.
19. Berggreen E, Wiig H. Lowering of interstitial fluid pressure in rat submandibular gland: a novel mechanism in saliva secretion. American journal of physiology Heart and circulatory physiology. 2006;290(4):H1460-8. Epub 2005/11/15.
20. Clough G, Smaje LH. Exchange area and surface properties of the microvasculature of the rabbit submandibular gland following duct ligation. The Journal of physiology. 1984;354:445-56. Epub 1984/09/01.
21. Boy C, Heusner TA, Poeppel TD, Redmann-Bischofs A, Unger N, Jentzen W, et al. (68)Ga-DOTATOC PET/CT and somatostatin receptor (sst1-sst5) expression in normal human tissue: correlation of sst2 mRNA and SUV(max). Eur J Nucl Med Mol Imaging. 2011;38(7):1224-36.
22. Hofland LJ, Lamberts SW. The Pathophysiological Consequences of Somatostatin Receptor Internalization and Resistance. Endocrine Reviews. 2003;24(1):28-47.
23. Winter G, Baur B, Andreolli E, Kull T, Witulla B, Solbach C, et al. Biological evaluation of the new glutamate-urea-based PSMA ligand Df-DUPA-Pep. Eur J Nucl Med Mol Imaging. 2013;40:S184-S5.
24. Siegel JA, Thomas SR, Stubbs JB, Stabin MG, Hays MT, Koral KF, et al. MIRD pamphlet no. 16: Techniques for quantitative radiopharmaceutical biodistribution data acquisition and analysis for use in human radiation dose estimates. J Nucl Med. 1999;40(2):37S-61S.
25. Hobbs RF, Sgouros G. Calculation of the biological effective dose for piecewise defined dose-rate fits. Med Phys. 2009;36(3):904-7.
26. Stabin MG, Sparks RB, Crowe E. OLINDA/EXM: The Second-Generation Personal Computer Software for Internal Dose Assessment in Nuclear Medicine. J Nucl Med. 2005;46(6):1023-7.
27. Stabin MG, Siegel JA. Physical models and dose factors for use in internal dose assessment. Health Phys. 2003;85(3):294-310.
28. Hindorf C, Glatting G, Chiesa C, Lindén O, Flux G. EANM Dosimetry Committee guidelines for bone marrow and whole-body dosimetry. Eur J Nucl Med Mol Imaging. 2010;37(6):1238-50.
29. Cremonesi M, Botta F, Di Dia A, Ferrari M, Bodei L, De Cicco C, et al. Dosimetry for treatment with radiolabelled somatostatin analogues. A review. Q J Nucl Med Mol Imaging. 2010;54(1):37-51. Epub 2010/02/20.
30. Konijnenberg M. From imaging to dosimetry and biological effects. Q J Nucl Med Mol Imaging. 2011;55(1):44-56. Epub 2011/03/10.
31. Dale RG. The application of the linear-quadratic dose-effect equation to fractionated and protracted radiotherapy. Br J Radiol. 1985;58(690):515-28.

PBPK Model compartments

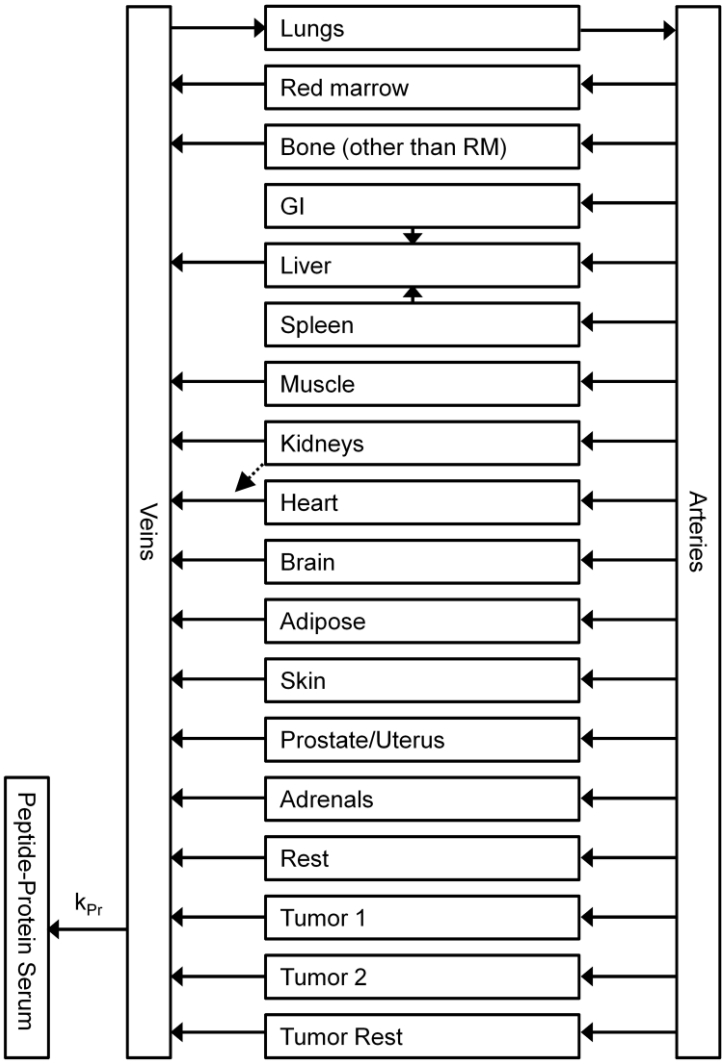

SUPPLEMENTAL FIGURE 1: Main model structure: All organs are represented by a rectangular compartment and are connected via blood flow. Each organ within this model, except arteries, veins, brain and protein serum, is divided into sub-compartments. The substance is cleared via kidneys. The compartment "Peptide-Protein serum" contains peptide bound to serum protein. As the fraction of bound peptide to proteins compared to the total amount is small and to reduce the complexity, only the „veins" were connected to this compartment. The corresponding fraction for each specific organ was considered in the fitting process by assigning the data to the specific compartments.

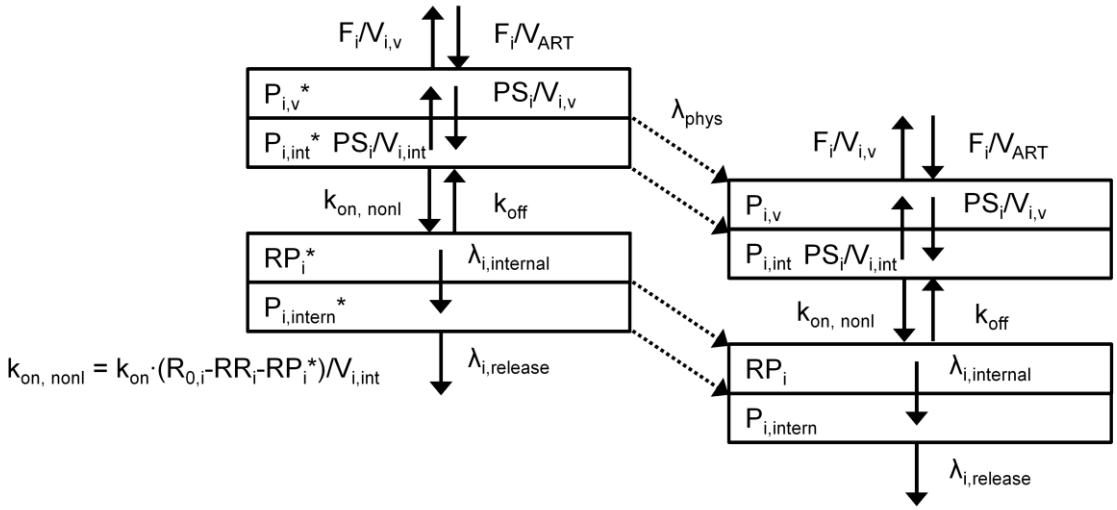

SUPPLEMENTAL FIGURE 2a: Red marrow, GI, spleen, muscle, prostate (uterus), adrenals, rest and tumor: The entire model consists of two systems, one for labeled (with *) and one for unlabeled peptide. The systems are connected by the competition for free receptors ($k_{on,nonl} = k_{on} \cdot (R_{0,i} - RR_i - RP_i^*)/V_{i,int}$) and by the physical decay (λ_{phys}). All physiological parameters are assumed equal for the labeled and unlabeled substance. k_{off} is the dissociation rate, the transport of peptide via serum flow to organ is described by F_i/V_{ART} (where F_i is serum flow and V_{ART} is serum volume of the arteries). $F_i/V_{i,v}$ describes the transport of peptide via serum flow out of organ. $V_{i,v}$ is the serum volume of the respective organ. RP_i is sst2 specific bound peptide to the cell surface. $P_{i,v}$ and $P_{i,int}$ are free peptide of the vascular ($V_{i,v}$) and interstitial space ($V_{i,int}$), respectively. PS_i is the permeability surface area product. $\lambda_{i,\ internal}$ is the internalisation rate of bound peptide and $\lambda_{i,\ release}$ the release rate of ^{111}In (and degraded peptide) from the cell.

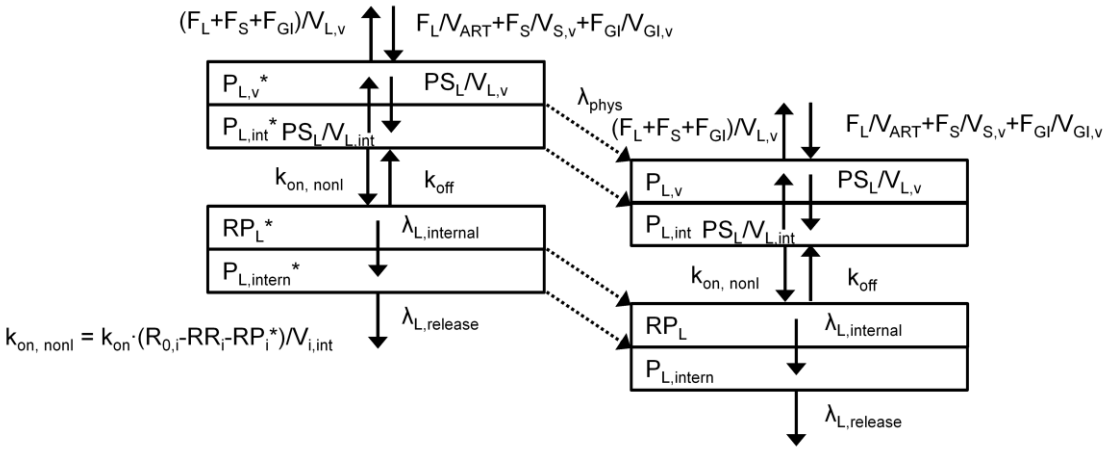

SUPPLEMENTAL FIGURE 2b: Liver: For the liver, the model description of Figure 2a applies but the plasma flow is composed of liver arterial, GI and spleen flow.

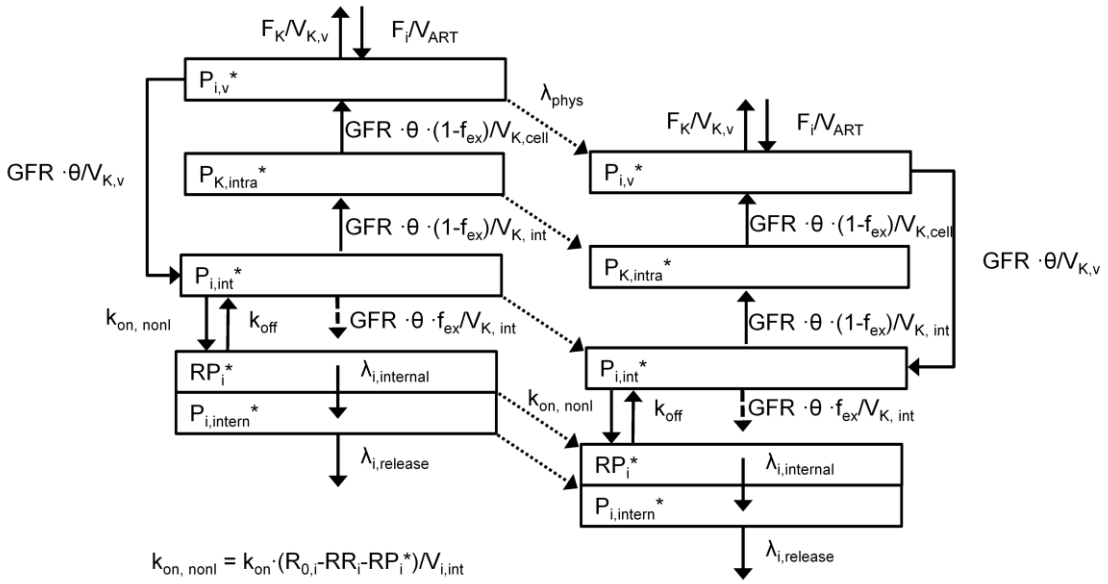

SUPPLEMENTAL FIGURE 2c: Kidneys: The peptide is transported via serum flow to the vascular compartment and then filtrated into the interstitial part. Due to the administration of amino acids the largest fraction (f_{ex} = 0.98, Table A) of peptide is excreted. All unspecific uptake mechanisms are modelled with flow GFR ·θ ·(1-f_{ex}) in and out of kidney cells.

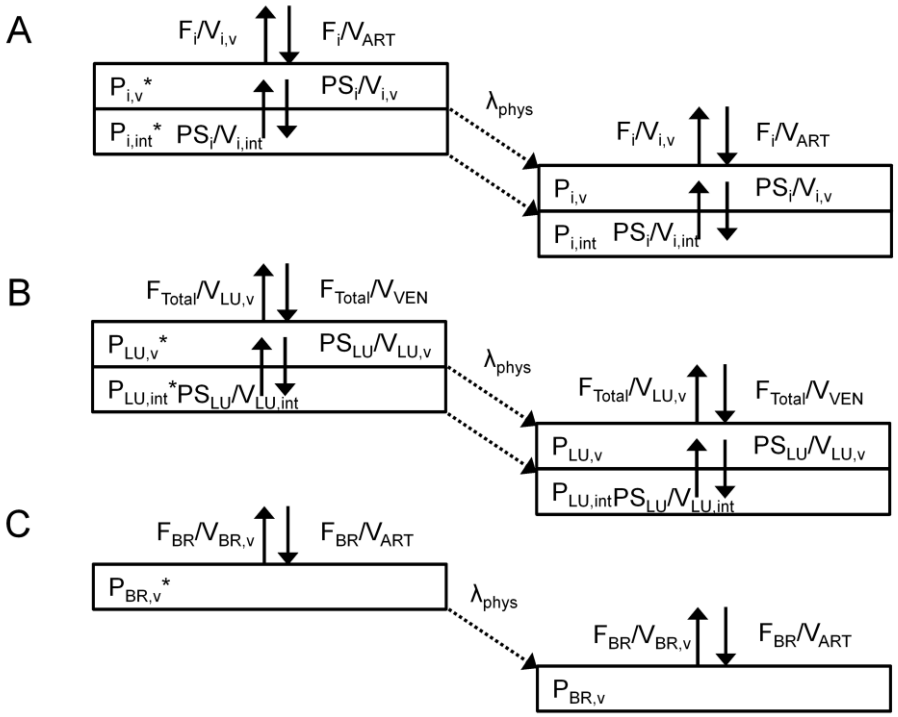

SUPPLEMENTAL FIGURE 3: sst2 negative tissue and brain: For adipose, bone (other than red marrow), skin, heart (A) and lung (B), the model on the organ level simplifies to the transport of peptide via serum flow and transcapillary extravasation. For brain (C) the model reduces to serum flow.

Supplemental Data. Fitted curves and estimated parameters

Patient	Measurements and Modell	Number of data points	Akaike weight	$[R_{K,0}]$	$[R_{S,0}]$	$[R_{L,0}]$	$[R_{REST,0}]$	$[R_{TU1,0}]$	$[R_{TU2,0}]$	$\lambda_{NT,release}$	$\lambda_{TU1,release}$	$\lambda_{TU2,release}$	$V_{TURE,total,}$	f_{TU1}	f_{TU2}	k_{PR}
			[unity]	[nmol/L]						[$min^{-1}\cdot10^{-4}$]			[L]	[ml min^{-1} g^{-1}]		[$min^{-1}\cdot10^{-4}$]
P1	N1 M3	39	1	6.5	8.7	1.4	0.5	15	9.2	0.7	1.1	1.8	-	0.10	0.20	4.7
	N2 M3	39	1	8.8	11	2.5	0.5	18	11	0.7	1.1	1.8	-	0.10	0.20	5.6
	N3 M3	39	1	7.3	9.2	2.0	0.5	17	12	0.7	1.1	1.8	-	0.1	0.2	3.8
P2	N4 M3	34	1	5.7	7.8	1.0	0.4	24	-	1.1	1.7	-	-	0.10	-	4.3
	N5 M3	34	1	5.7	7.8	1.0	0.4	24	-	0.5	1.7	-	-	0.10	-	4.3
P3	N6 M1	38	1	6.2	17	0.9	0.4	5.0	34	0.5	3.0	1.7	-	0.90	0.90	4.0
P4	N7 M1	34	1	8.8	12	1.1	0.9	30	-	1.7	2.1	2.1	-	1.00	1.00	2.1
P5	N8 M2	29	0.8	7.1	13	1.2	0.5 fixed	29	-	2.1	0.0	0.0	0 fixed	0.10	-	24
	N8 M3	29	0.2	7.1	13	1.2	0.5 fixed	27	-	2.3	0.0	0.0	0 fixed	0.11	-	23
P6	N9 M1	32	1	7.5	-	1.5	0.5 fixed	19	35	1.2	2.0	1.1	0.1	1.0	1.0	17
P7	N10 M3	39	1	2.8	3.9	1.1	0.5 fixed	11	7	1.2	0.0	0.0	0.0	0.03	0.02	10
P8	N11 M3	39	1	2.3	4.7	0.6	0.5 fixed	16	25	0.6	0.0	0.0	0.2	0.02	1.00	10
P9	N12 M3	39	1	8.7	18	2.1	0.5 fixed	14	7	1.4	2.1	0.8	1.2	0.06	0.03	17

The relative SD of all parameters were < 50%. All elements of the correlation matrix were < 0.8.

For patient 1 (N1-3) and 2 (N4-5) an iterative two-stage parametric population fit using all pre-therapeutic measurements for parameter estimation was conducted. The total tumor volume could be delineated for meningioma but not for patients with metastasizing NETs. Therefore, the models were first fitted to time activity data of meningioma patients. The estimated value for the receptor concentration of the remaining tissue, $[R_{Rest,0}]$ was then used as a fixed value for the individual fitting of the NET patients. Thus, the additional tumor volume (other than the explicitly delineated lesions) was estimated. For patient 5 also the average liver receptor concentration was fixed, because the high tumor load did not allow to distinguish between normal and tumor tissue in liver .

Preliminary fits showed that the internalization rates of kidney, liver and spleen were similar and in the order of 10^{-3}. To reduce parameter correlation, the kidney and tumor internalization rate were fixed to $\lambda_{K,\,int} = 0.0017\ min^{-1}$ and $\lambda_{TU,\,int} = 0.001\ min^{-1}$, respectively. A sensitivity analysis (Supplement D) showed little influence of these assumptions on the results.

The overall error (bias and uncertainty) of the data could not be determined. However, the estimated relative standard error within the data was < 10 % for all curves except for the serum measurements of data set N1 and N5.

1A

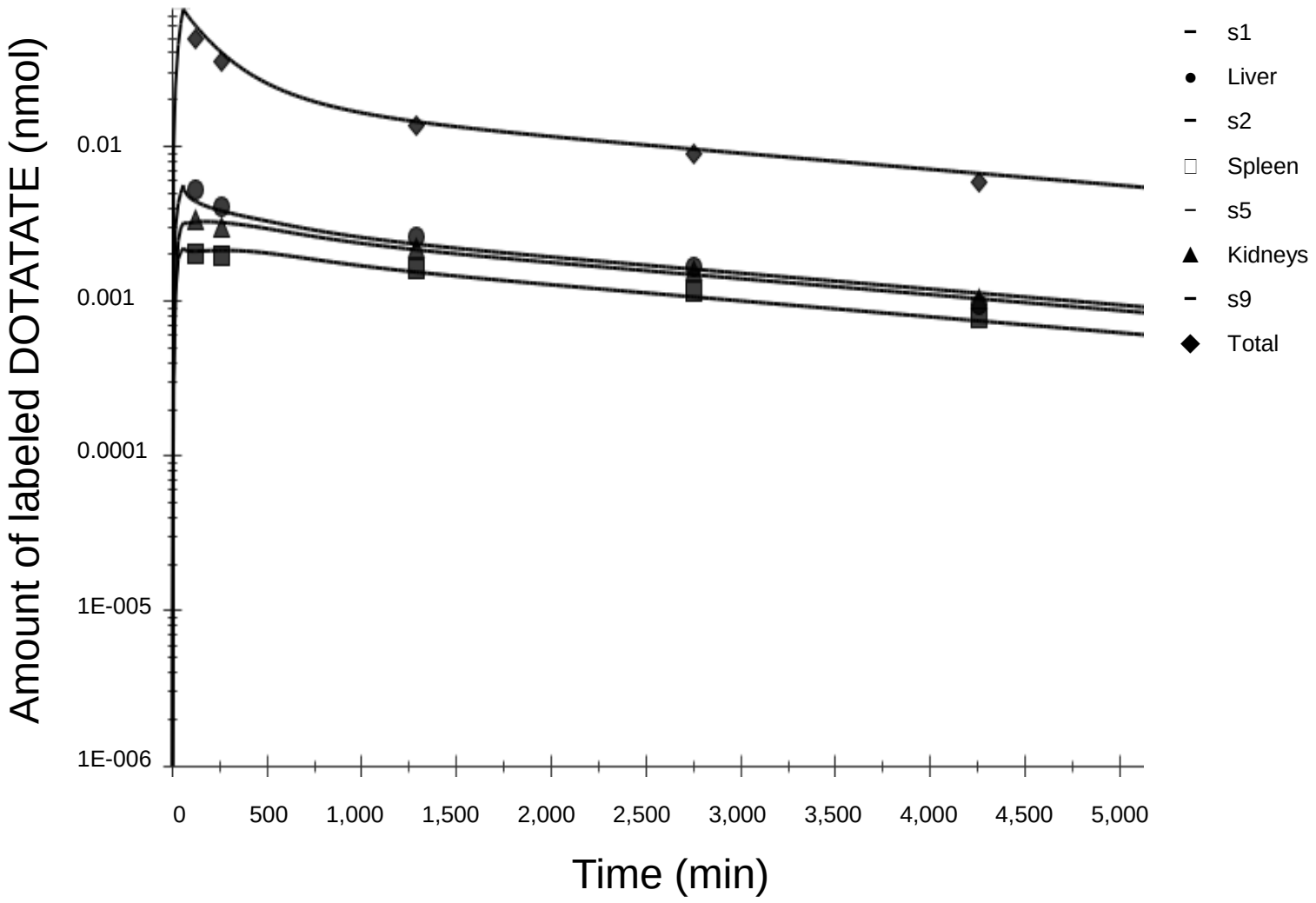
Amount of labeled DOTATATE (nmol)
0.01
0.001
0.0001
1E-005
1E-006
0
500
1,000
1,500
2,000
2,500
3,000
3,500
4,000
4,500
5,000
Time (min)
s1
Liver
s2
Spleen
s5
Kidneys
s9
Total

1B

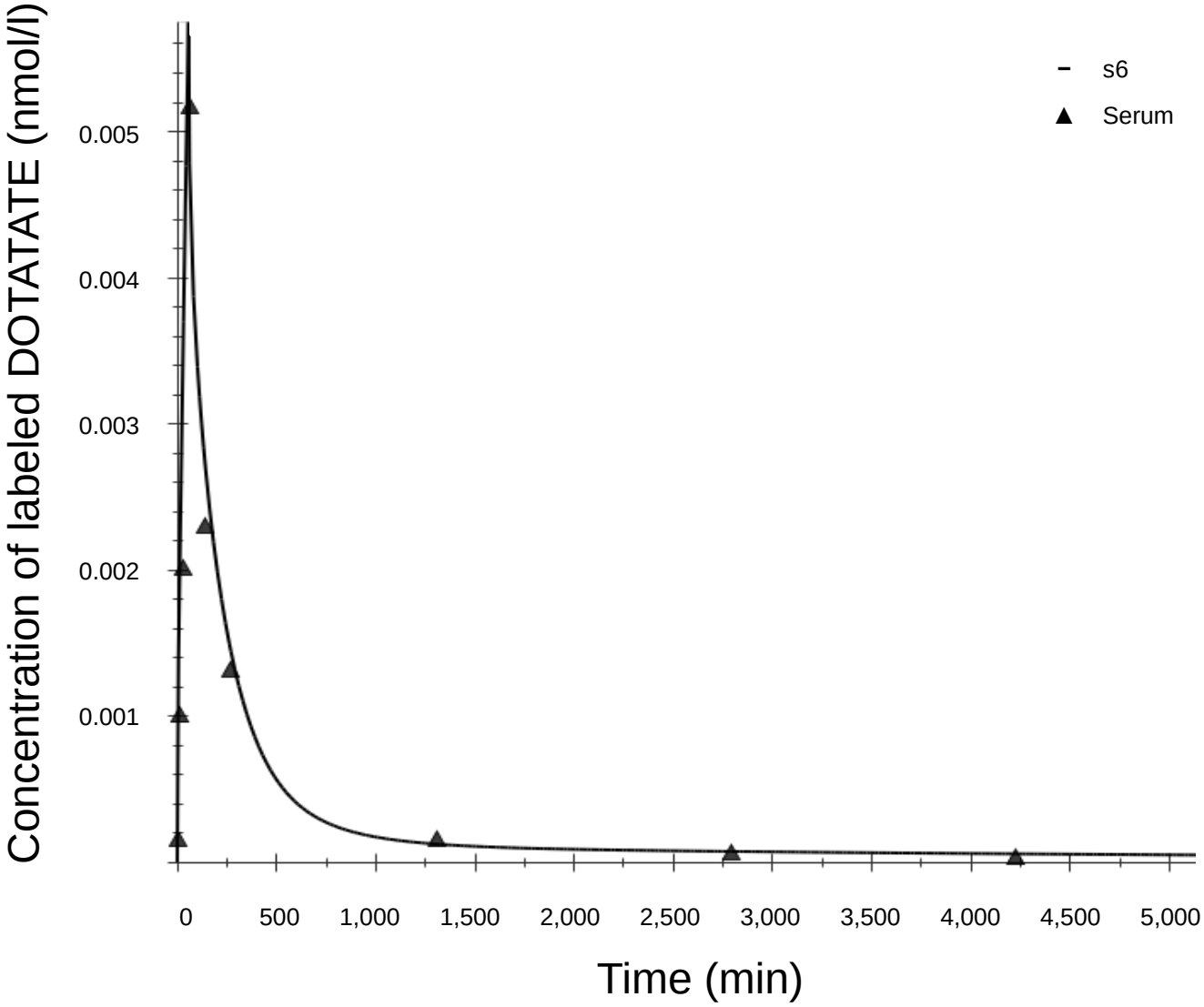
Concentration of labeled DOTATATE (nmol/l)
0.005
0.004
0.003
0.002
0.001
0
500
1,000
1,500
2,000
2,500
3,000
3,500
4,000
4,500
5,000
Time (min)
s6
Serum

1C

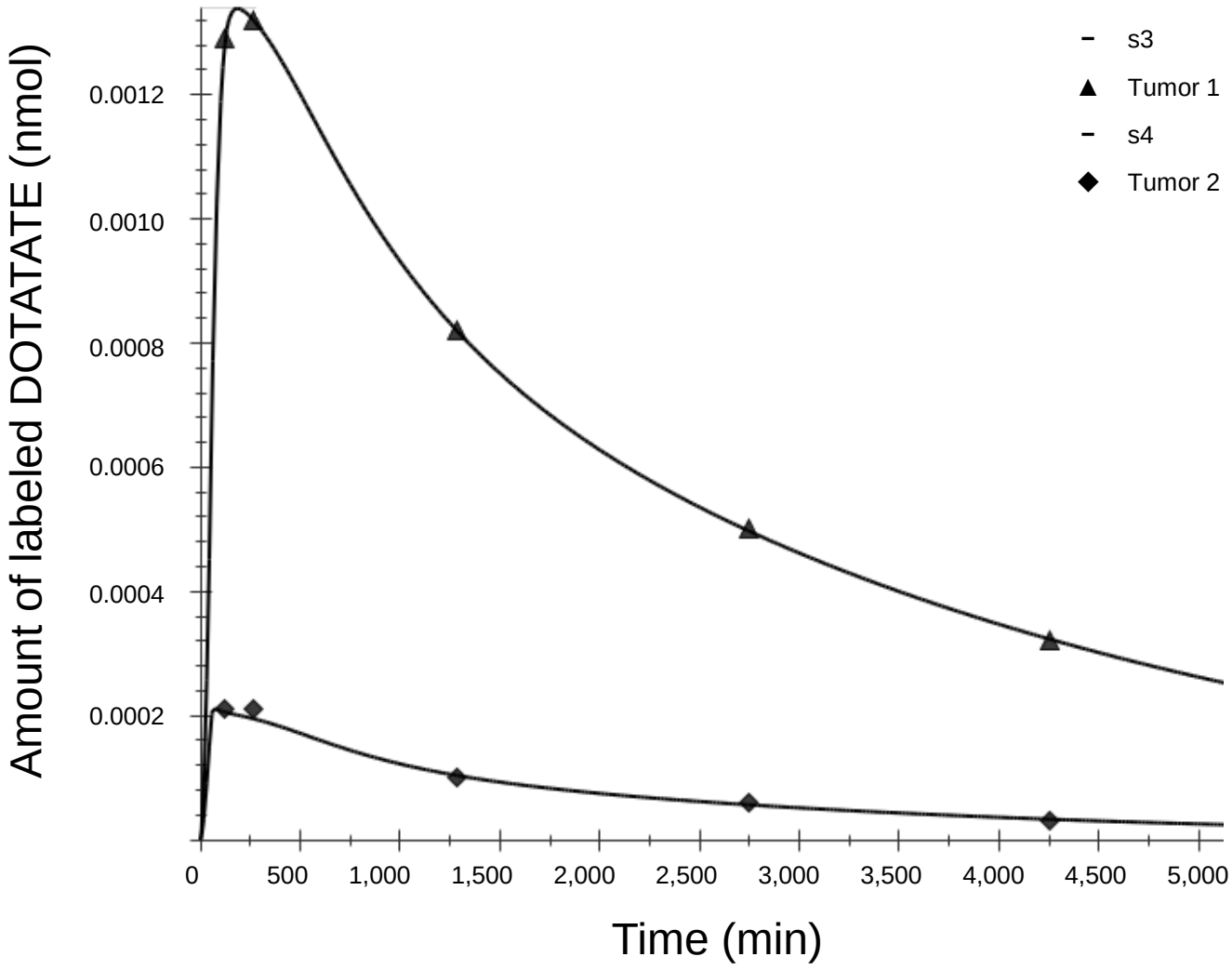
Amount of labeled DOTATATE (nmol)
0.0012
0.0010
0.0008
0.0006
0.0004
0.0002
0
500
1,000
1,500
2,000
2,500
3,000
3,500
4,000
4,500
5,000
Time (min)
s3
Tumor 1
s4
Tumor 2

2A

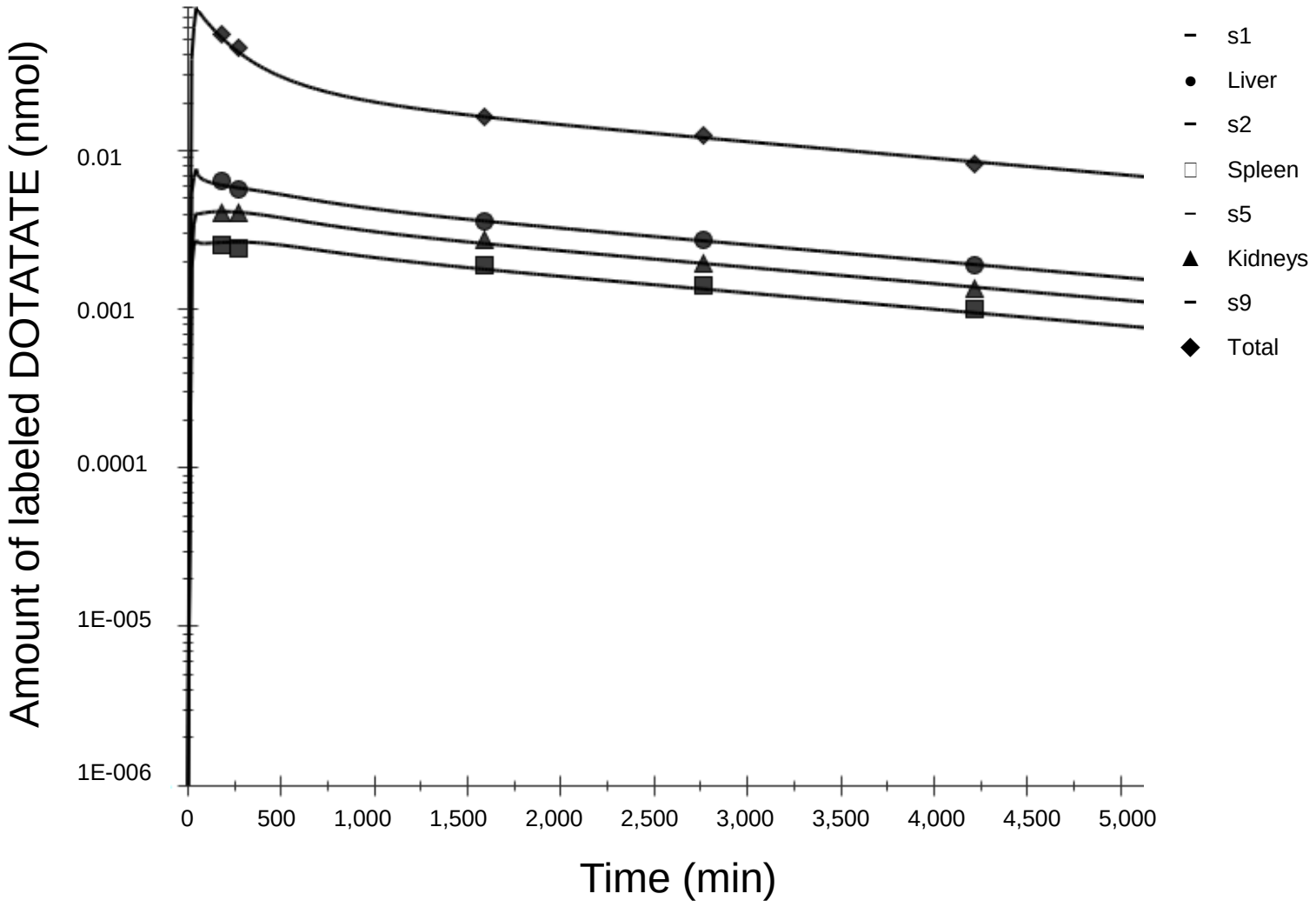
Amount of labeled DOTATATE (nmol)
0.01
0.001
0.0001
1E-005
1E-006
0
500
1,000
1,500
2,000
2,500
3,000
3,500
4,000
4,500
5,000
Time (min)
s1
Liver
s2
Spleen
s5
Kidneys
s9
Total

2B

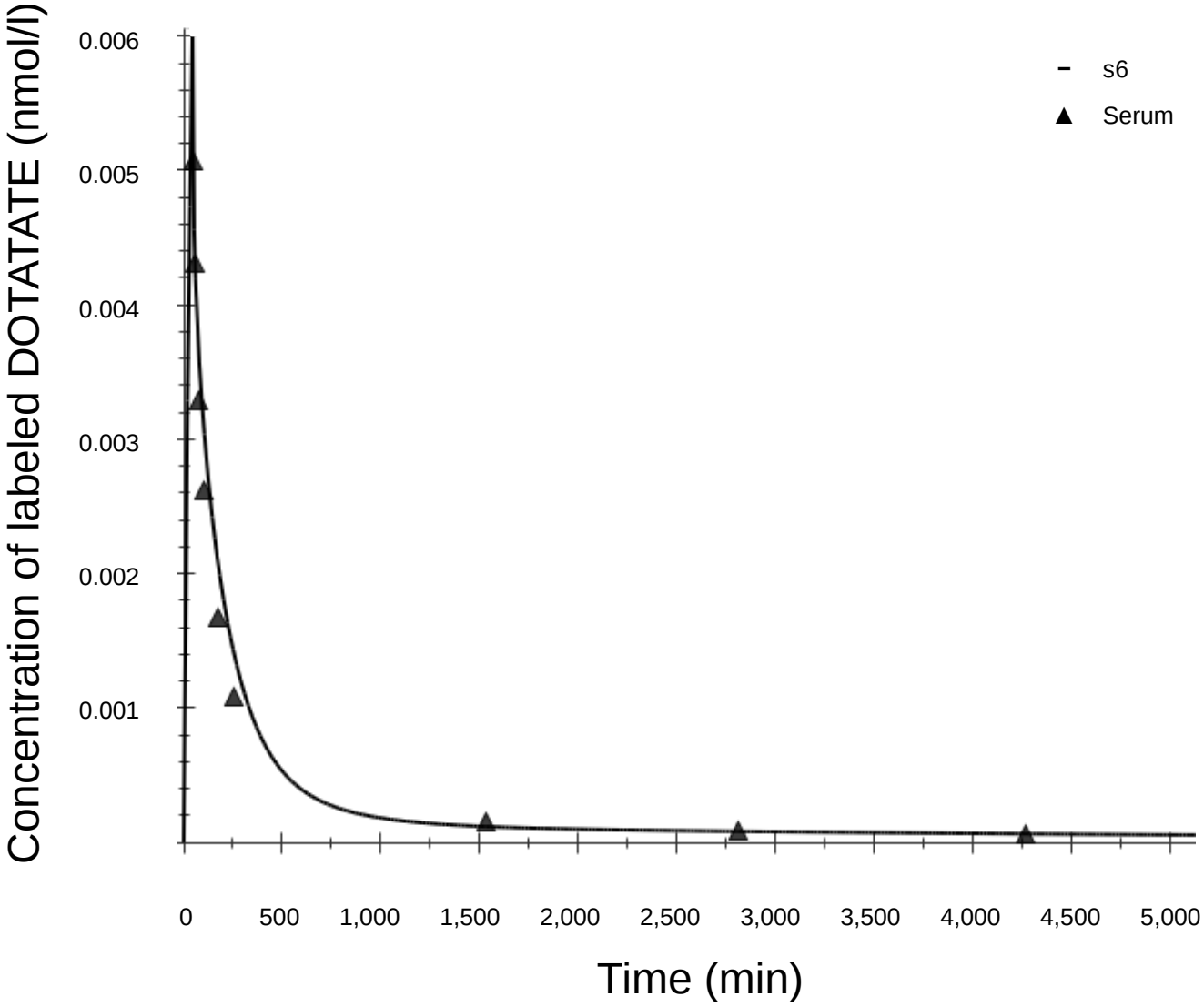
Concentration of labeled DOTATATE (nmol/l)
0.006
0.005
0.004
0.003
0.002
0.001
s6
Serum
0
500
1,000
1,500
2,000
2,500
3,000
3,500
4,000
4,500
5,000
Time (min)

2C

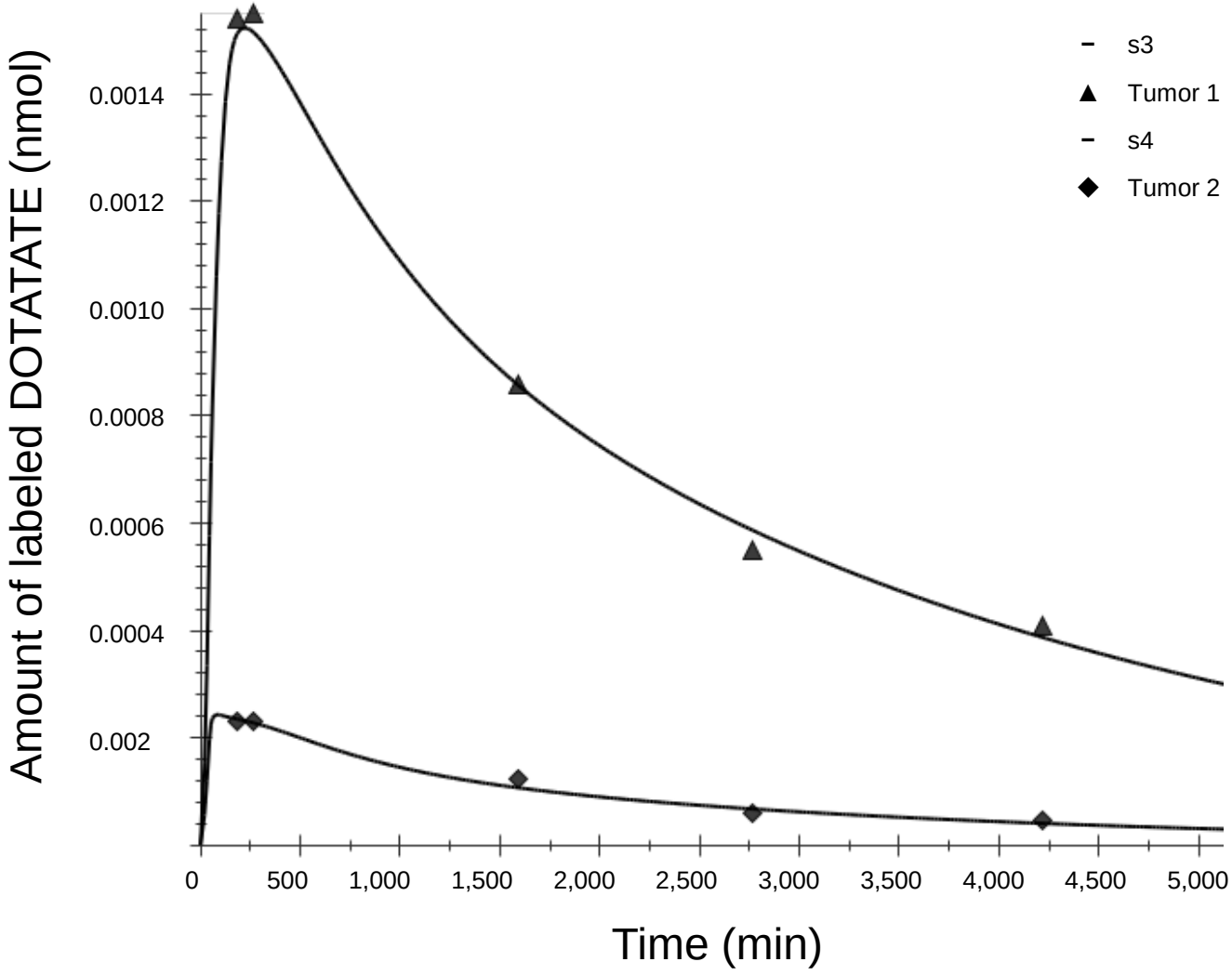
Amount of labeled DOTATATE (nmol)
0.0014
0.0012
0.0010
0.0008
0.0006
0.0004
0.002
0
500
1,000
1,500
2,000
2,500
3,000
3,500
4,000
4,500
5,000
Time (min)
s3
Tumor 1
s4
Tumor 2

3A

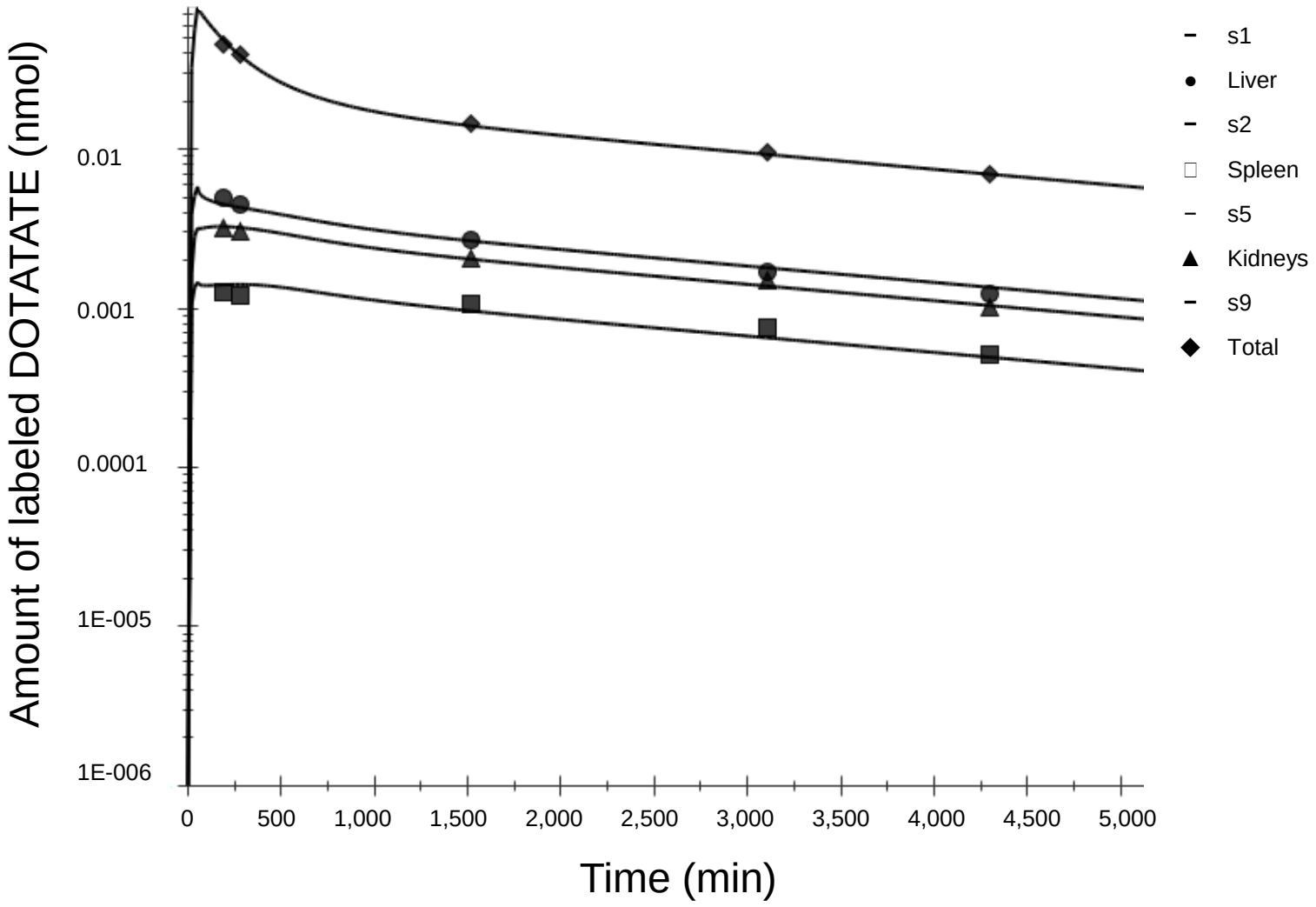
Amount of labeled DOTATATE (nmol)
0.01
0.001
0.0001
1E-005
1E-006
0
500
1,000
1,500
2,000
2,500
3,000
3,500
4,000
4,500
5,000
Time (min)
s1
Liver
s2
Spleen
s5
Kidneys
s9
Total

3B

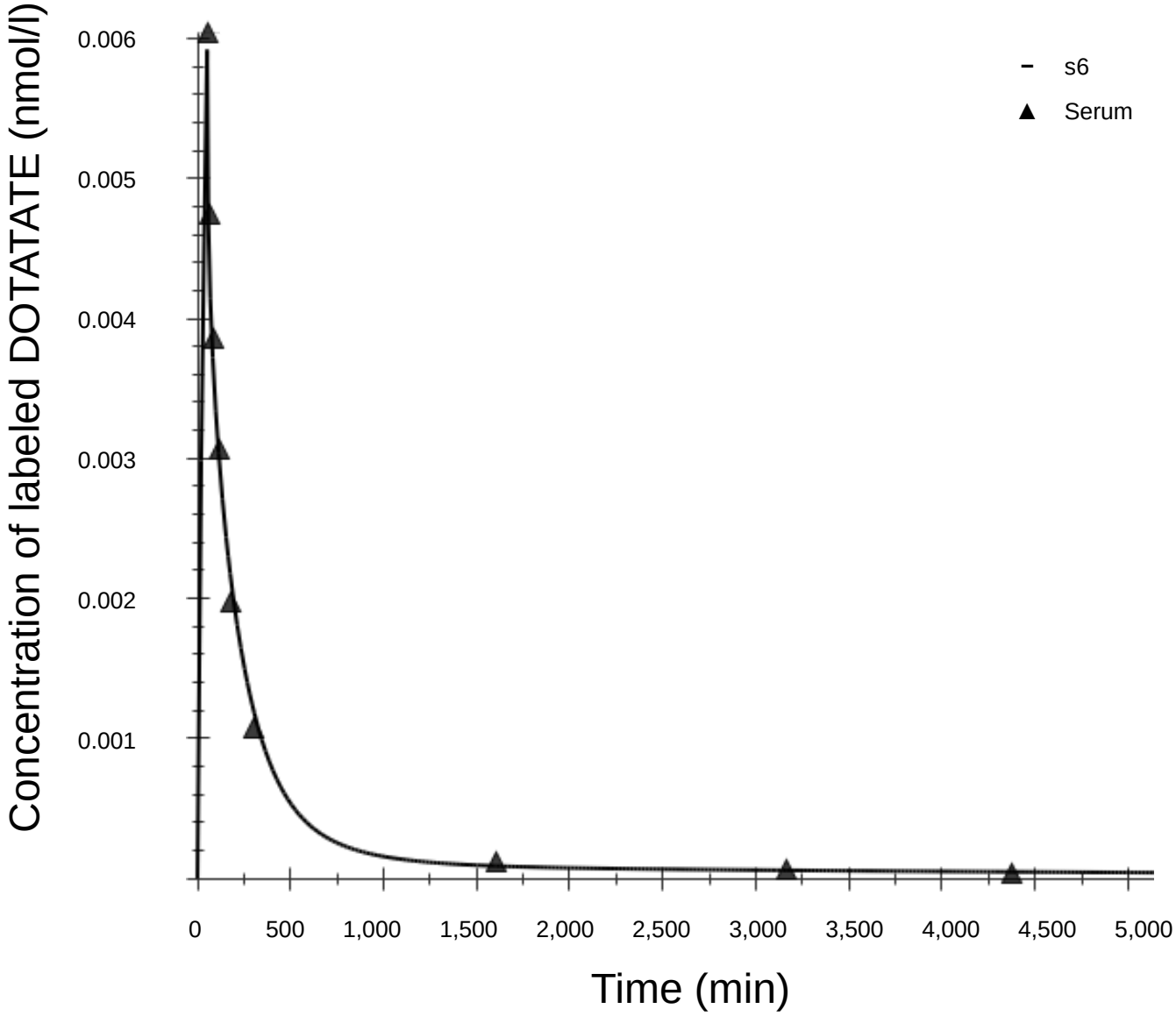
Concentration of labeled DOTATATE (nmol/l)
0.006
0.005
0.004
0.003
0.002
0.001
0
500
1,000
1,500
2,000
2,500
3,000
3,500
4,000
4,500
5,000
Time (min)
s6
Serum

3C

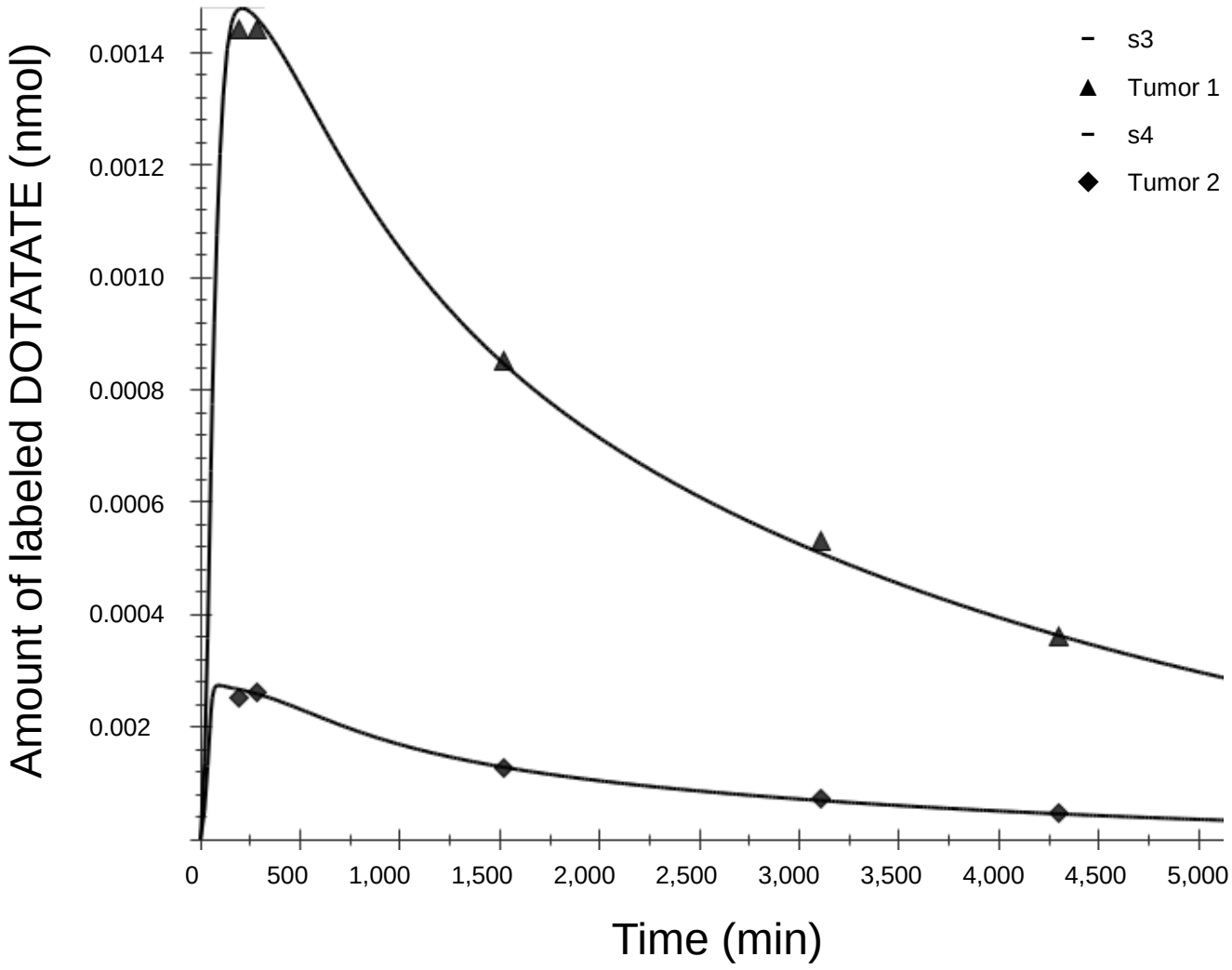
Amount of labeled DOTATATE (nmol)
0.0014
0.0012
0.0010
0.0008
0.0006
0.0004
0.002
0
500
1,000
1,500
2,000
2,500
3,000
3,500
4,000
4,500
5,000
Time (min)
s3
Tumor 1
s4
Tumor 2

4A

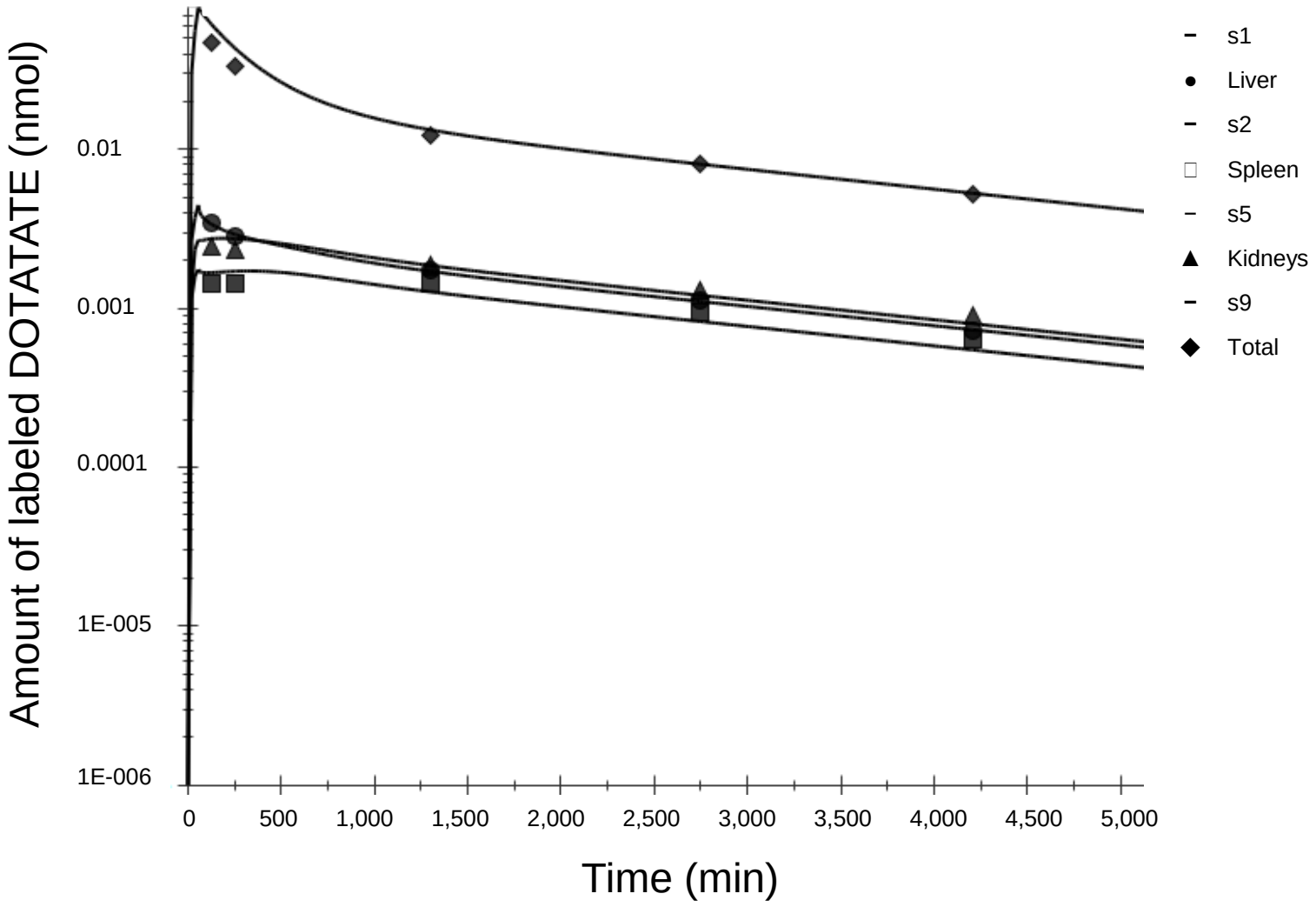
Amount of labeled DOTATATE (nmol)
0.01
0.001
0.0001
1E-005
1E-006
0
500
1,000
1,500
2,000
2,500
3,000
3,500
4,000
4,500
5,000
Time (min)
s1
Liver
s2
Spleen
s5
Kidneys
s9
Total

4B

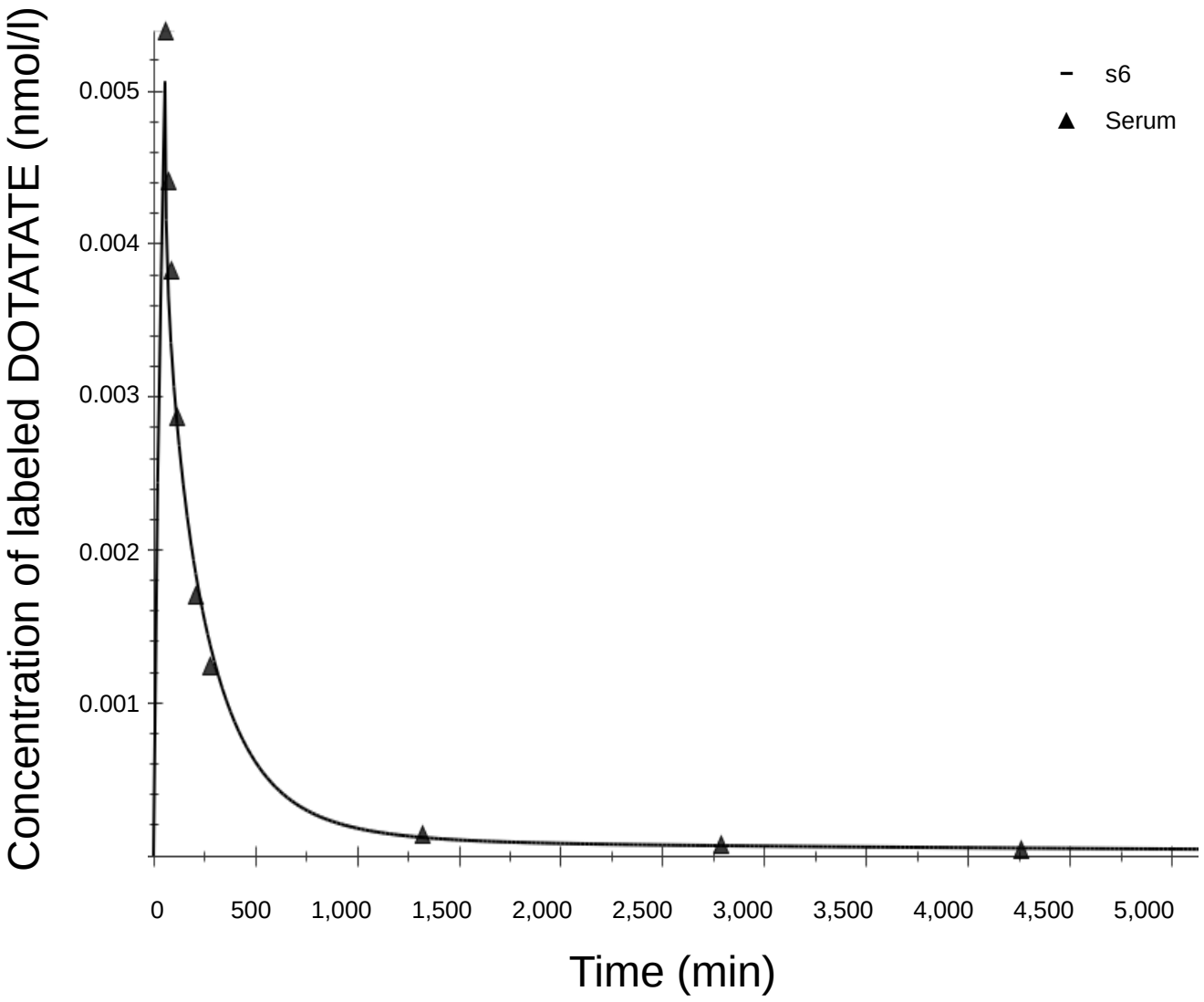
Concentration of labeled DOTATATE (nmol/l)
0.005
0.004
0.003
0.002
0.001
0
500
1,000
1,500
2,000
2,500
3,000
3,500
4,000
4,500
5,000
Time (min)
s6
Serum

4C

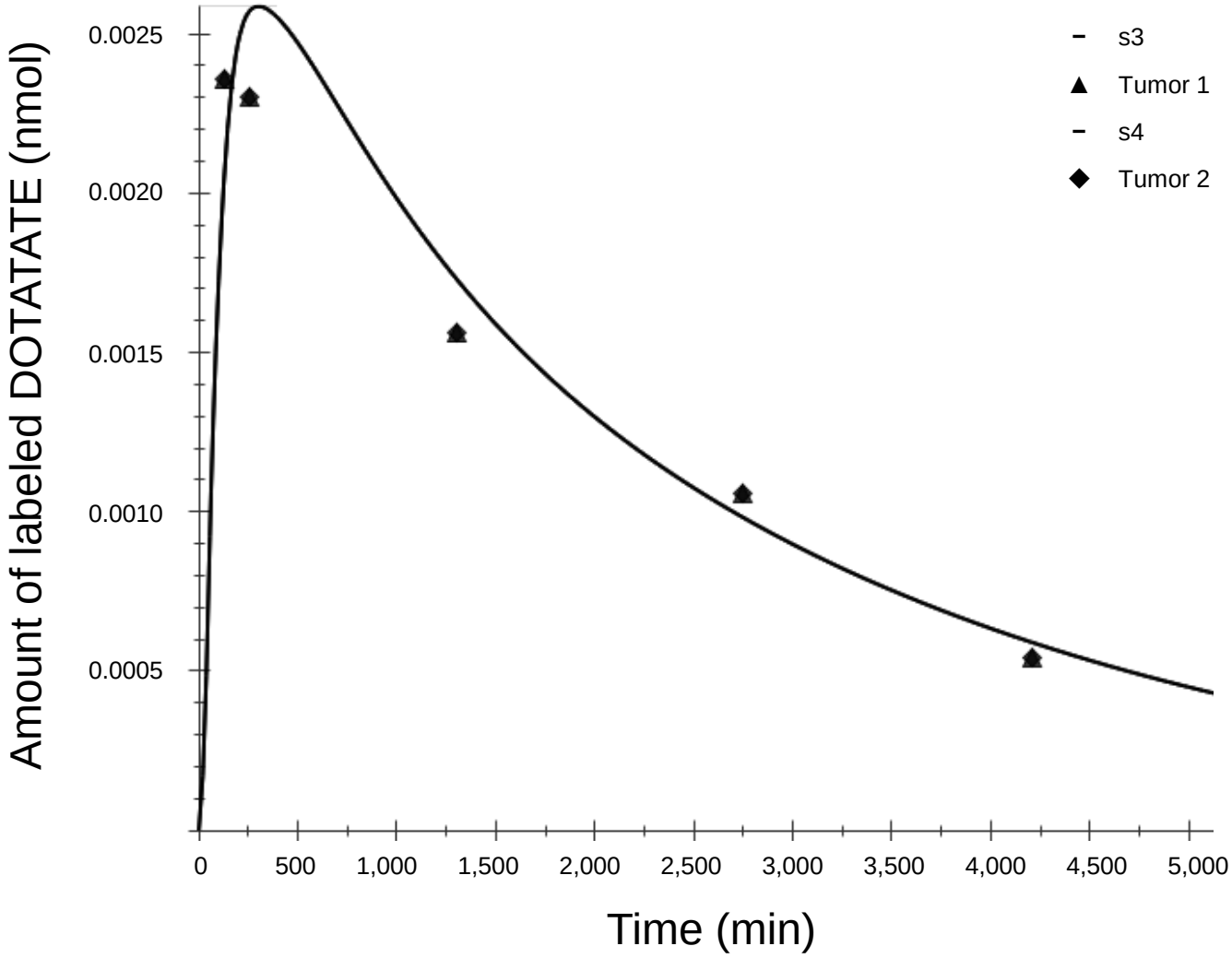
Amount of labeled DOTATATE (nmol)
0.0025
0.0020
0.0015
0.0010
0.0005
0
500
1,000
1,500
2,000
2,500
3,000
3,500
4,000
4,500
5,000
Time (min)
s3
Tumor 1
s4
Tumor 2

5A

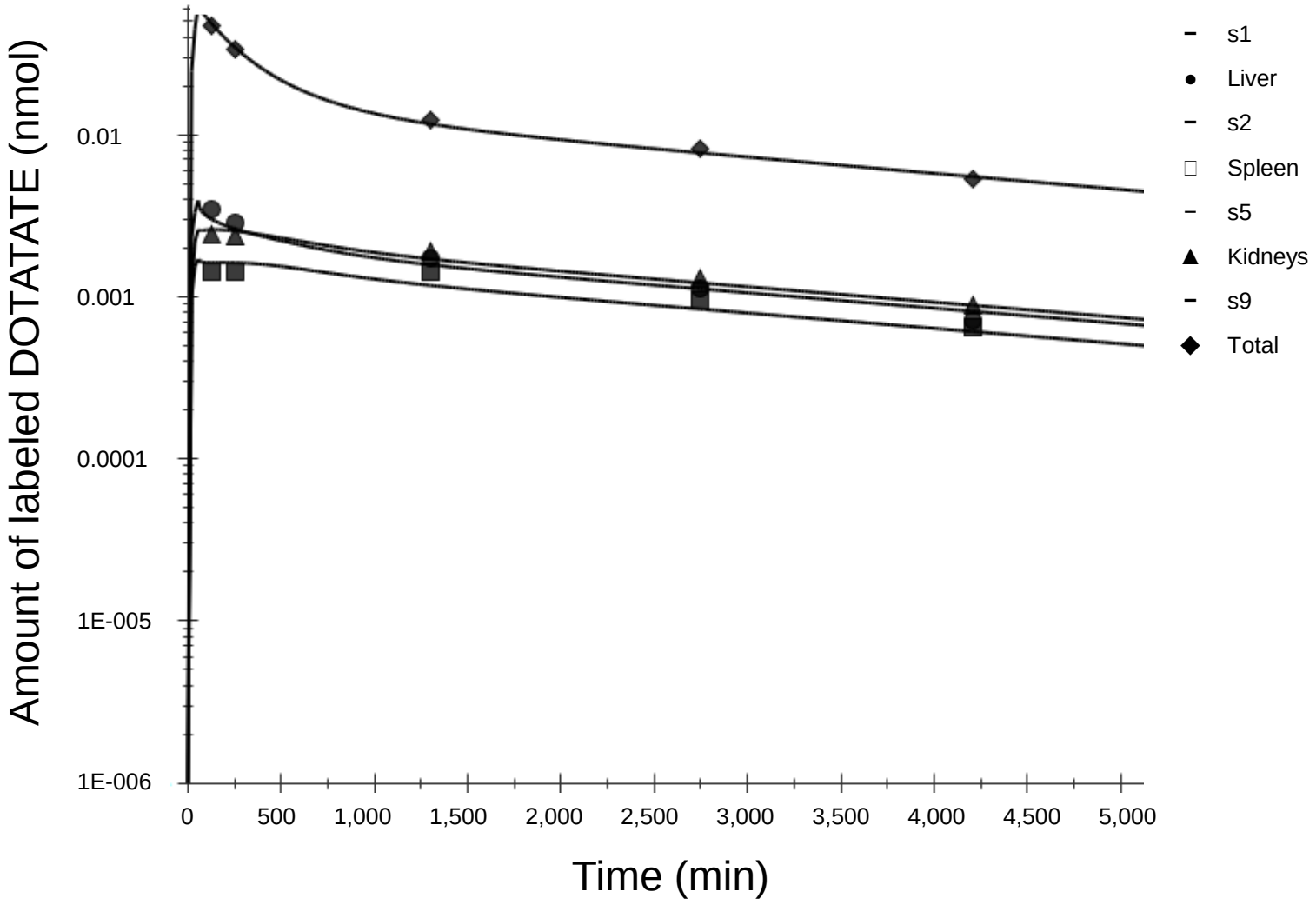
Amount of labeled DOTATATE (nmol)
0.01
0.001
0.0001
1E-005
1E-006
0
500
1,000
1,500
2,000
2,500
3,000
3,500
4,000
4,500
5,000
Time (min)
s1
Liver
s2
Spleen
s5
Kidneys
s9
Total

5B

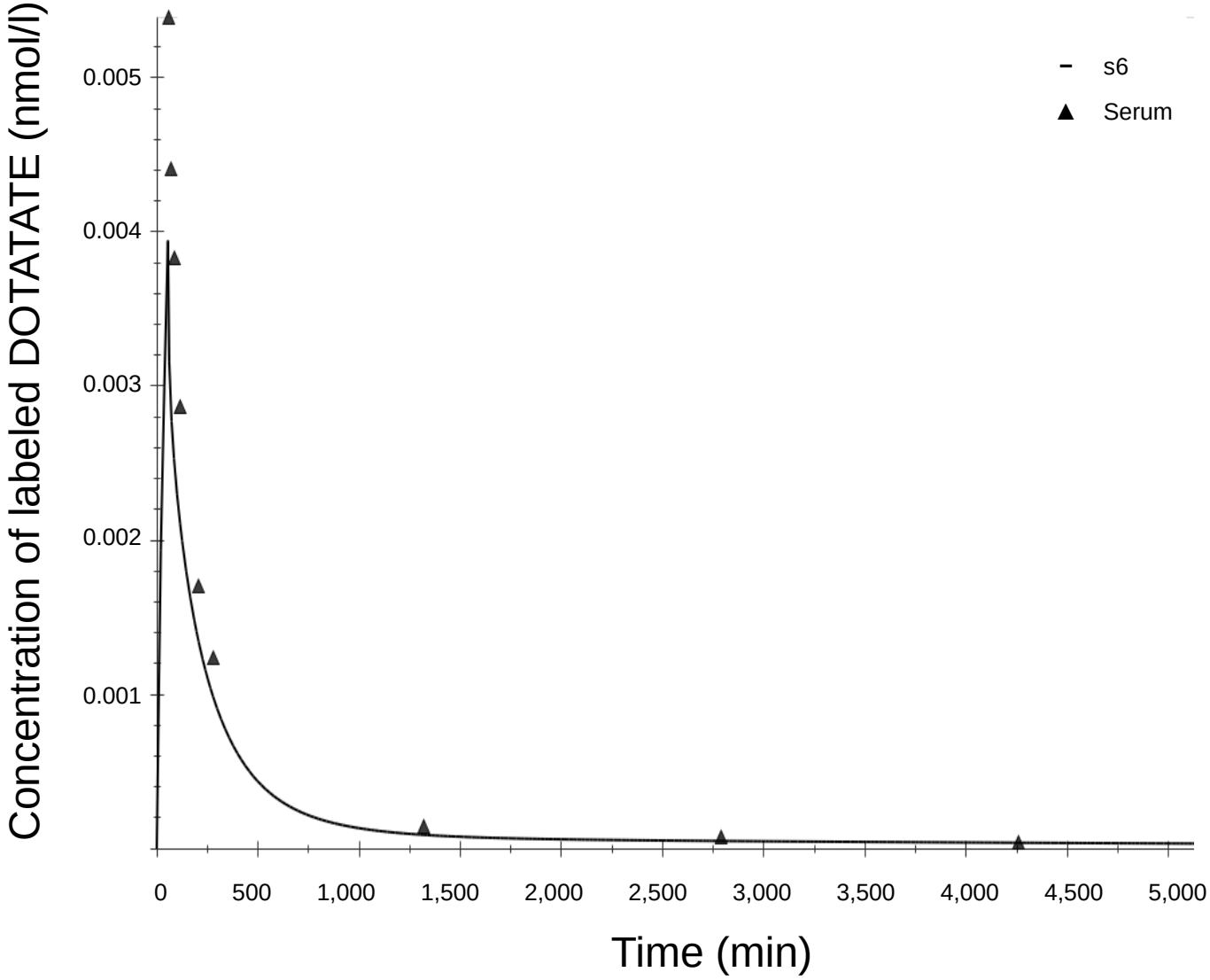
Concentration of labeled DOTATATE (nmol/l)
0.005
0.004
0.003
0.002
0.001
0
500
1,000
1,500
2,000
2,500
3,000
3,500
4,000
4,500
5,000
Time (min)
s6
Serum

5C

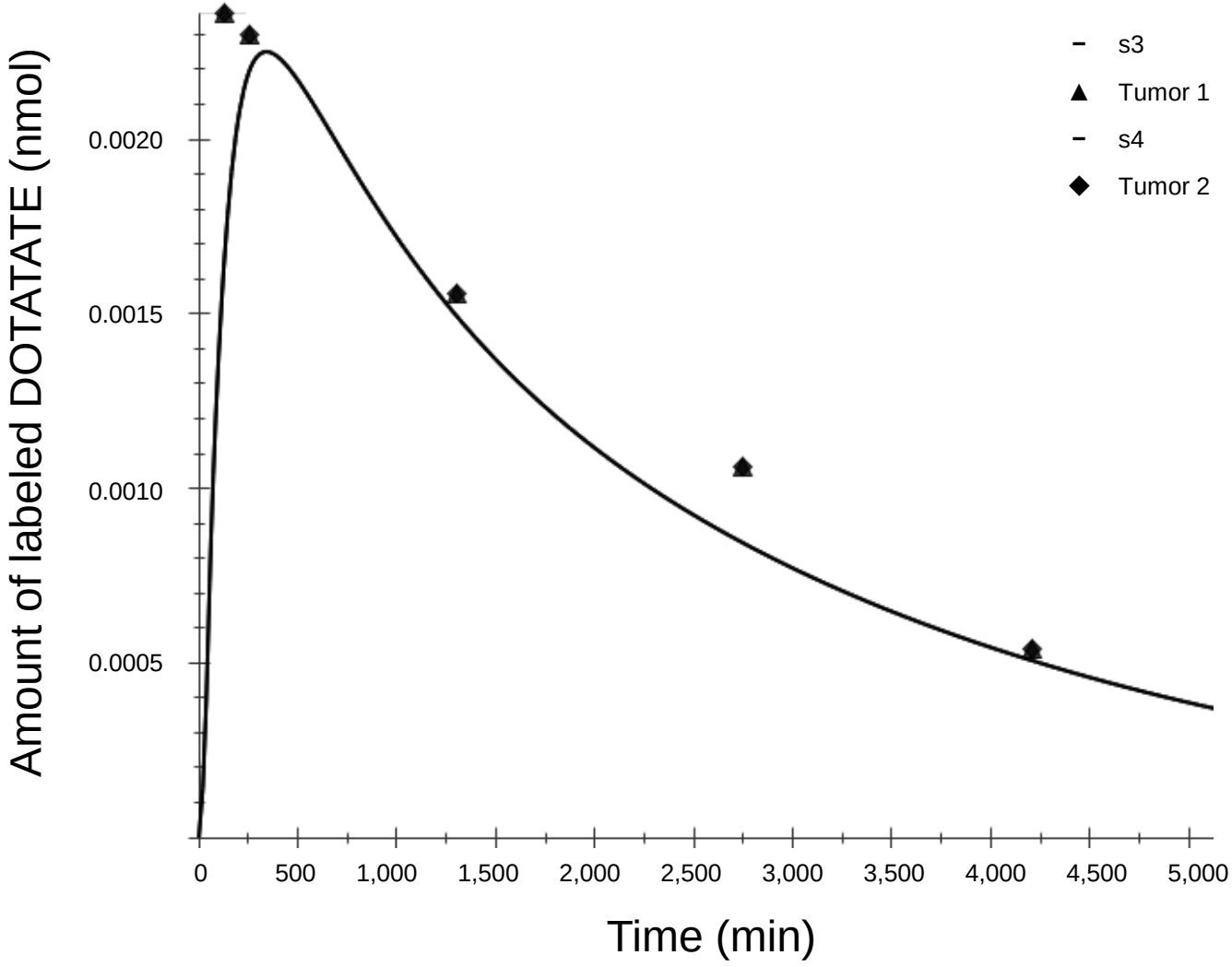
Amount of labeled DOTATATE (nmol)
0.0020
0.0015
0.0010
0.0005
0
500
1,000
1,500
2,000
2,500
3,000
3,500
4,000
4,500
5,000
Time (min)
s3
Tumor 1
s4
Tumor 2

6A

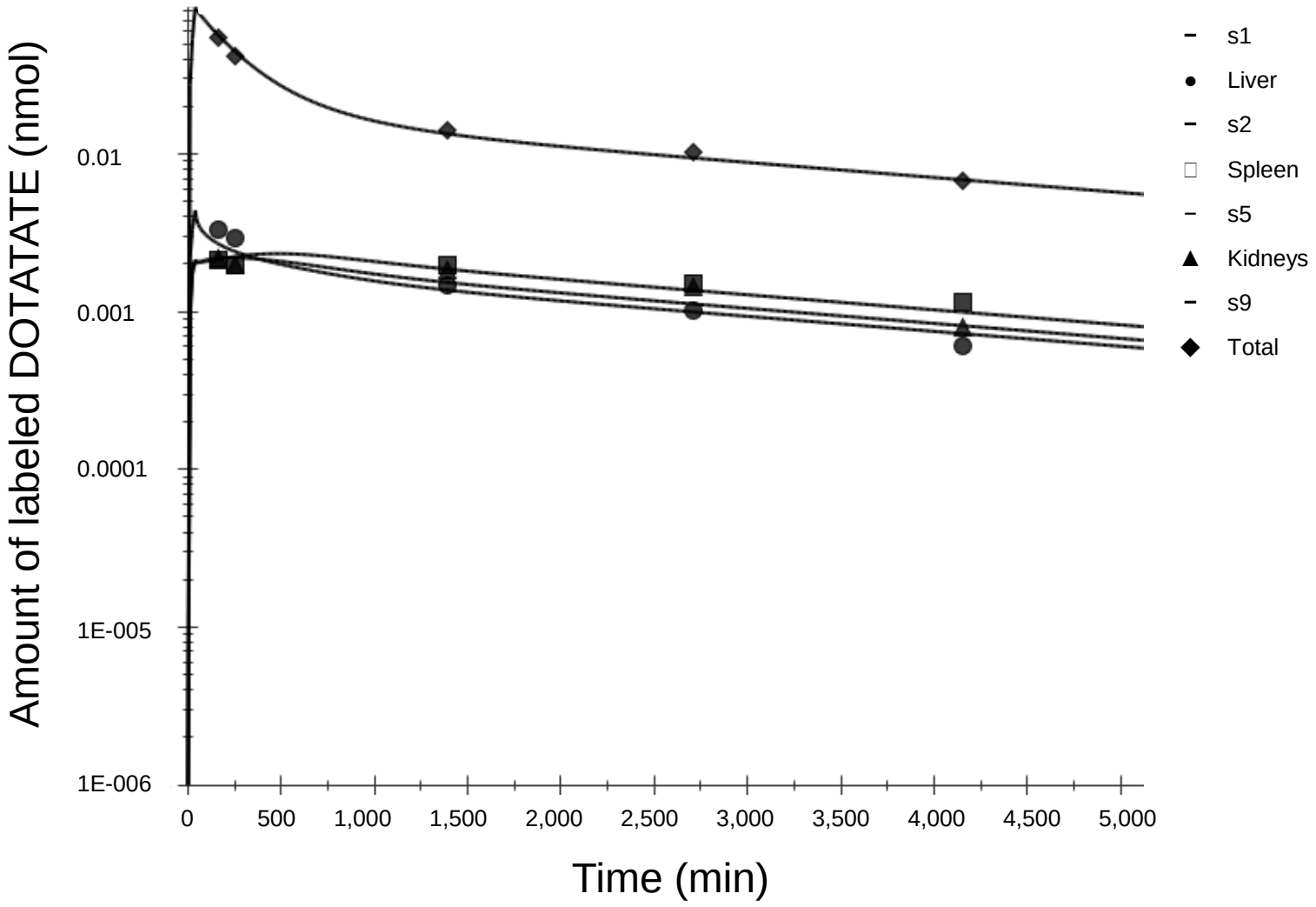
Amount of labeled DOTATATE (nmol)
0.01
0.001
0.0001
1E-005
1E-006
0
500
1,000
1,500
2,000
2,500
3,000
3,500
4,000
4,500
5,000
Time (min)
s1
Liver
s2
Spleen
s5
Kidneys
s9
Total

6B

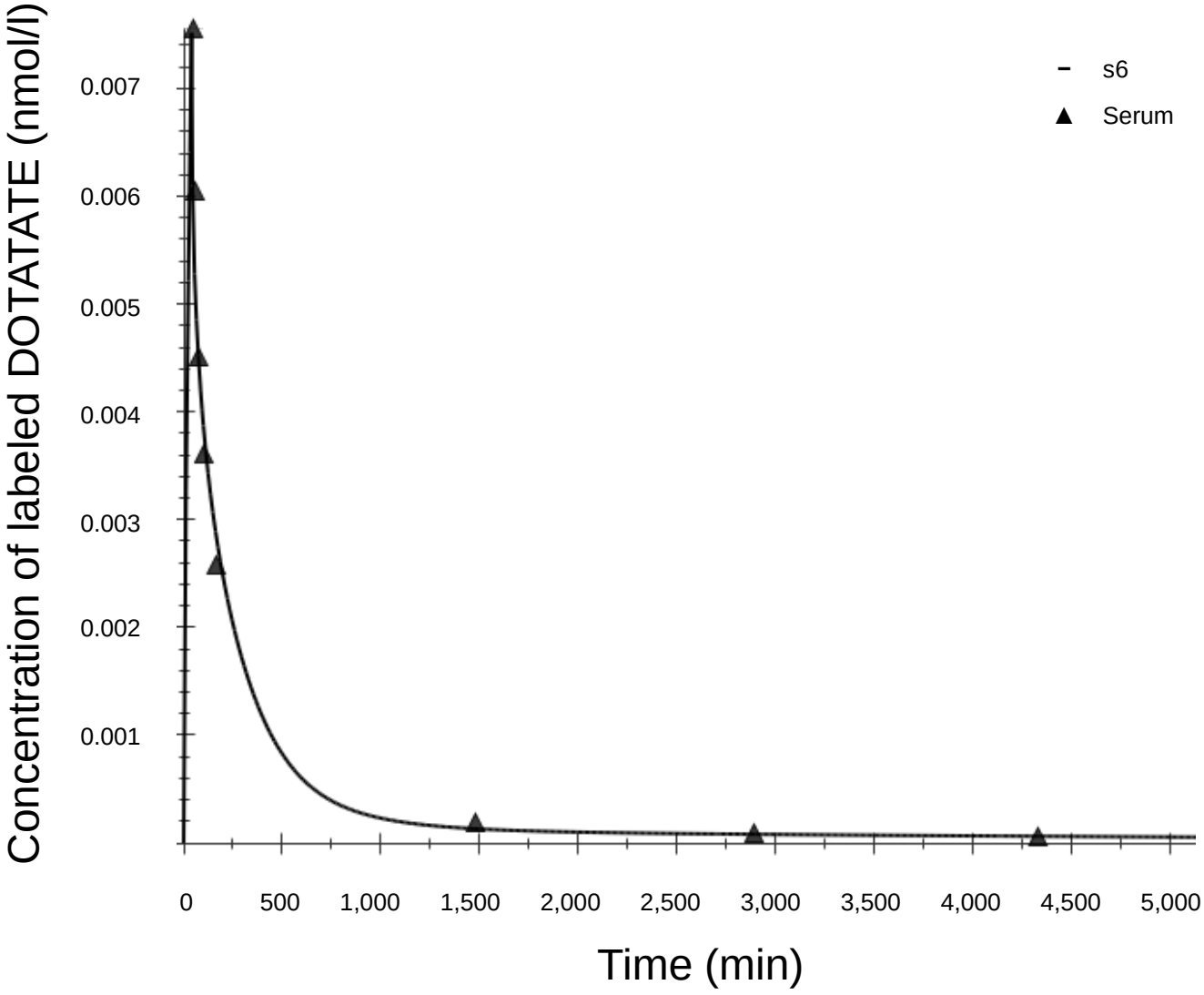
Concentration of labeled DOTATATE (nmol/l)
0.007
0.006
0.005
0.004
0.003
0.002
0.001
0
500
1,000
1,500
2,000
2,500
3,000
3,500
4,000
4,500
5,000
Time (min)
s6
Serum

6C

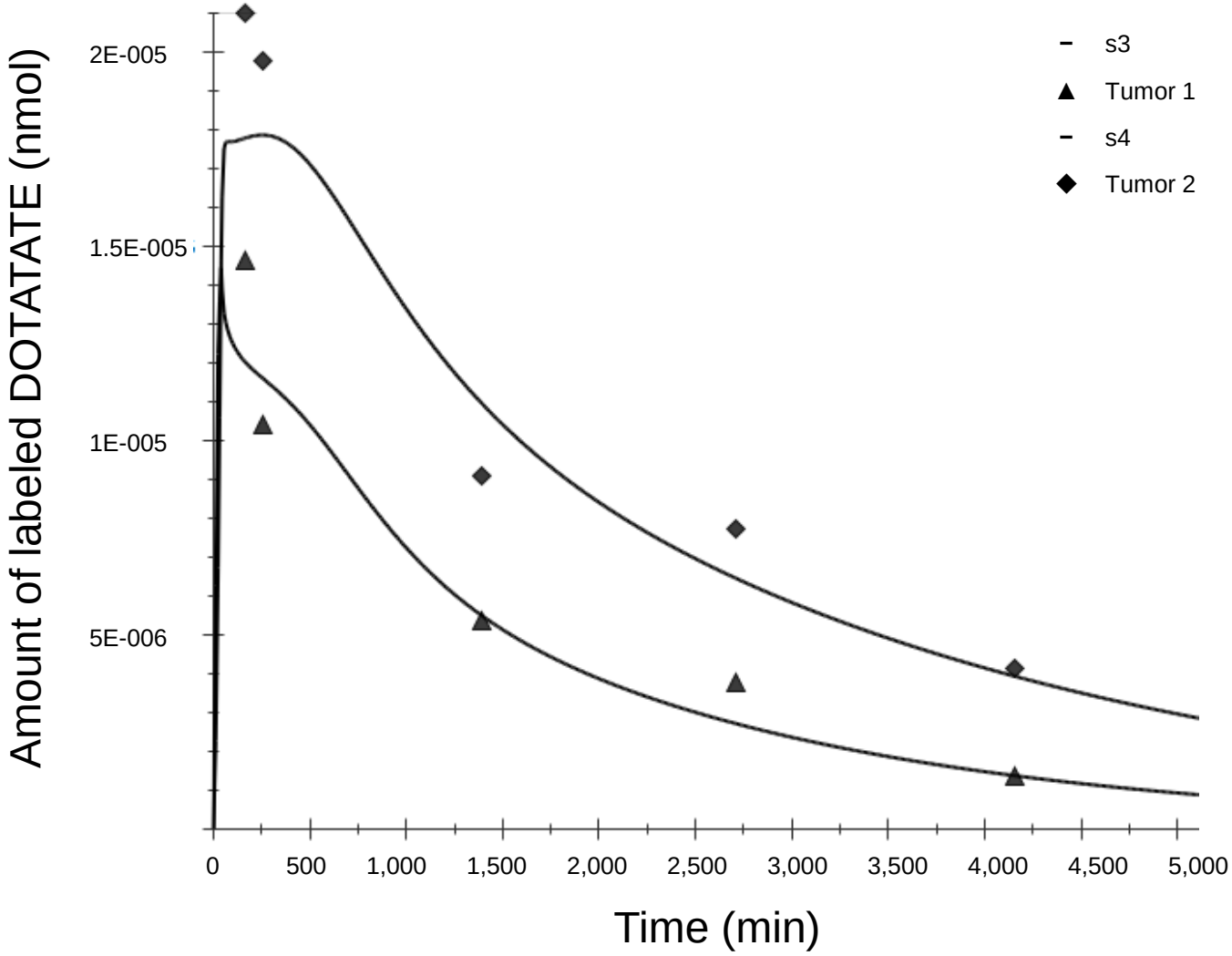
Amount of labeled DOTATATE (nmol)
2E-005
1.5E-005
1E-005
5E-006
0
500
1,000
1,500
2,000
2,500
3,000
3,500
4,000
4,500
5,000
Time (min)
s3
Tumor 1
s4
Tumor 2

7A

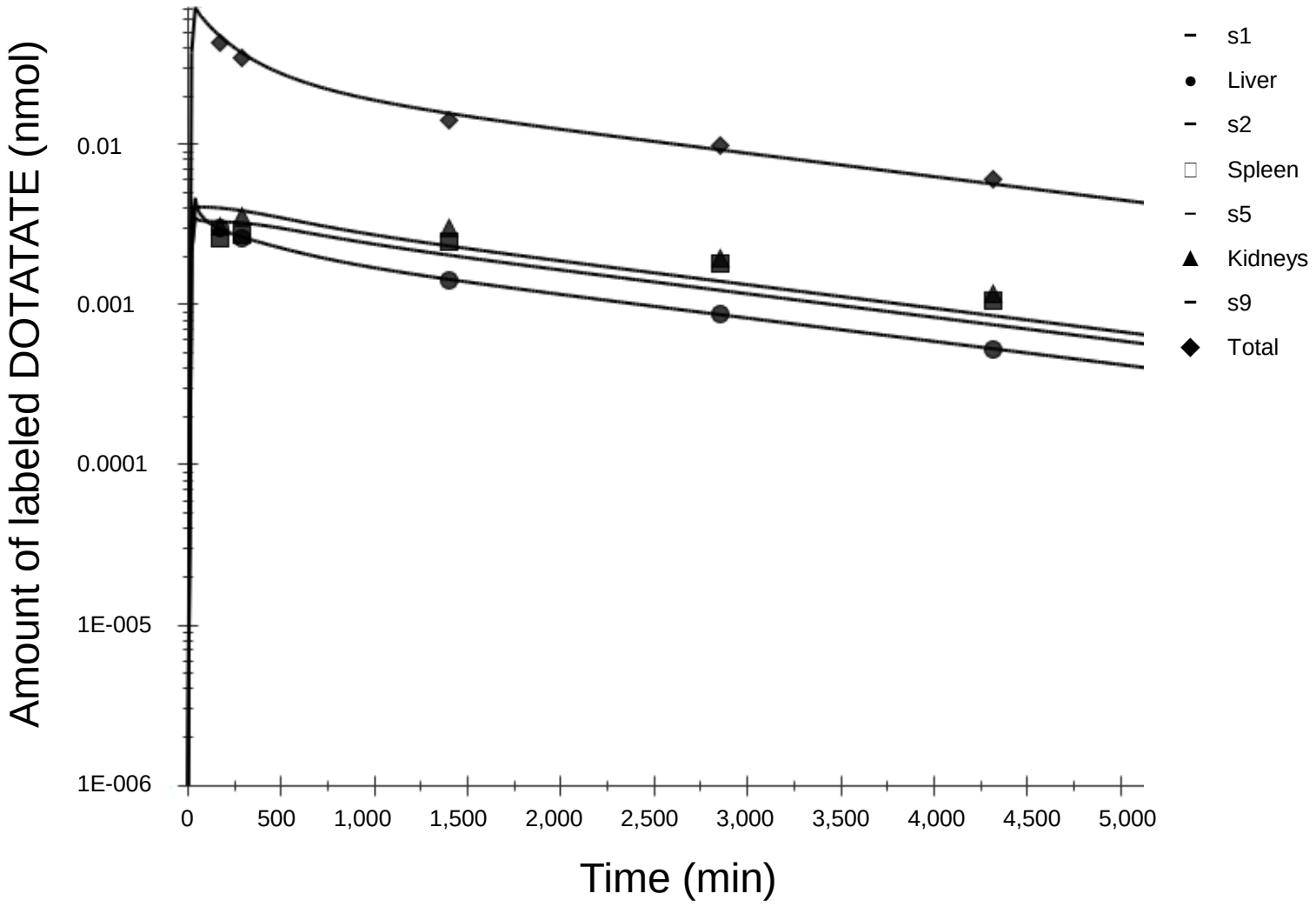
Amount of labeled DOTATATE (nmol)
0.01
0.001
0.0001
1E-005
1E-006
0
500
1,000
1,500
2,000
2,500
3,000
3,500
4,000
4,500
5,000
Time (min)
s1
Liver
s2
Spleen
s5
Kidneys
s9
Total

7B

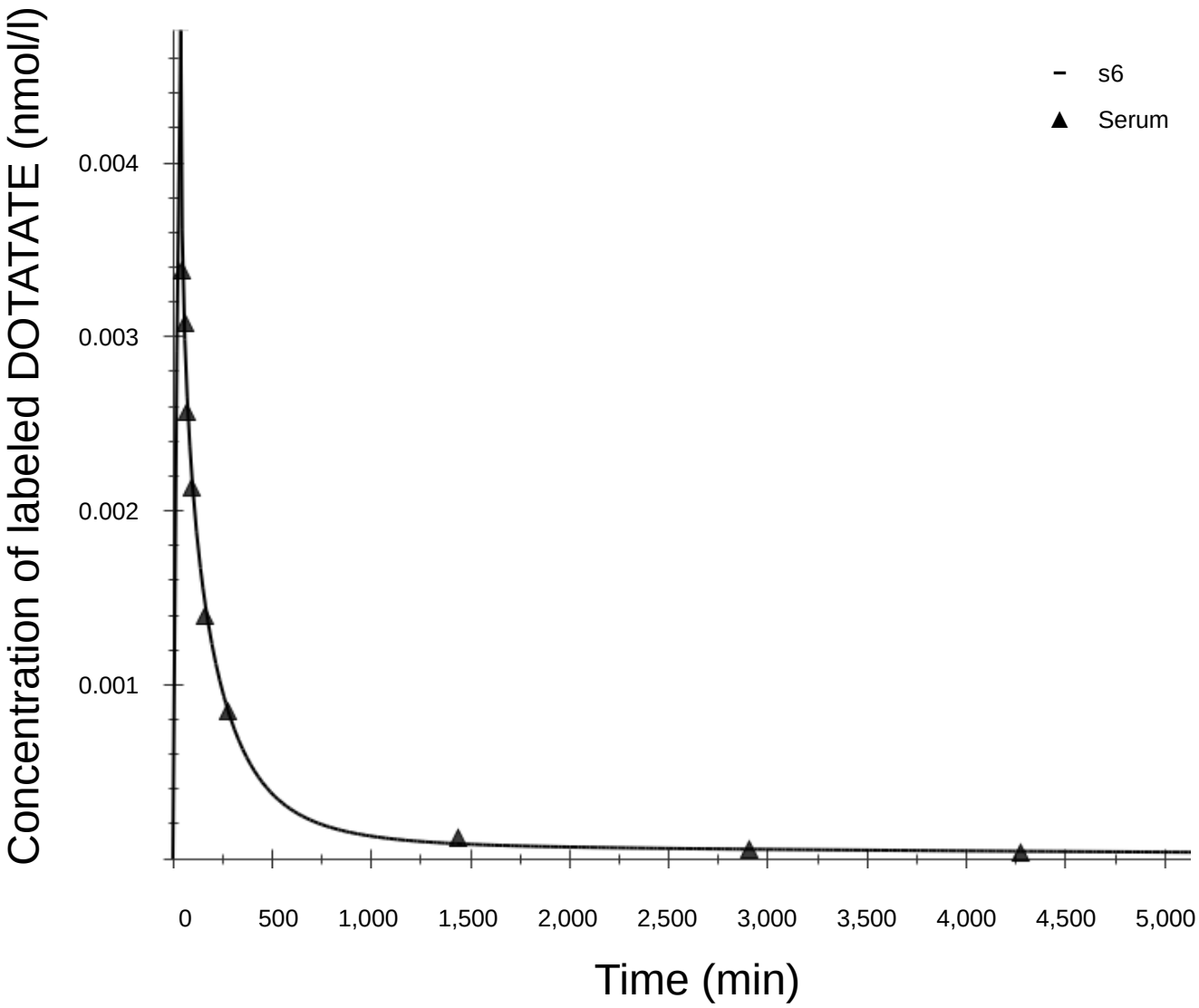
Concentration of labeled DOTATATE (nmol/l)
0.004
0.003
0.002
0.001
0
500
1,000
1,500
2,000
2,500
3,000
3,500
4,000
4,500
5,000
Time (min)
s6
Serum

7C

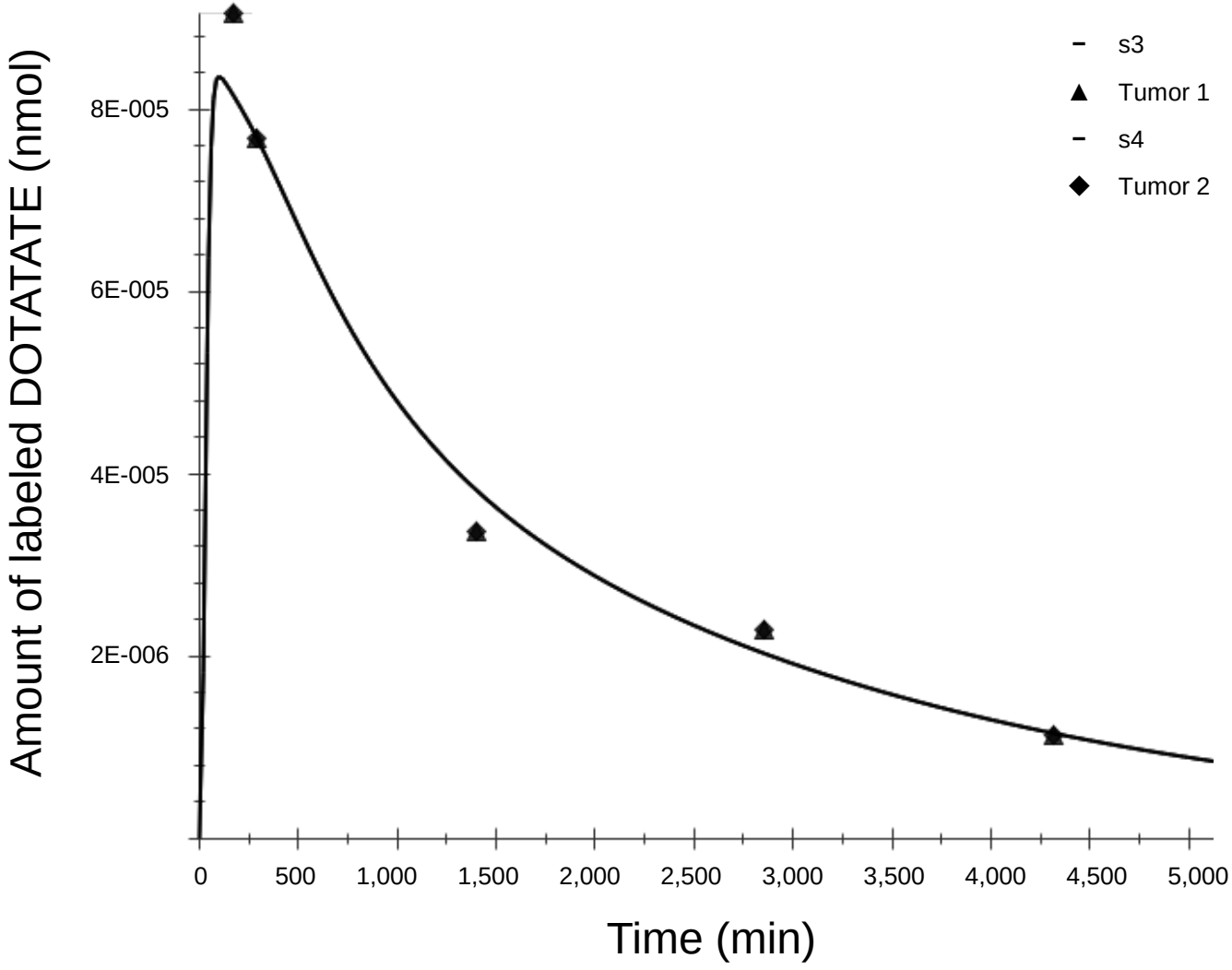
Amount of labeled DOTATATE (nmol)
8E-005
6E-005
4E-005
2E-006
0
500
1,000
1,500
2,000
2,500
3,000
3,500
4,000
4,500
5,000
Time (min)
s3
Tumor 1
s4
Tumor 2

8A

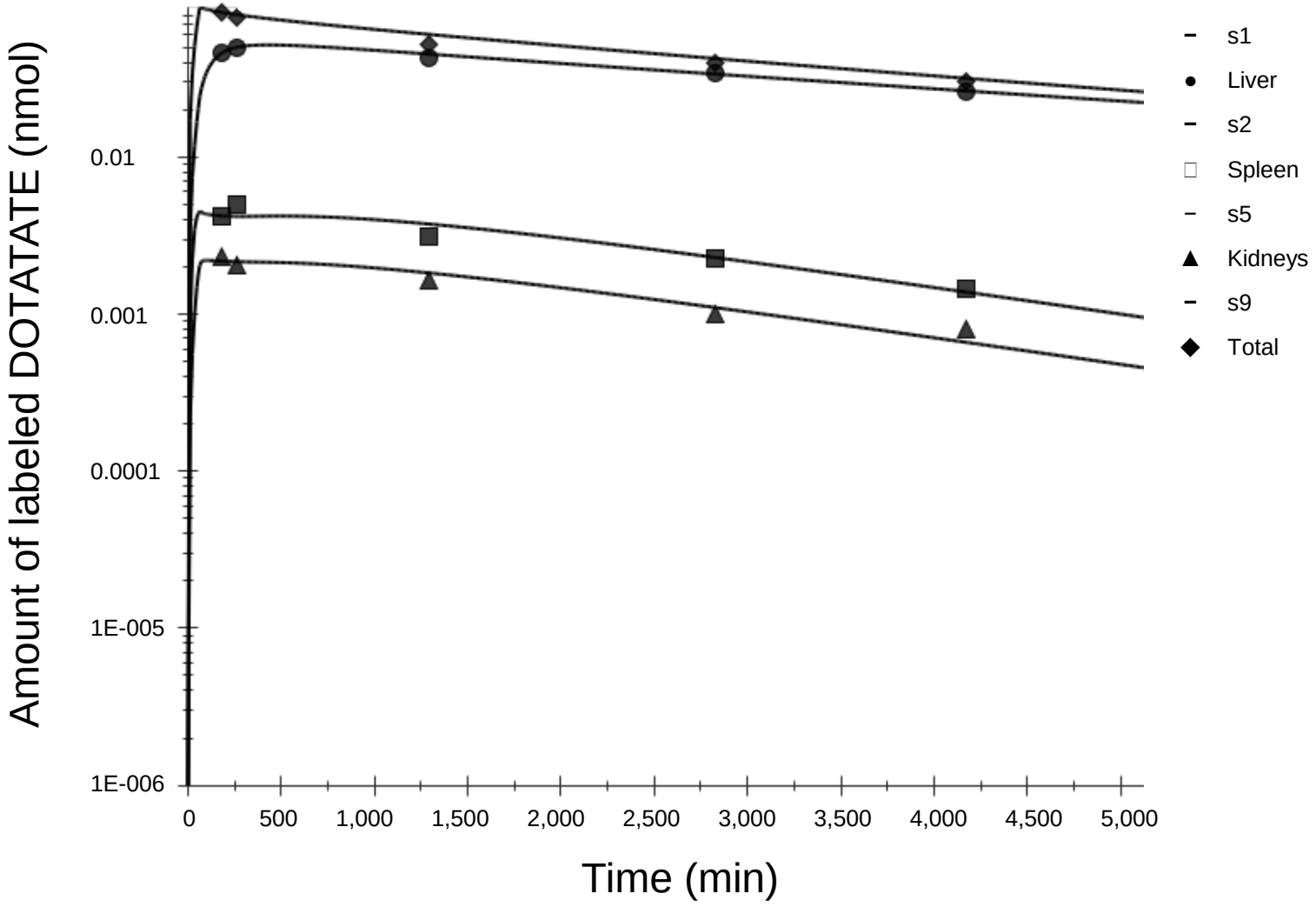
Amount of labeled DOTATATE (nmol)
0.01
0.001
0.0001
1E-005
1E-006
0
500
1,000
1,500
2,000
2,500
3,000
3,500
4,000
4,500
5,000
Time (min)
s1
Liver
s2
Spleen
s5
Kidneys
s9
Total

8B

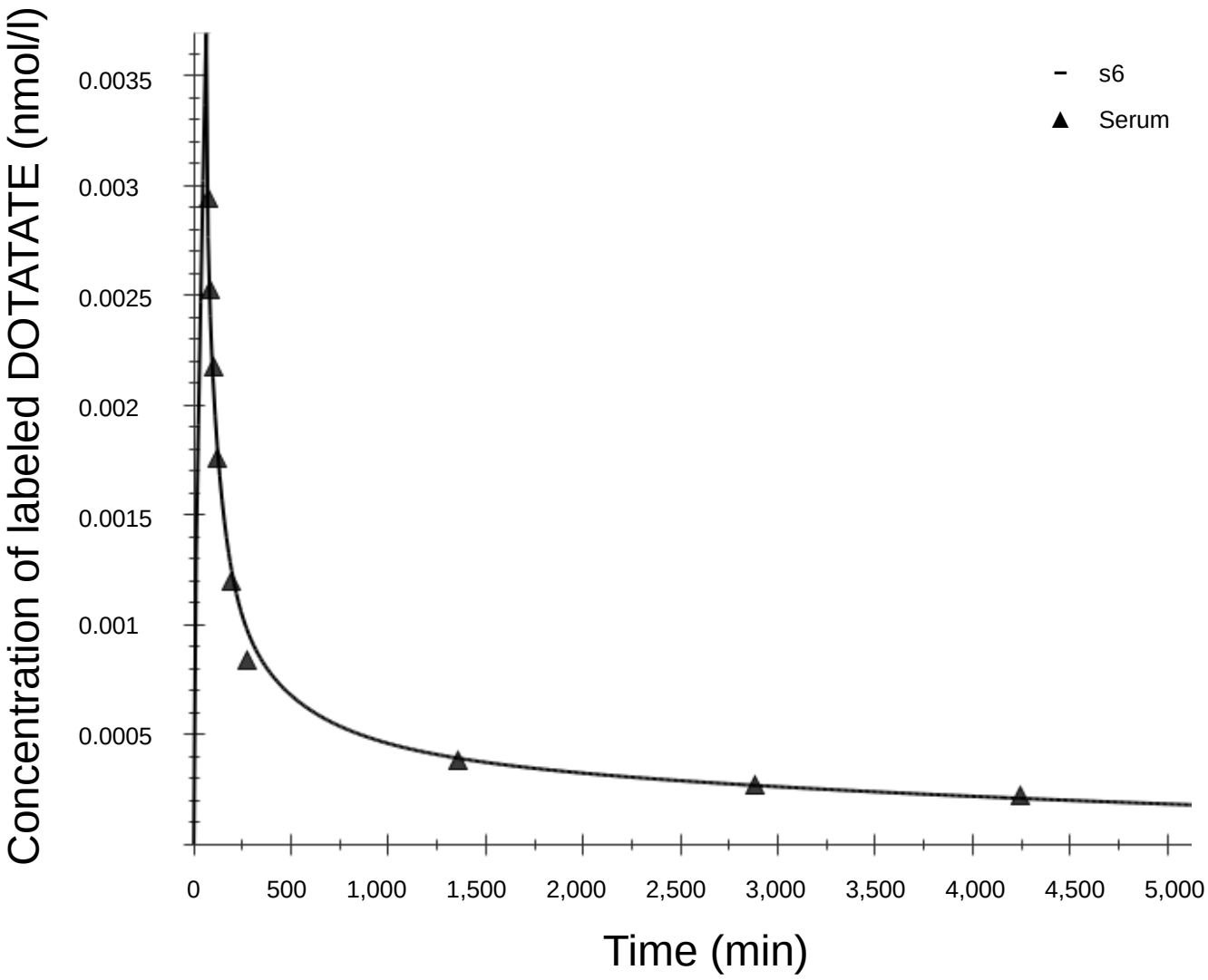
Concentration of labeled DOTATATE (nmol/l)
0.0035
0.003
0.0025
0.002
0.0015
0.001
0.0005
0
500
1,000
1,500
2,000
2,500
3,000
3,500
4,000
4,500
5,000
Time (min)
s6
Serum

8C

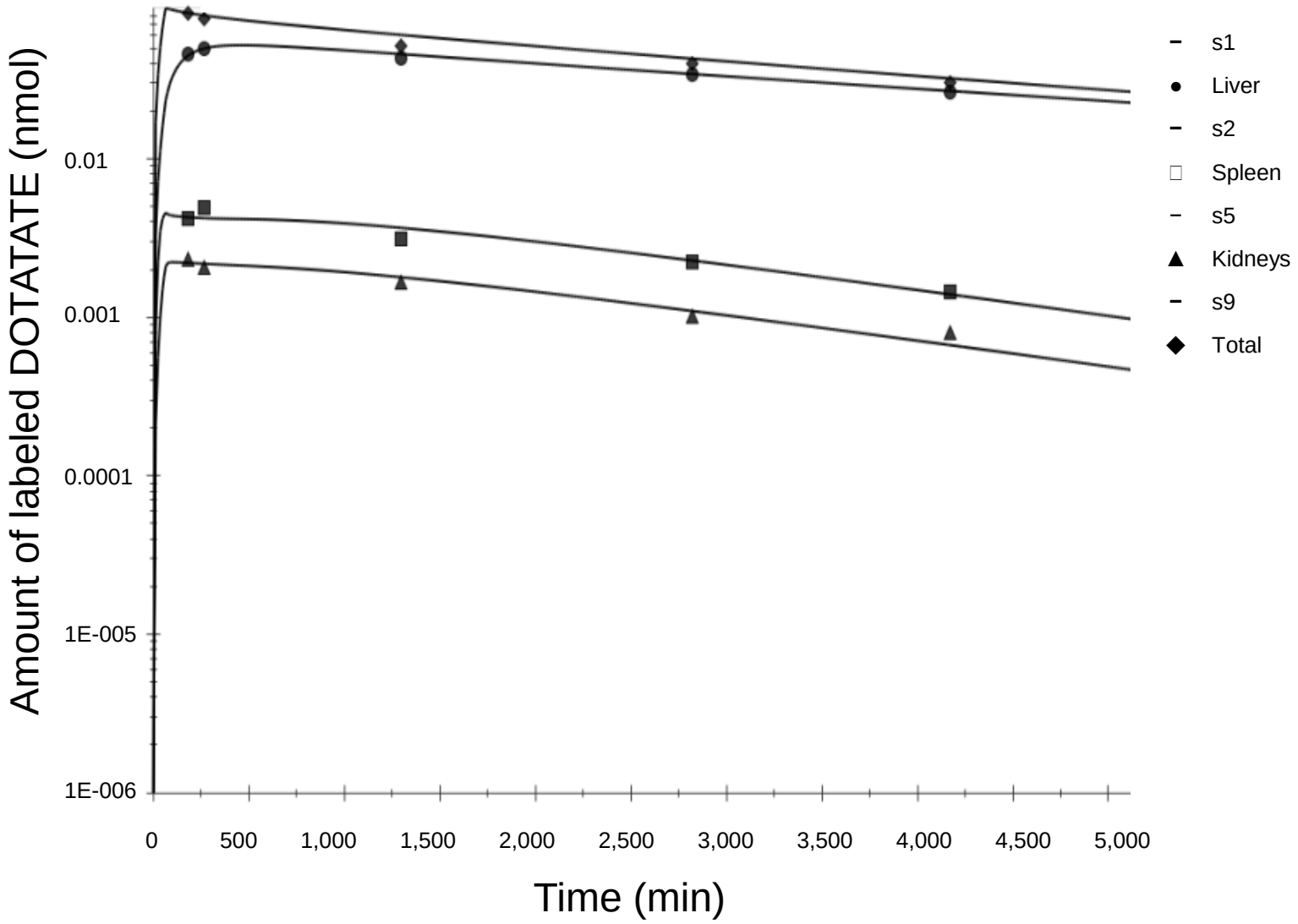
Amount of labeled DOTATATE (nmol)
0.01
0.001
0.0001
1E-005
1E-006
0
500
1,000
1,500
2,000
2,500
3,000
3,500
4,000
4,500
5,000
Time (min)
s1
Liver
s2
Spleen
s5
Kidneys
s9
Total

8D

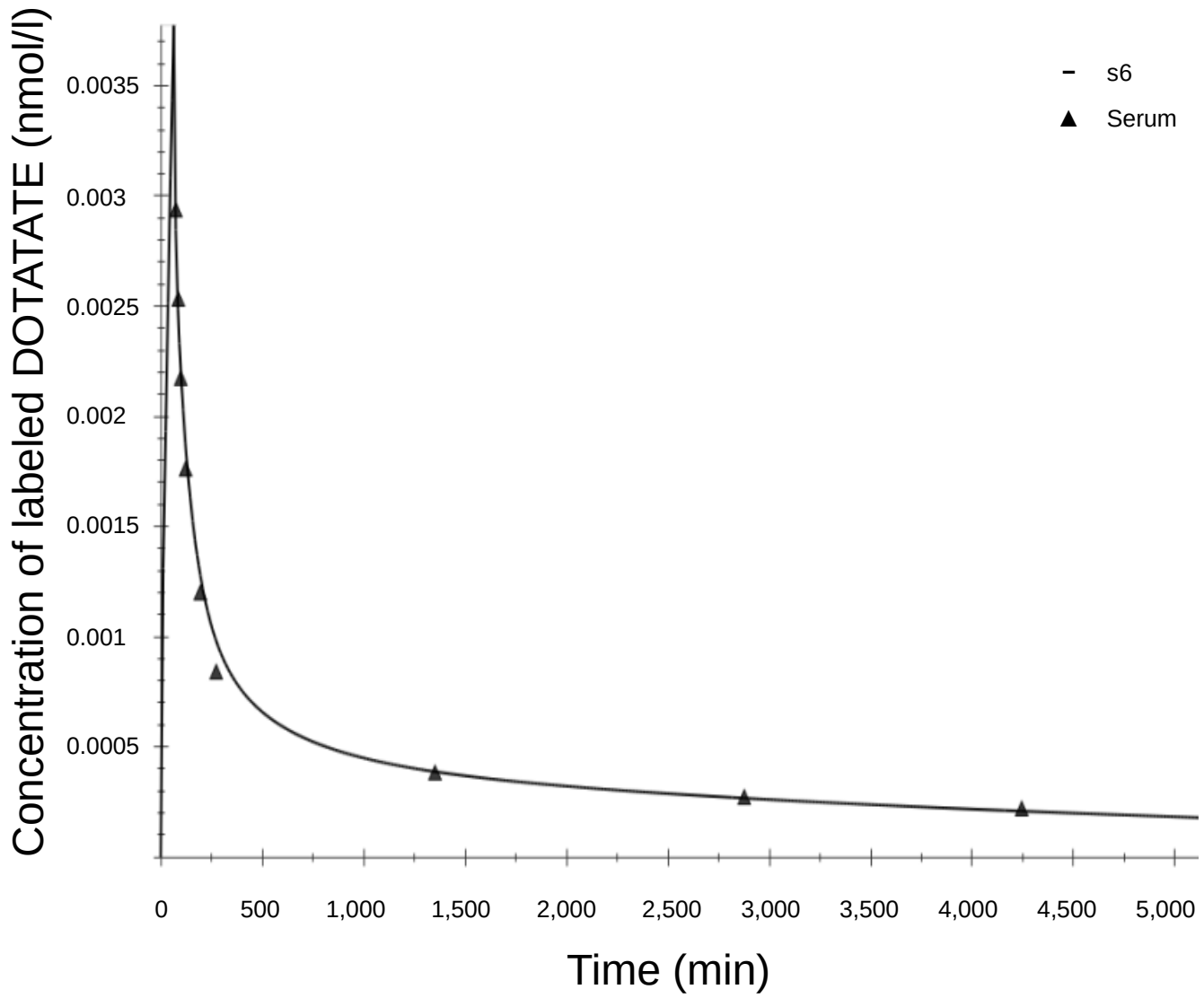
Concentration of labeled DOTATATE (nmol/l)
0.0035
0.003
0.0025
0.002
0.0015
0.001
0.0005
0
500
1,000
1,500
2,000
2,500
3,000
3,500
4,000
4,500
5,000
Time (min)
s6
Serum

9A

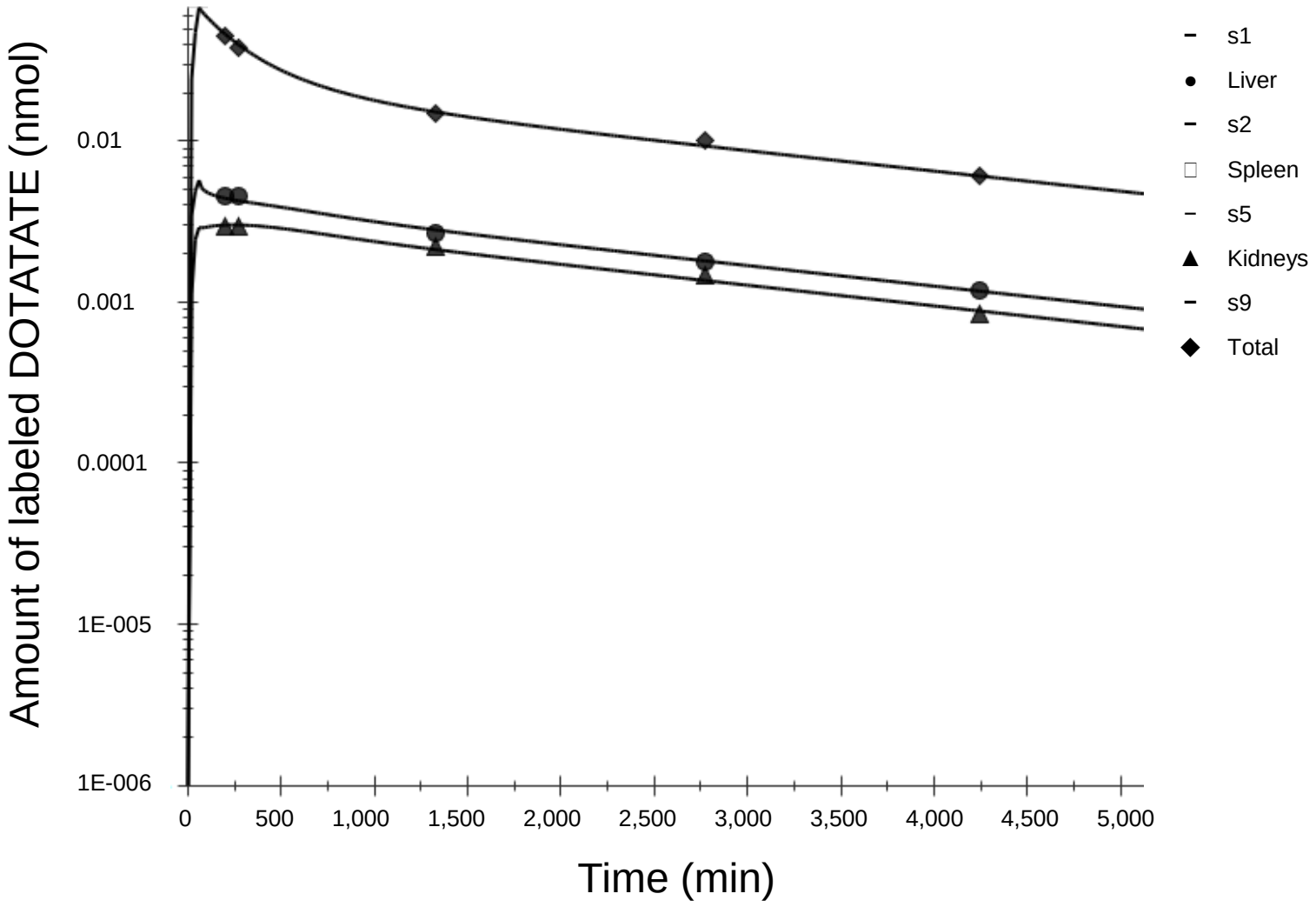
Amount of labeled DOTATATE (nmol)
0.01
0.001
0.0001
1E-005
1E-006
0
500
1,000
1,500
2,000
2,500
3,000
3,500
4,000
4,500
5,000
Time (min)
s1
Liver
s2
Spleen
s5
Kidneys
s9
Total

9B

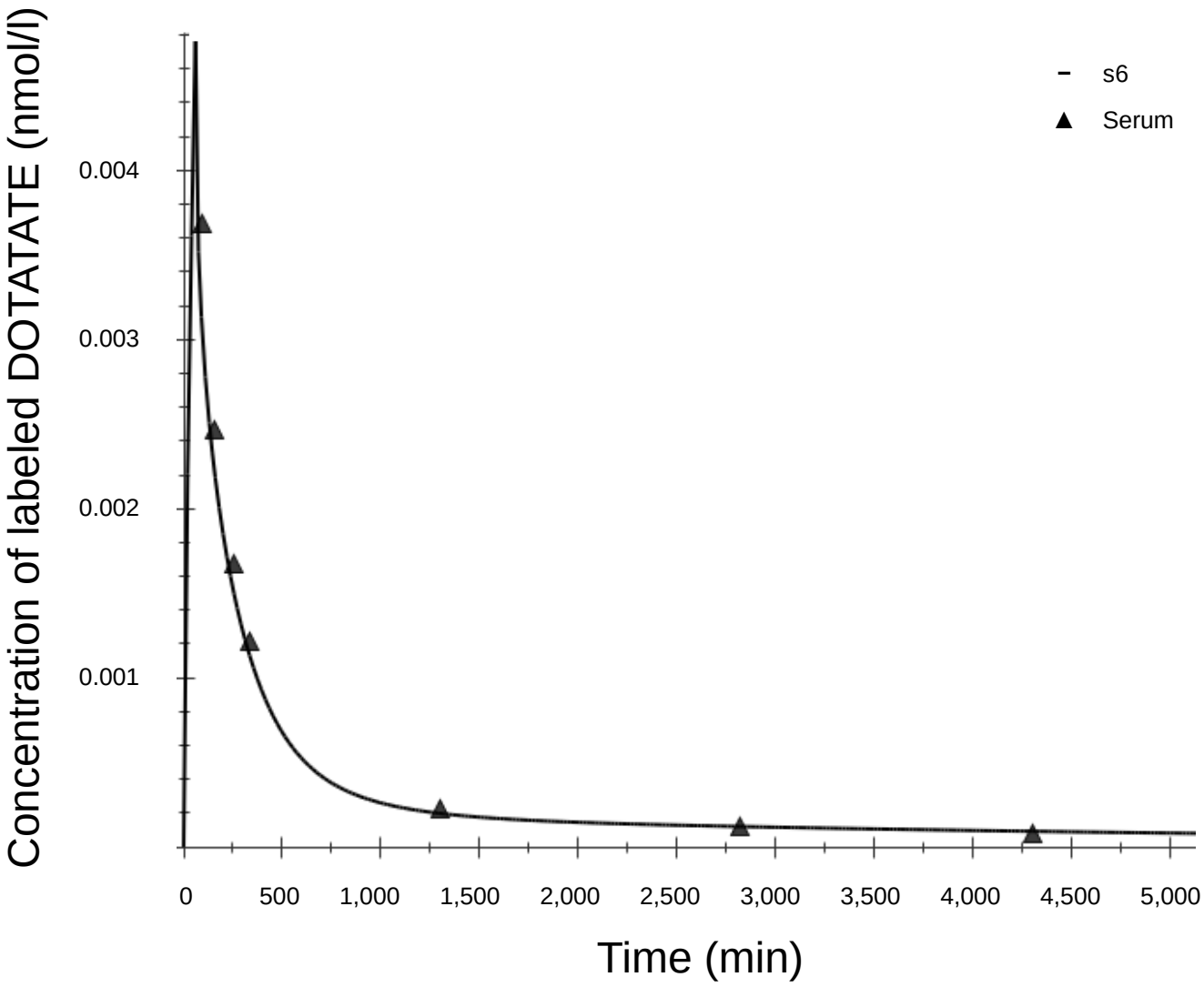
Concentration of labeled DOTATATE (nmol/l)
0.004
0.003
0.002
0.001
0
500
1,000
1,500
2,000
2,500
3,000
3,500
4,000
4,500
5,000
Time (min)
s6
Serum

9C

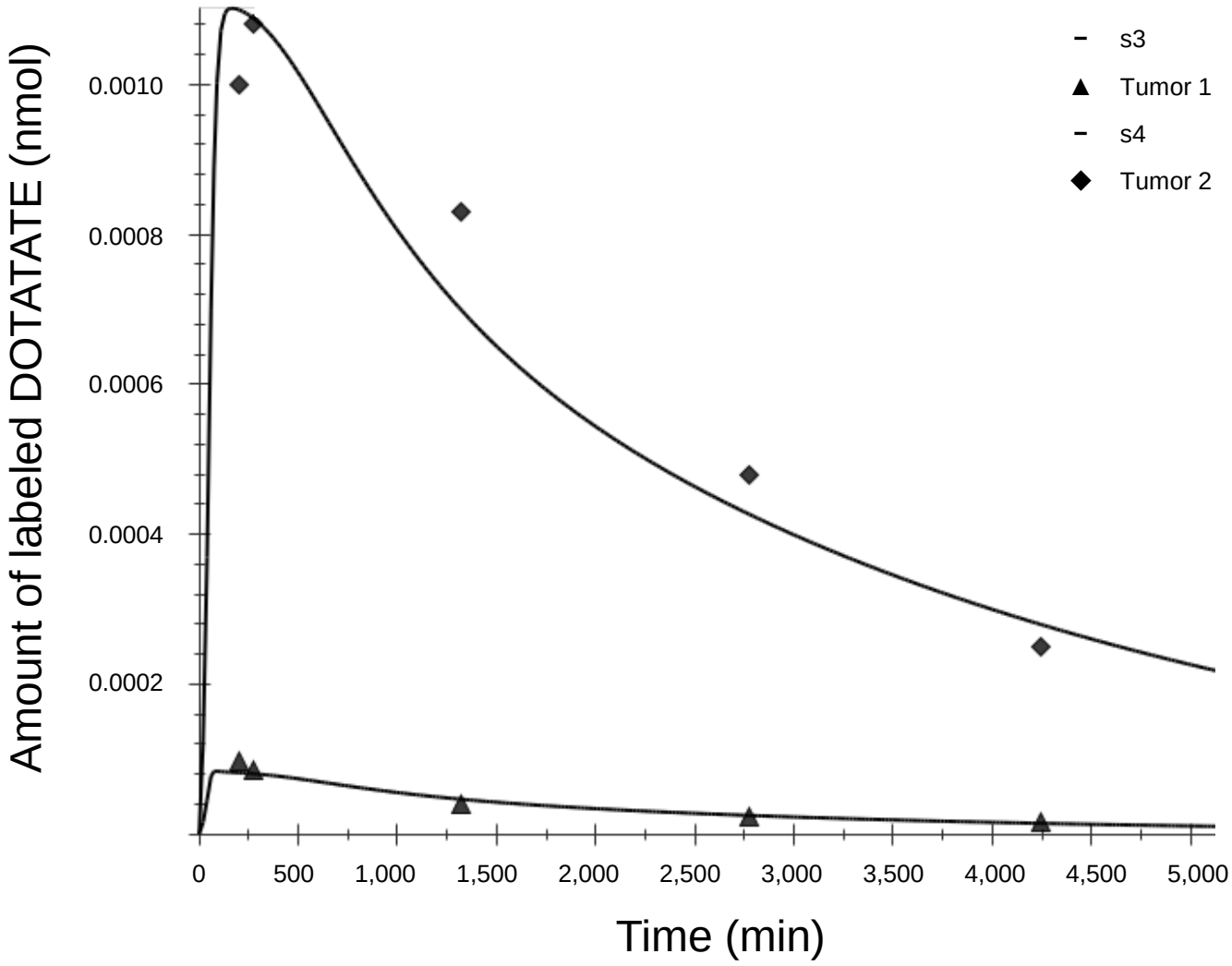
Amount of labeled DOTATATE (nmol)
0.0010
0.0008
0.0006
0.0004
0.0002
0
500
1,000
1,500
2,000
2,500
3,000
3,500
4,000
4,500
5,000
Time (min)
s3
Tumor 1
s4
Tumor 2

9D

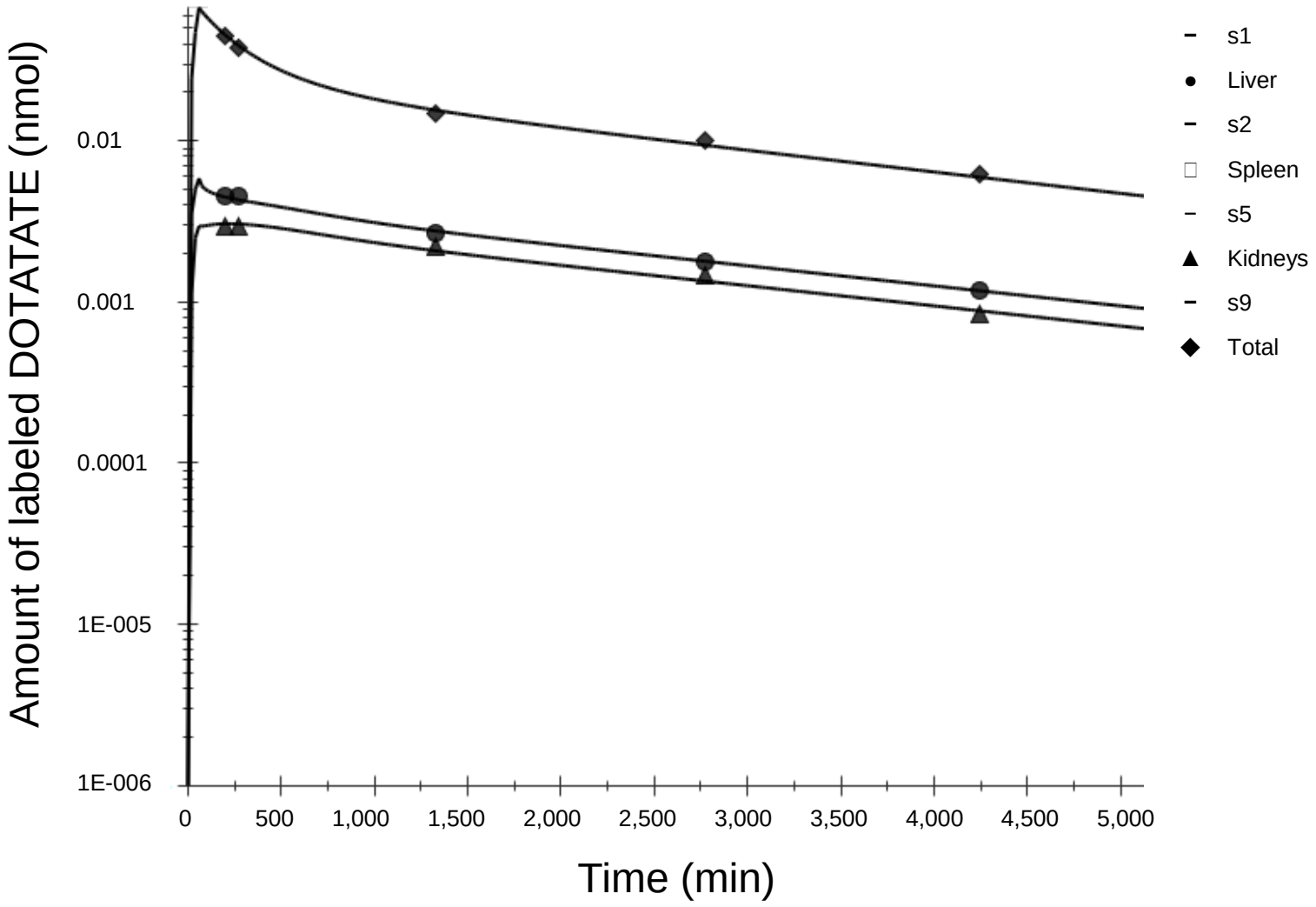
Amount of labeled DOTATATE (nmol)
0.01
0.001
0.0001
1E-005
1E-006
0
500
1,000
1,500
2,000
2,500
3,000
3,500
4,000
4,500
5,000
Time (min)
s1
Liver
s2
Spleen
s5
Kidneys
s9
Total

9E

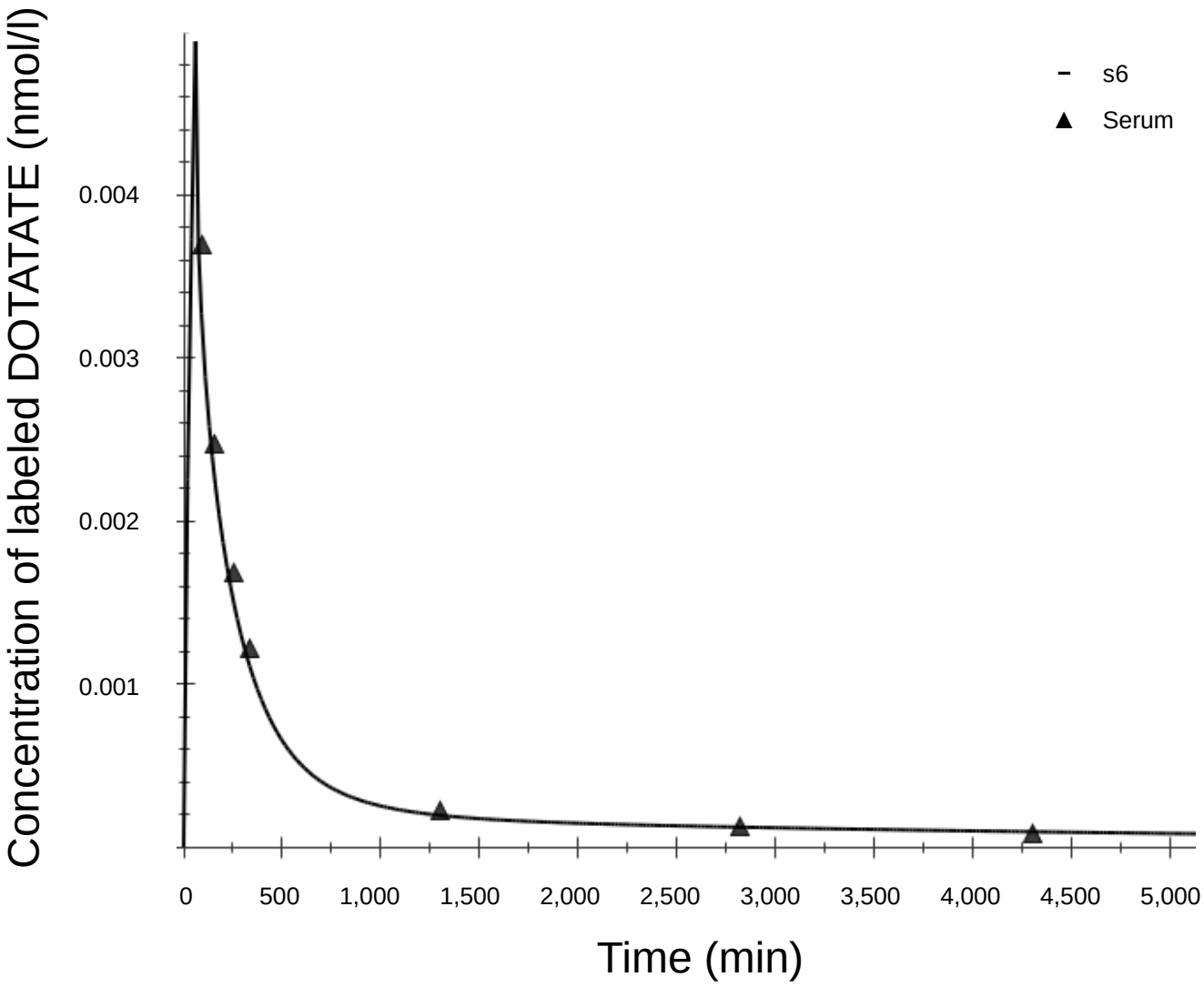
Concentration of labeled DOTATATE (nmol/l)
0.004
0.003
0.002
0.001
0
500
1,000
1,500
2,000
2,500
3,000
3,500
4,000
4,500
5,000
Time (min)
s6
Serum

9F

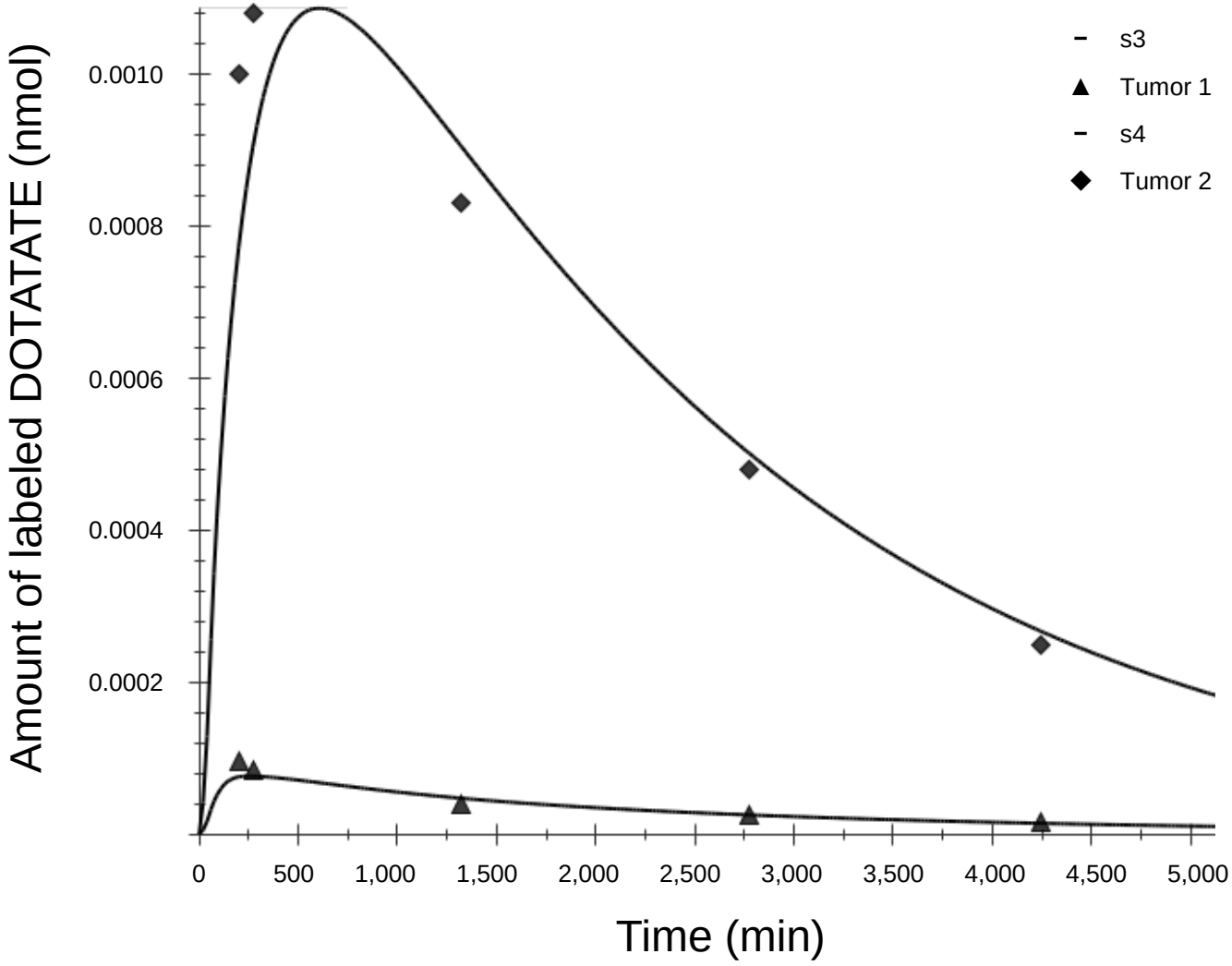
Amount of labeled DOTATATE (nmol)
0.0010
0.0008
0.0006
0.0004
0.0002
0
500
1,000
1,500
2,000
2,500
3,000
3,500
4,000
4,500
5,000
Time (min)
s3
Tumor 1
s4
Tumor 2

10A

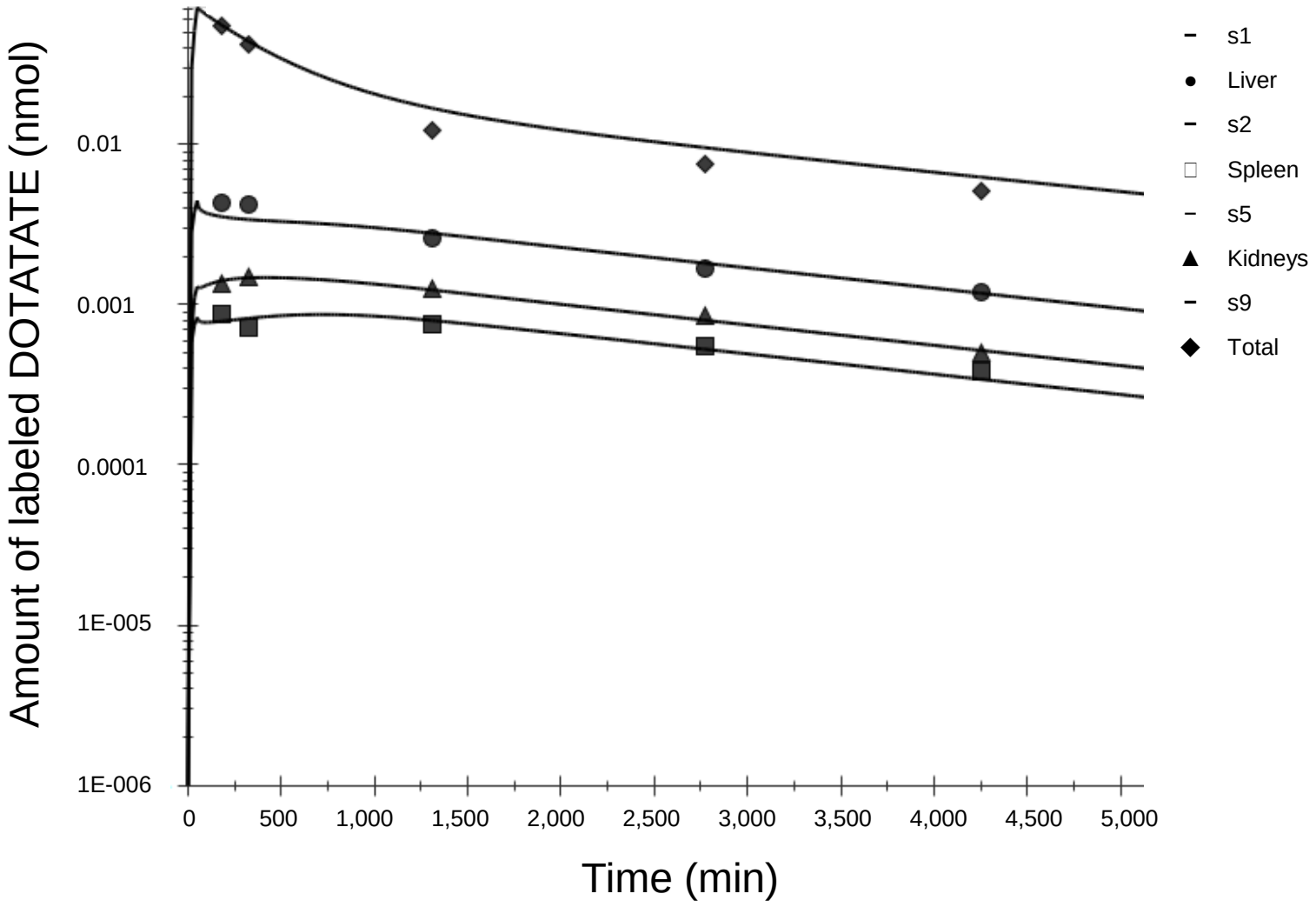
Amount of labeled DOTATATE (nmol)
0.01
0.001
0.0001
1E-005
1E-006
0
500
1,000
1,500
2,000
2,500
3,000
3,500
4,000
4,500
5,000
Time (min)
s1
Liver
s2
Spleen
s5
Kidneys
s9
Total

10B

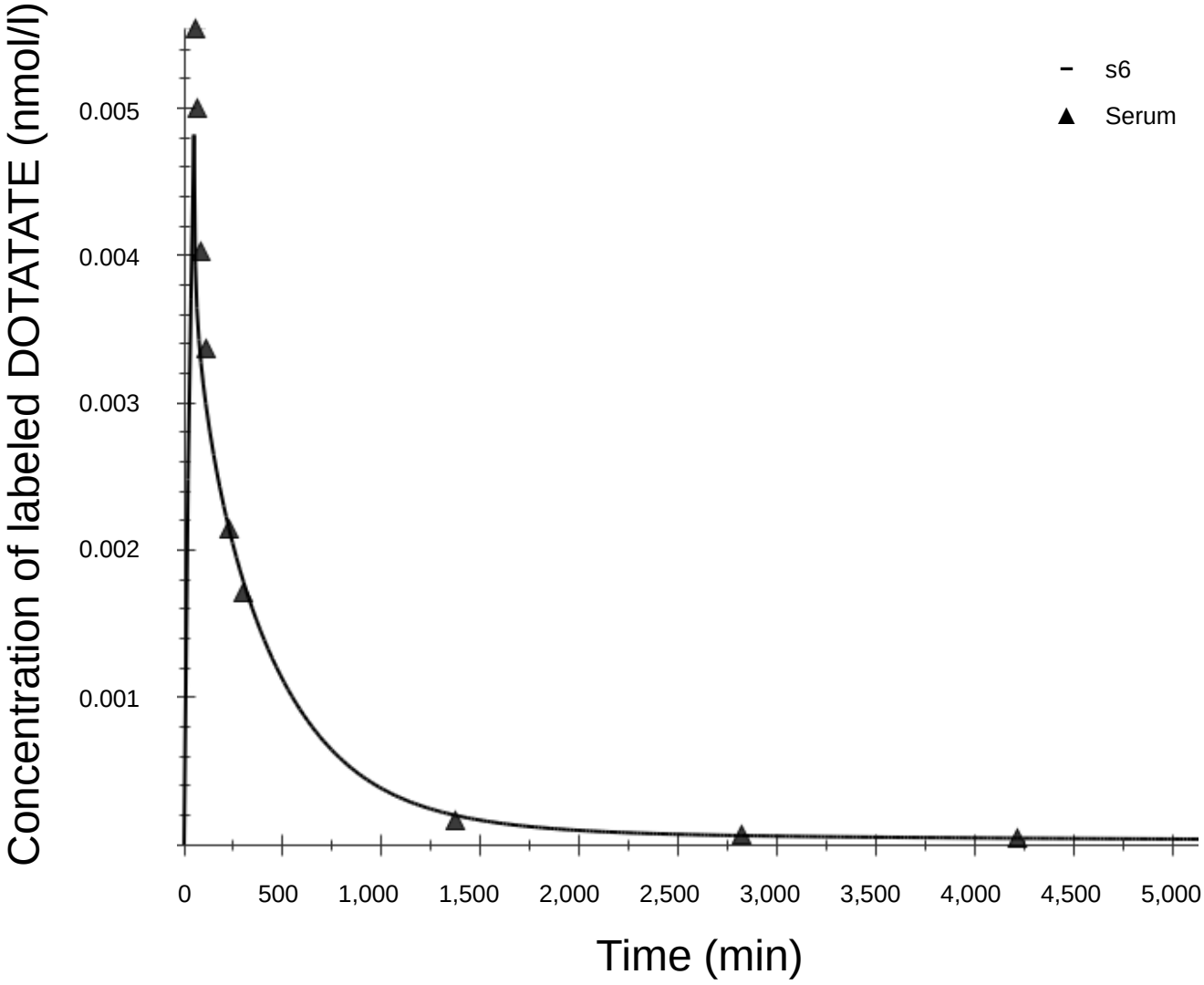
Concentration of labeled DOTATATE (nmol/l)
0.005
0.004
0.003
0.002
0.001
0
500
1,000
1,500
2,000
2,500
3,000
3,500
4,000
4,500
5,000
Time (min)
s6
Serum

10C

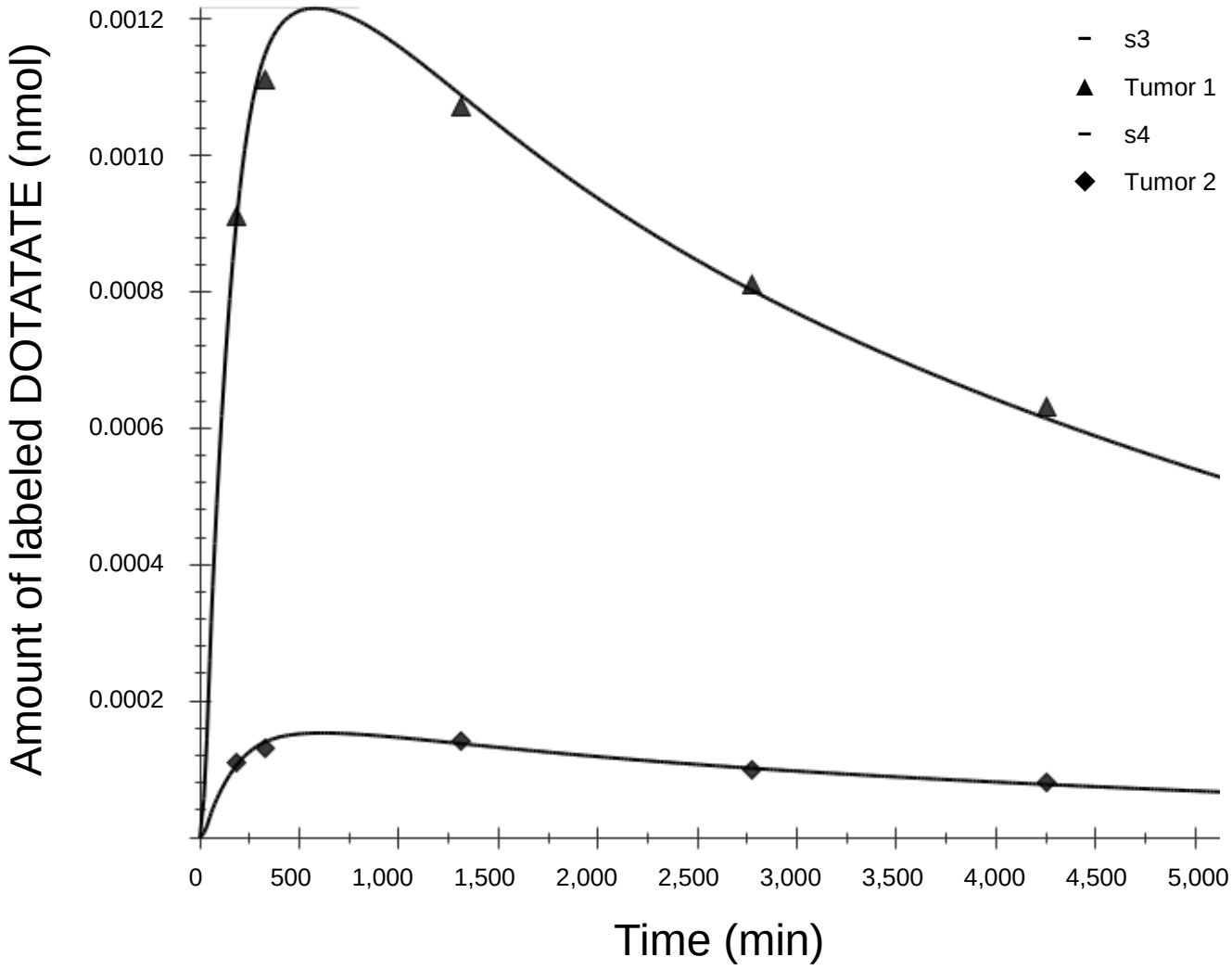
Amount of labeled DOTATATE (nmol)
0.0012
0.0010
0.0008
0.0006
0.0004
0.0002
0
500
1,000
1,500
2,000
2,500
3,000
3,500
4,000
4,500
5,000
Time (min)
s3
Tumor 1
s4
Tumor 2

11A

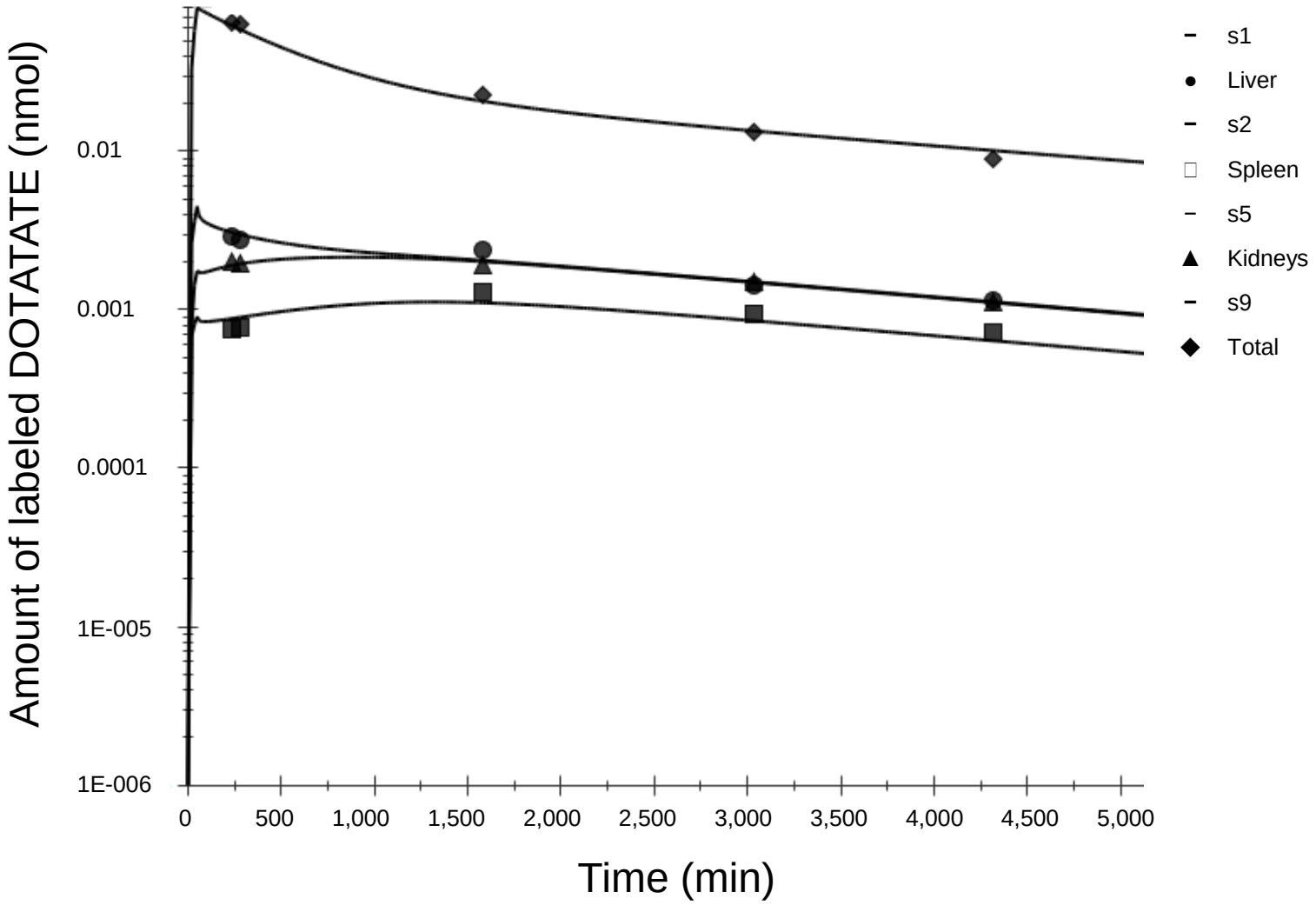
Amount of labeled DOTATATE (nmol)
0.01
0.001
0.0001
1E-005
1E-006
0
500
1,000
1,500
2,000
2,500
3,000
3,500
4,000
4,500
5,000
Time (min)
s1
Liver
s2
Spleen
s5
Kidneys
s9
Total

11B

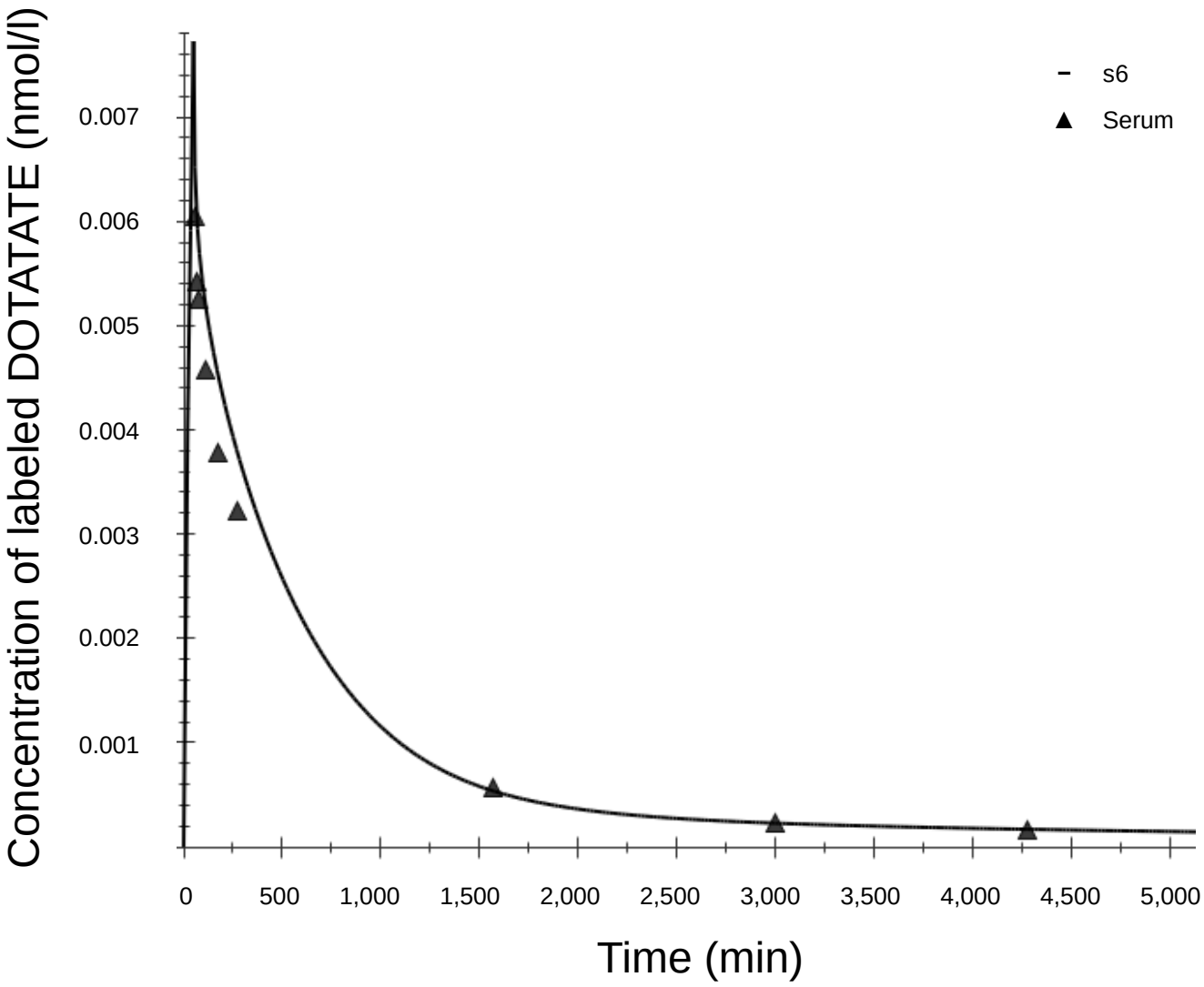
Concentration of labeled DOTATATE (nmol/l)
0.007
0.006
0.005
0.004
0.003
0.002
0.001
0
500
1,000
1,500
2,000
2,500
3,000
3,500
4,000
4,500
5,000
Time (min)
s6
Serum

11C

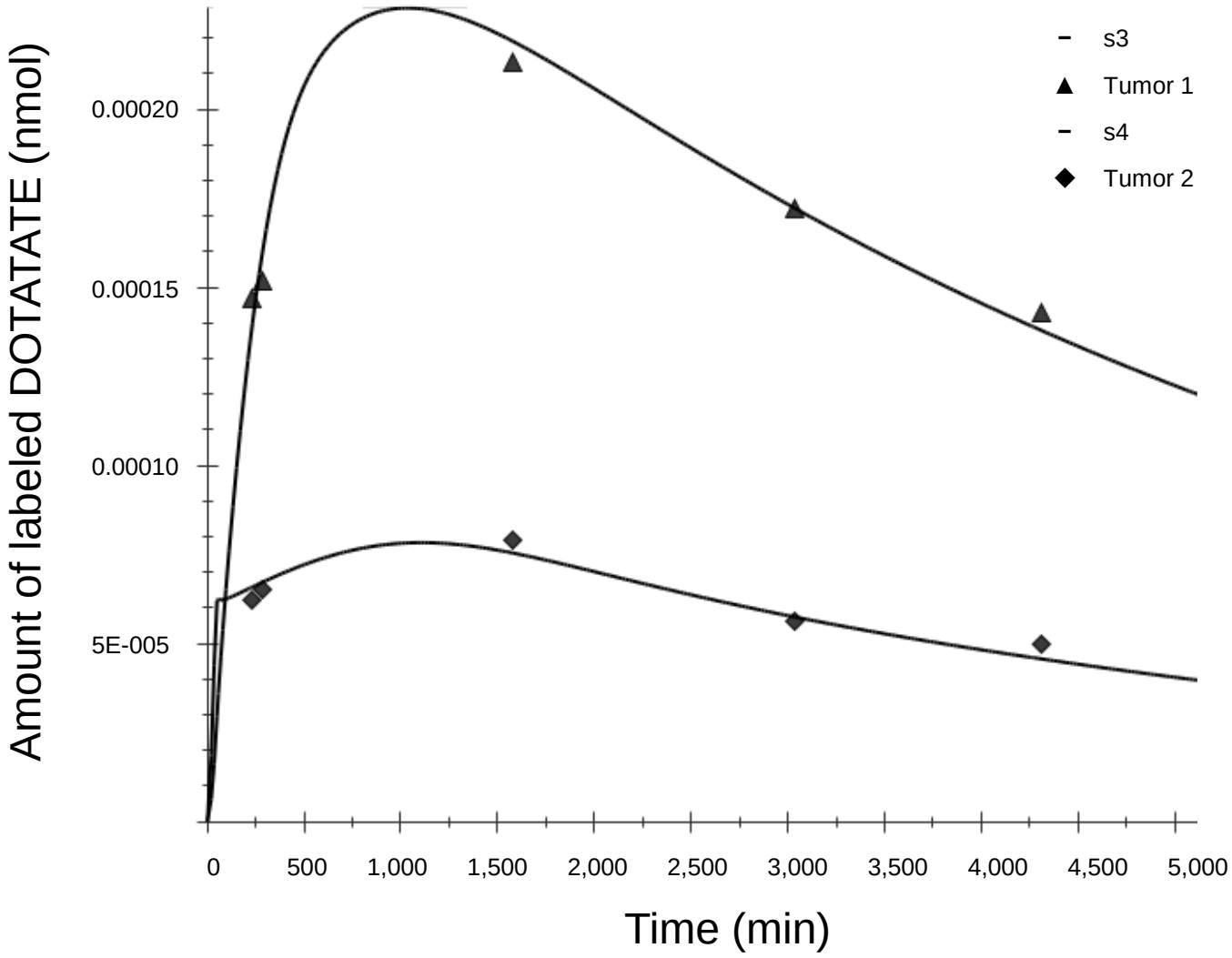
Amount of labeled DOTATATE (nmol)
0.00020
0.00015
0.00010
5E-005
0
500
1,000
1,500
2,000
2,500
3,000
3,500
4,000
4,500
5,000
Time (min)
s3
Tumor 1
s4
Tumor 2

12A

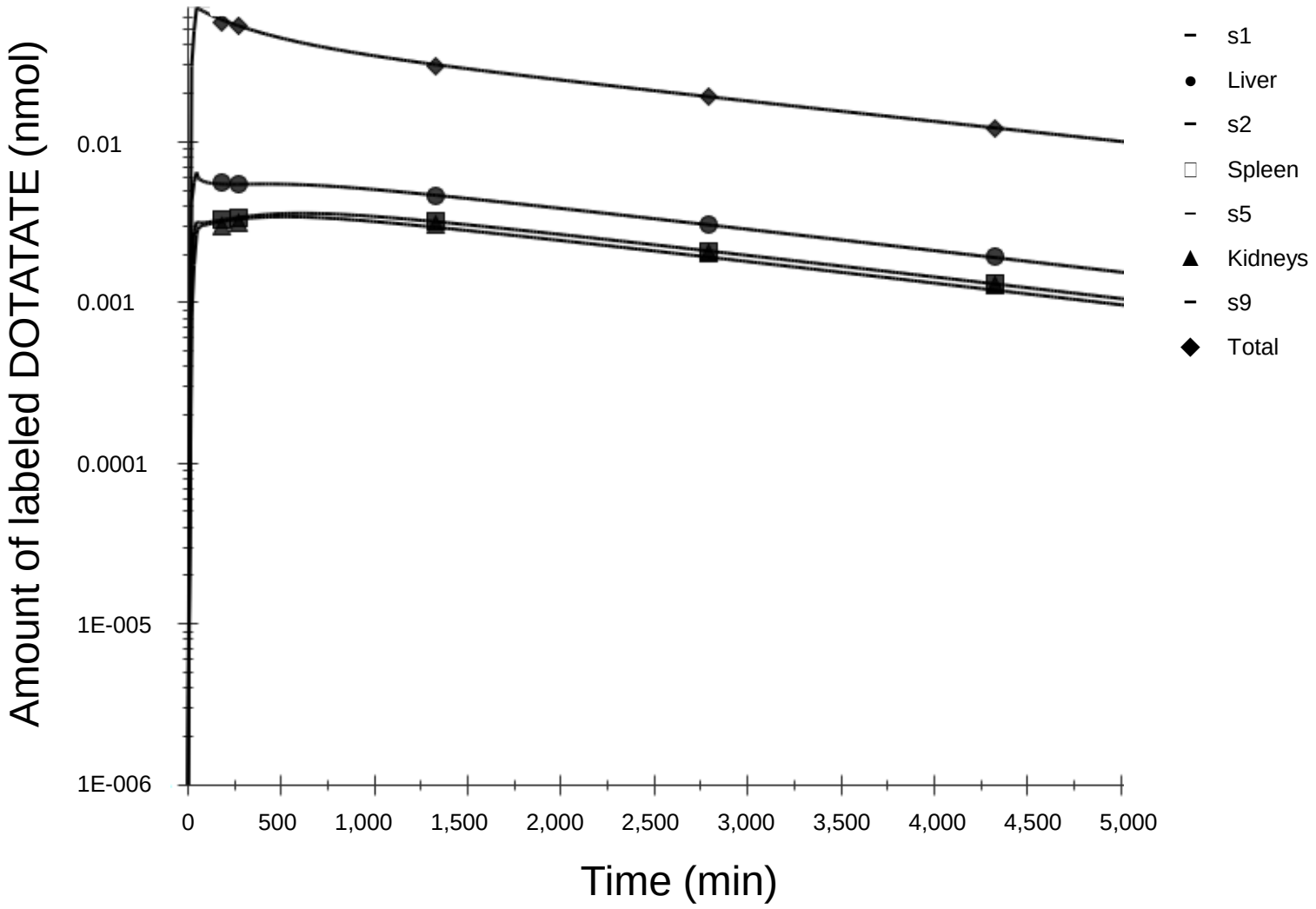
Amount of labeled DOTATATE (nmol)
0.01
0.001
0.0001
1E-005
1E-006
0
500
1,000
1,500
2,000
2,500
3,000
3,500
4,000
4,500
5,000
Time (min)
s1
Liver
s2
Spleen
s5
Kidneys
s9
Total

12B

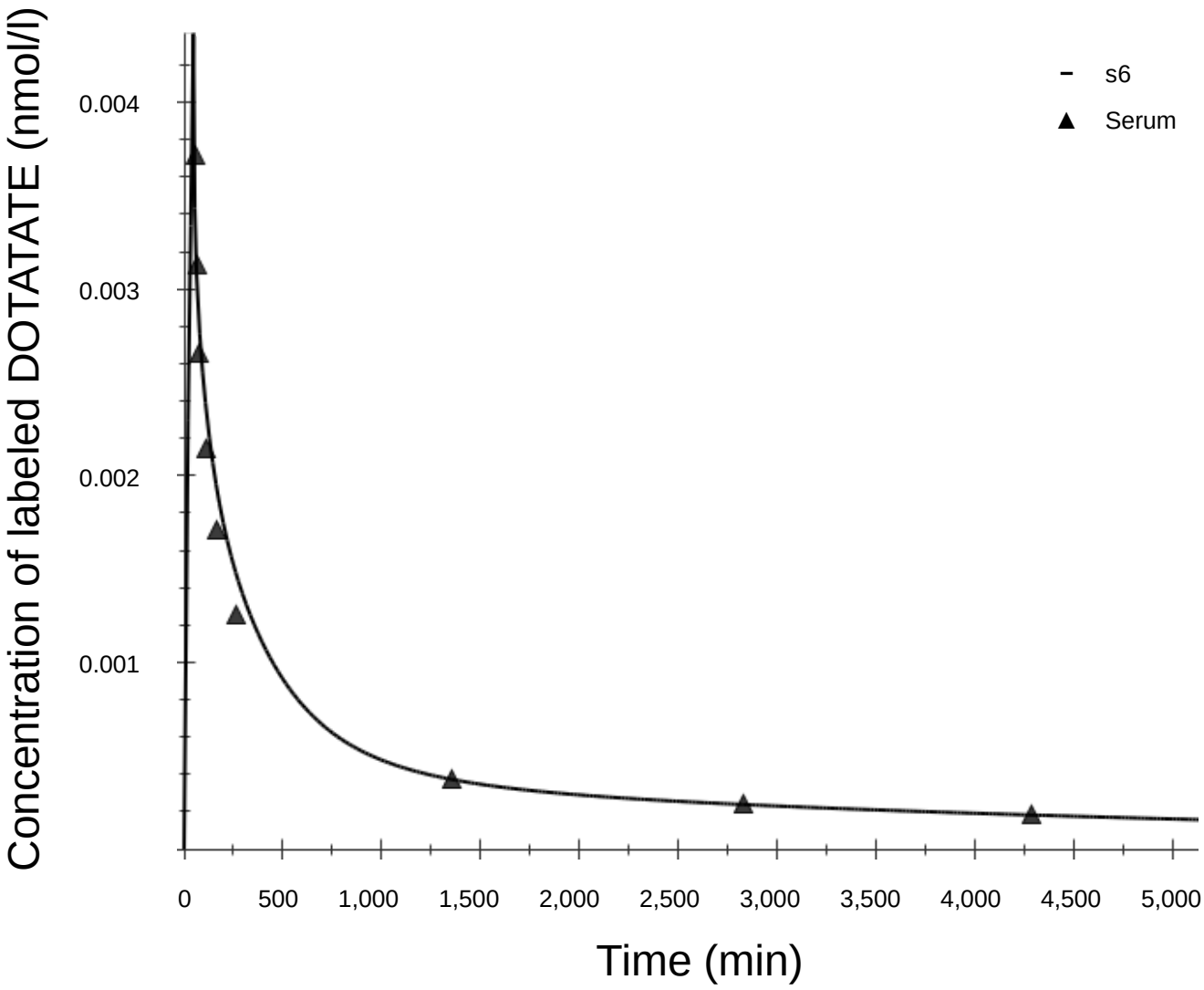
Concentration of labeled DOTATATE (nmol/l)
0.004
0.003
0.002
0.001
0
500
1,000
1,500
2,000
2,500
3,000
3,500
4,000
4,500
5,000
Time (min)
s6
Serum

12C

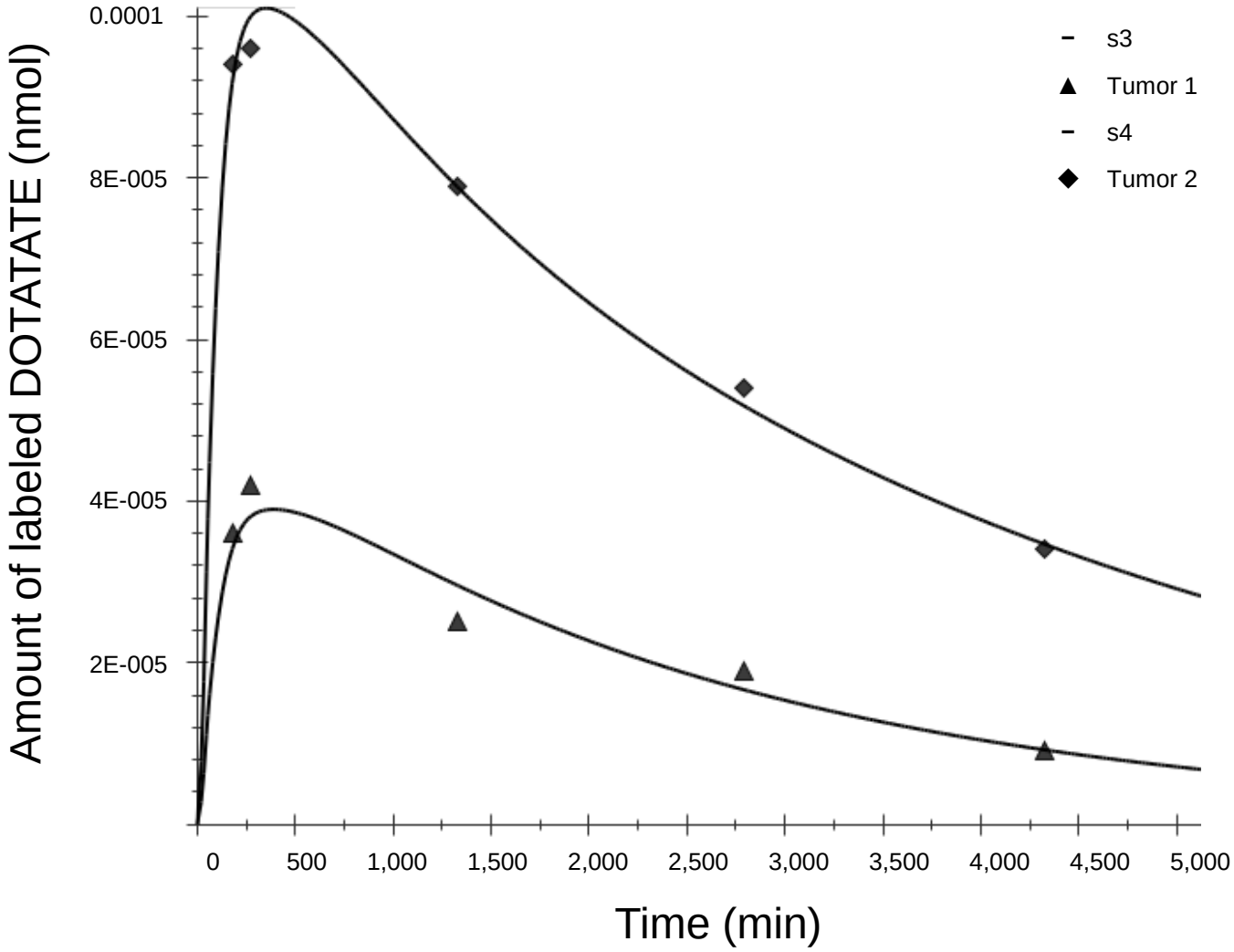
Amount of labeled DOTATATE (nmol)
0.0001
8E-005
6E-005
4E-005
2E-005
0
500
1,000
1,500
2,000
2,500
3,000
3,500
4,000
4,500
5,000
Time (min)
s3
Tumor 1
s4
Tumor 2

Supplemental Data

Optimal BED ratio simulations for N1-N12 (Figures 1-12)

Figure 1

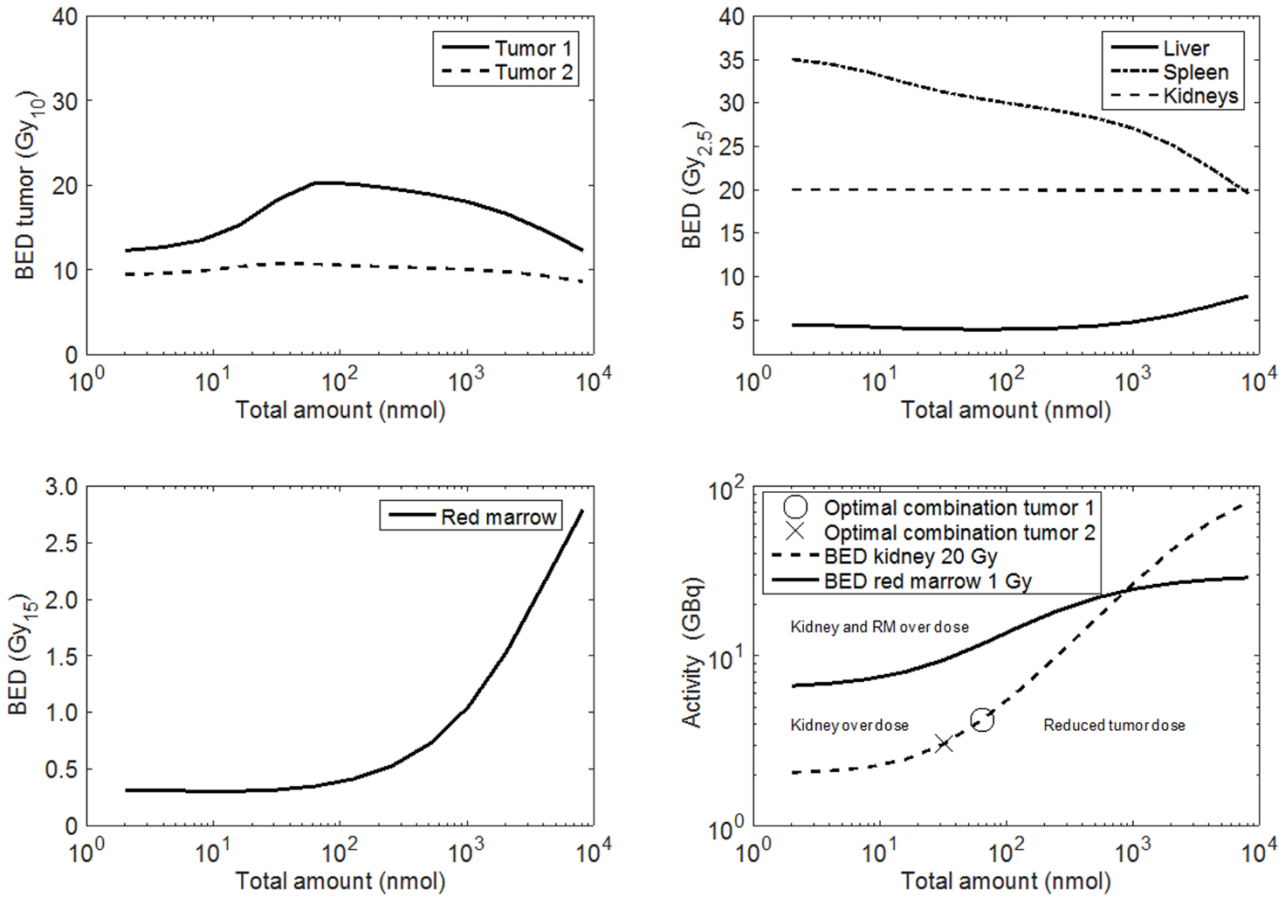
Tumor 1
Tumor 2
BED tumor (Gy10)
Total amount (nmol)
Liver
Spleen
Kidneys
BED (Gy2.5)
Total amount (nmol)
Red marrow
BED (Gy15)
Total amount (nmol)
Optimal combination tumor 1
Optimal combination tumor 2
BED kidney 20 Gy
BED red marrow 1 Gy
Kidney and RM over dose
Kidney over dose
Reduced tumor dose
Activity (GBq)
Total amount (nmol)

Figure 2

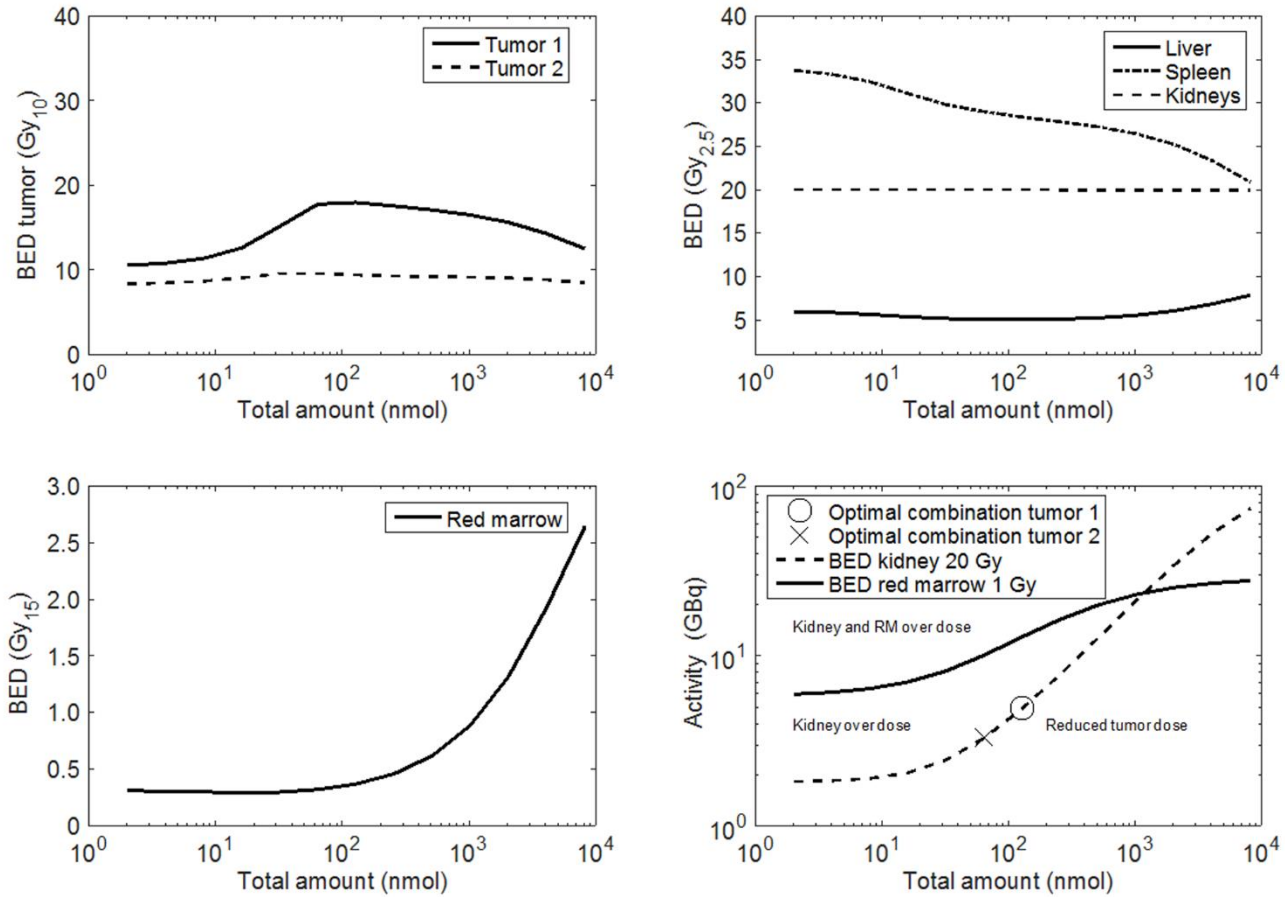
Tumor 1
Tumor 2
BED tumor (Gy10)
Total amount (nmol)
Liver
Spleen
Kidneys
BED (Gy2.5)
Total amount (nmol)
Red marrow
BED (Gy15)
Total amount (nmol)
Optimal combination tumor 1
Optimal combination tumor 2
BED kidney 20 Gy
BED red marrow 1 Gy
Kidney and RM over dose
Kidney overdose
Reduced tumor dose
Activity (GBq)
Total amount (nmol)

Figure 3

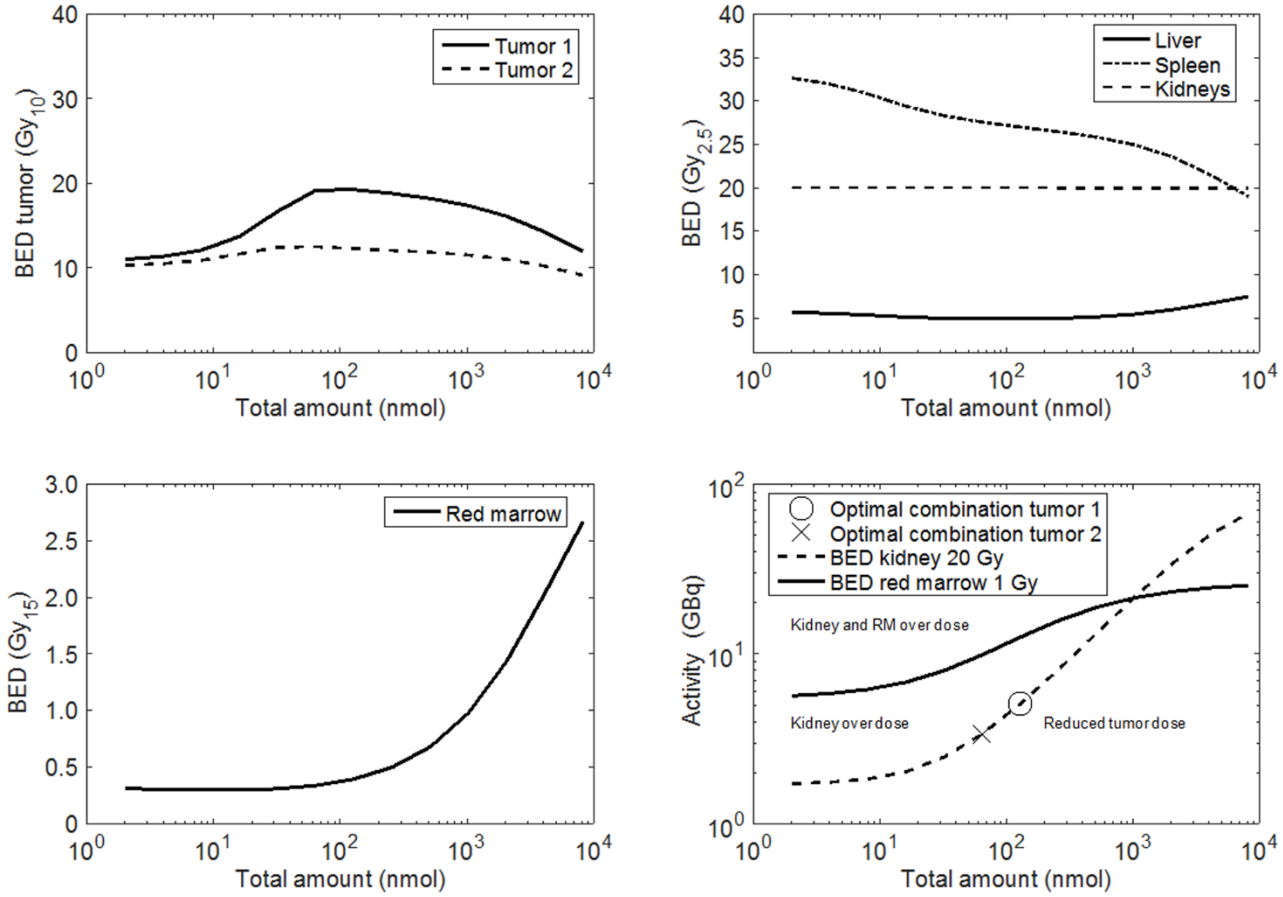
Tumor 1
Tumor 2
BED tumor (Gy10)
Total amount (nmol)
Liver
Spleen
Kidneys
BED (Gy2.5)
Total amount (nmol)
Red marrow
BED (Gy15)
Total amount (nmol)
Optimal combination tumor 1
Optimal combination tumor 2
BED kidney 20 Gy
BED red marrow 1 Gy
Kidney and RM over dose
Kidney over dose
Reduced tumor dose
Activity (GBq)
Total amount (nmol)

Figure 4

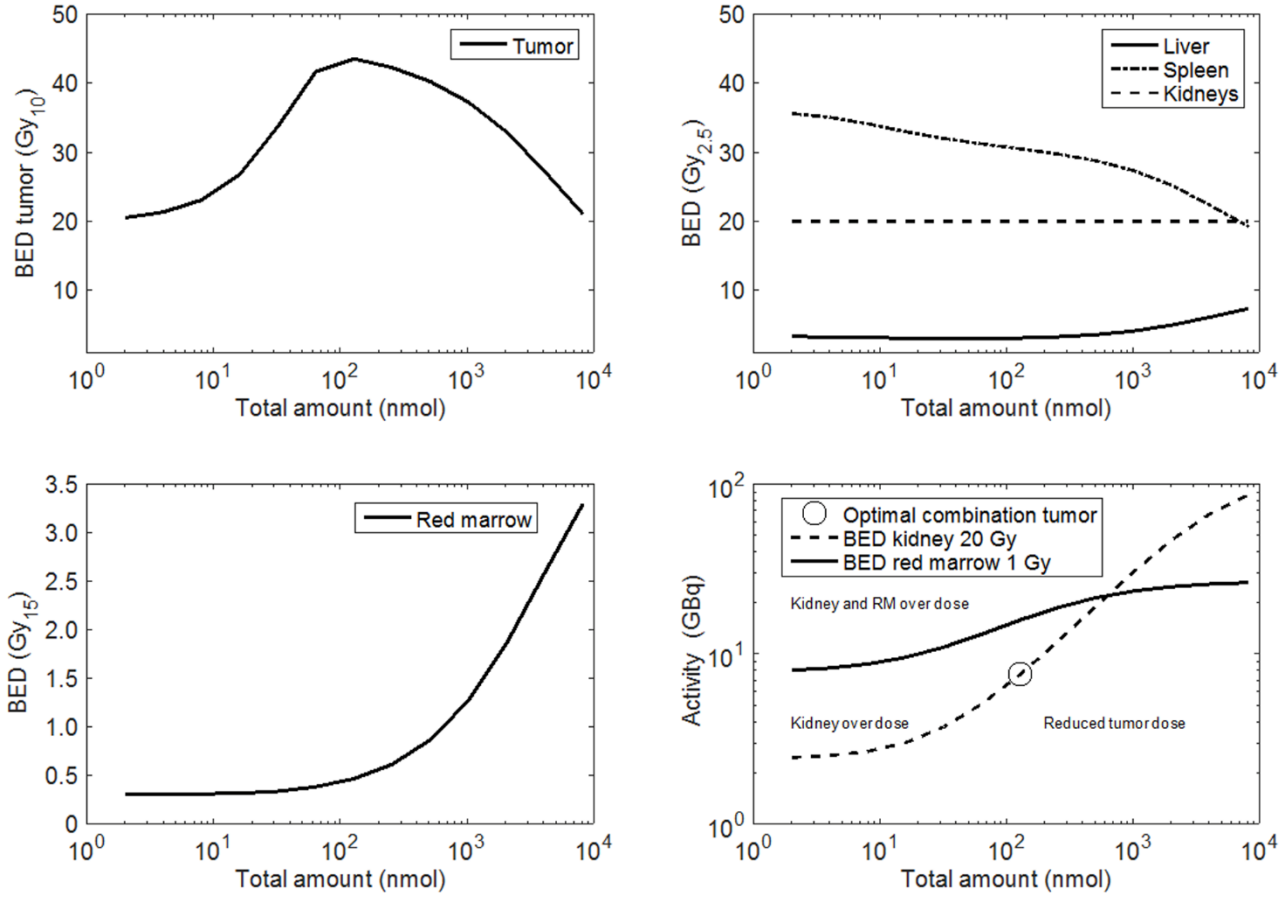
Tumor
BED tumor (Gy10)
Total amount (nmol)
Liver
Spleen
Kidneys
BED (Gy2.5)
Total amount (nmol)
Red marrow
BED (Gy15)
Total amount (nmol)
Optimal combination tumor
BED kidney 20 Gy
BED red marrow 1 Gy
Kidney and RM overdose
Kidney overdose
Reduced tumor dose
Activity (GBq)
Total amount (nmol)

Figure 5

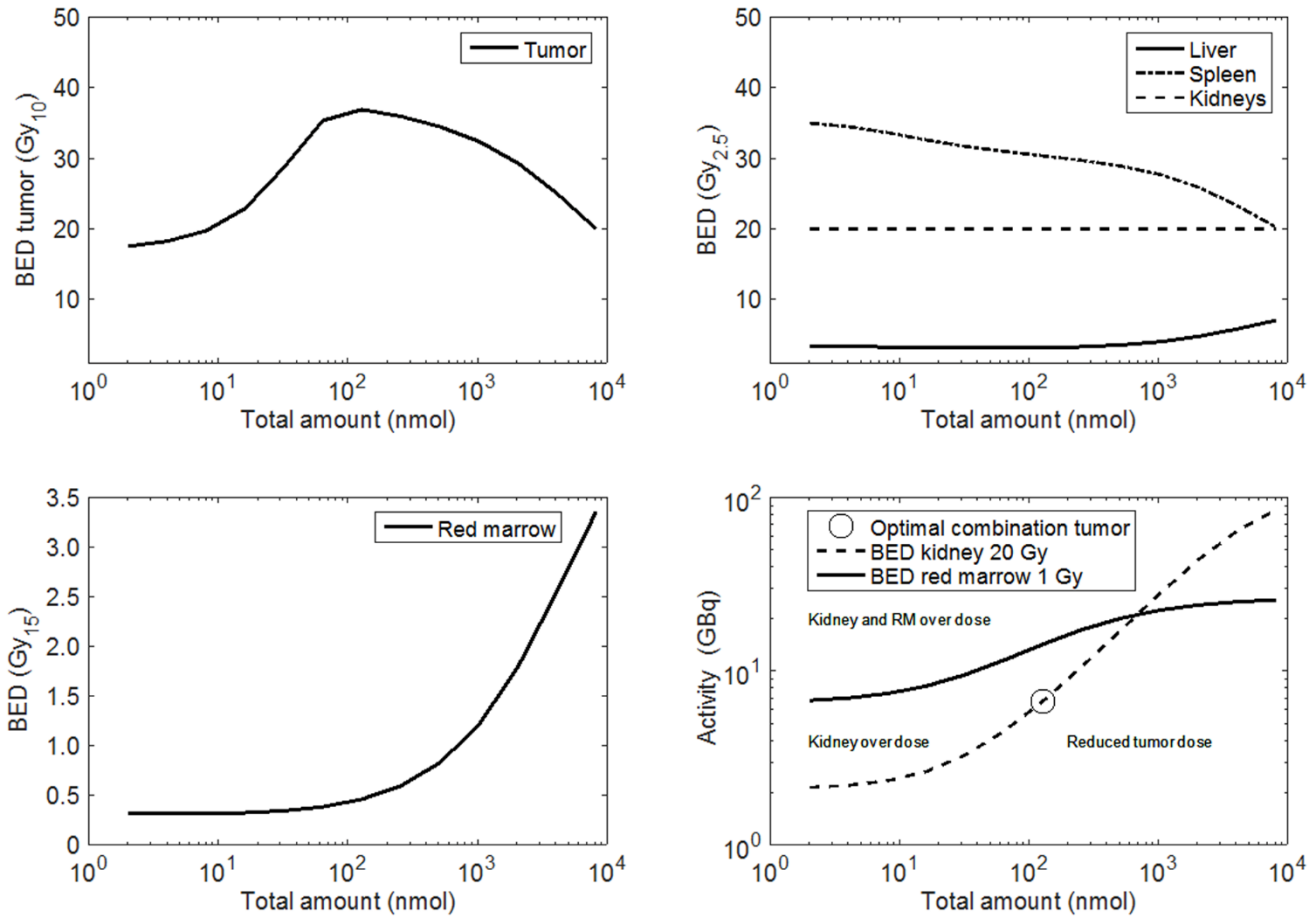
Tumor
BED tumor (Gy10)
Total amount (nmol)
Liver
Spleen
Kidneys
BED (Gy2.5)
Total amount (nmol)
Red marrow
BED (Gy15)
Total amount (nmol)
Optimal combination tumor
BED kidney 20 Gy
BED red marrow 1 Gy
Kidney and RM over dose
Kidney over dose
Reduced tumor dose
Activity (GBq)
Total amount (nmol)

Figure 6

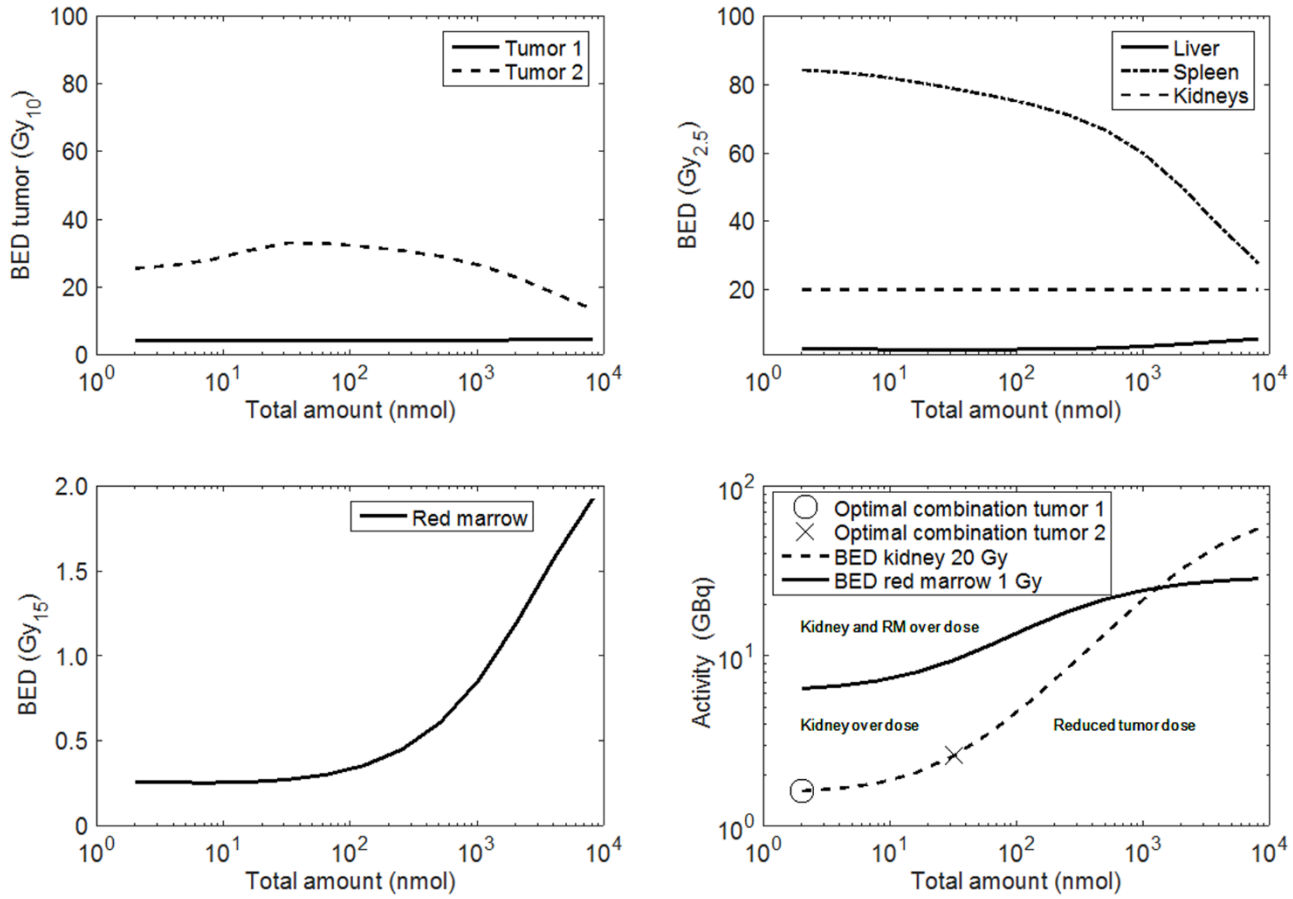
Tumor 1
Tumor 2
BED tumor (Gy10)
Total amount (nmol)
Liver
Spleen
Kidneys
BED (Gy2.5)
Total amount (nmol)
Red marrow
BED (Gy15)
Total amount (nmol)
Optimal combination tumor 1
Optimal combination tumor 2
BED kidney 20 Gy
BED red marrow 1 Gy
Kidney and RM over dose
Kidney over dose
Reduced tumor dose
Activity (GBq)
Total amount (nmol)

Figure 7

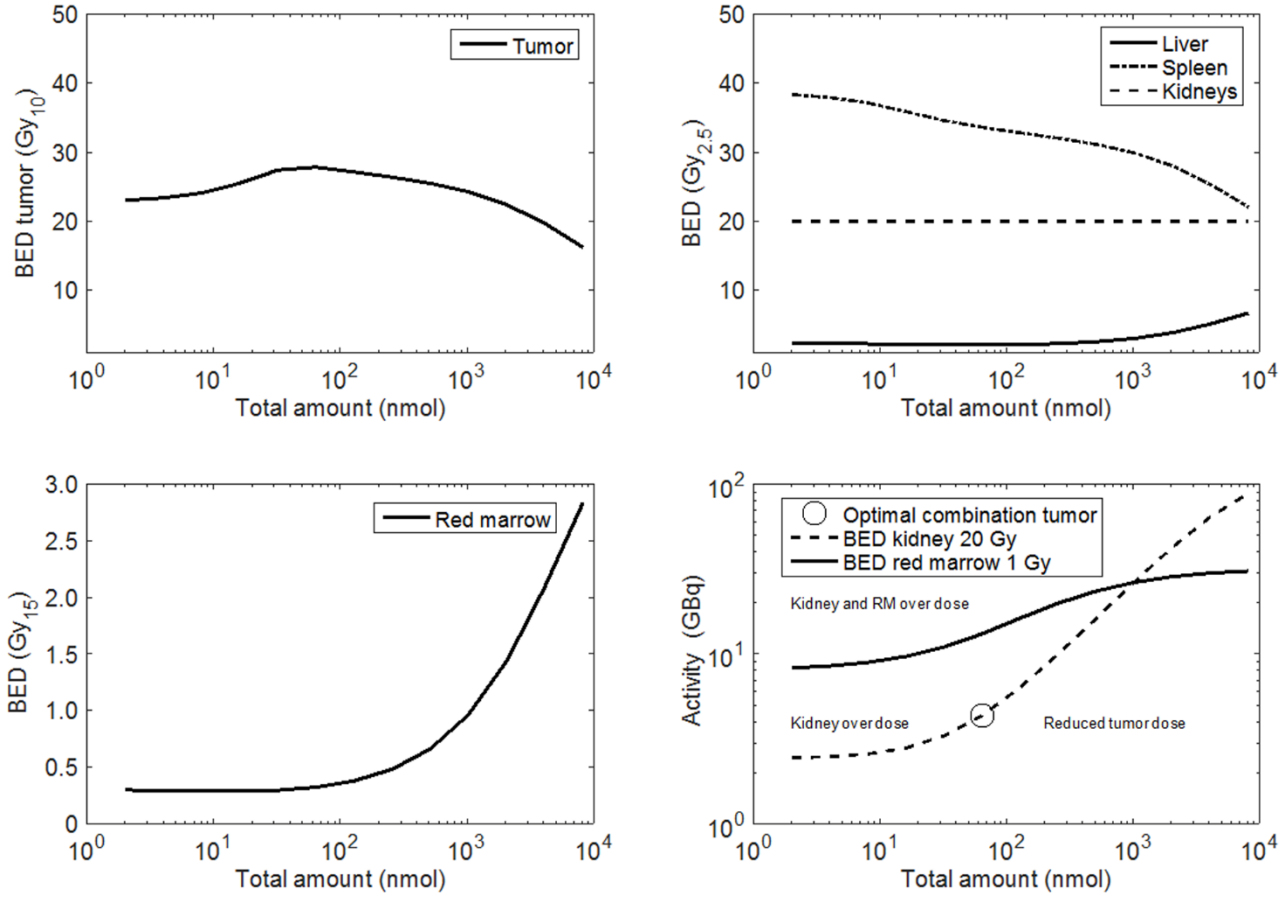
Tumor
BED tumor (Gy10)
Total amount (nmol)
Liver
Spleen
Kidneys
BED (Gy2.5)
Total amount (nmol)
Red marrow
BED (Gy15)
Total amount (nmol)
Optimal combination tumor
BED kidney 20 Gy
BED red marrow 1 Gy
Kidney and RM overdose
Kidney overdose
Reduced tumor dose
Activity (GBq)
Total amount (nmol)

Figure 8

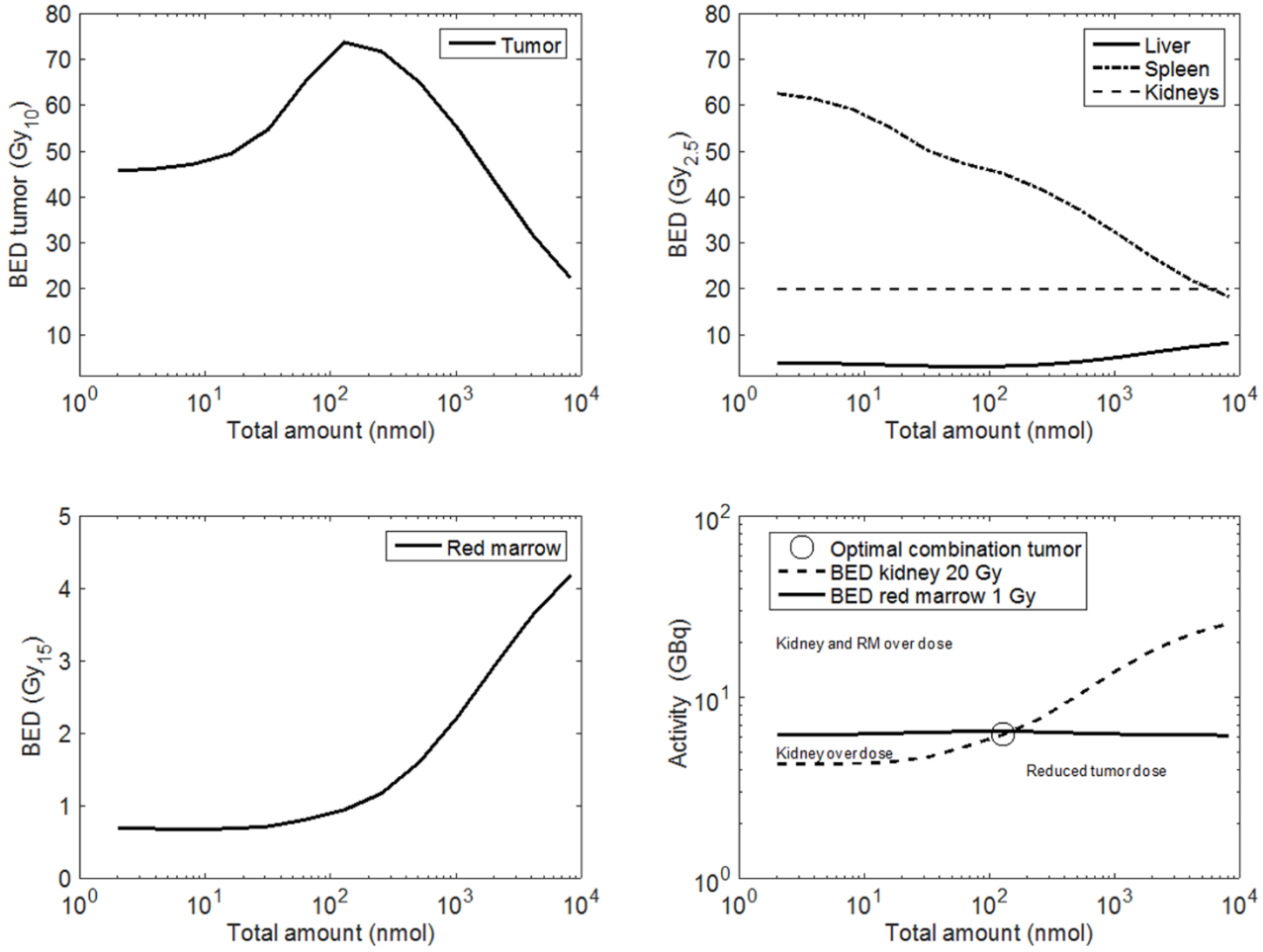
Tumor
BED tumor (Gy10)
Total amount (nmol)
Liver
Spleen
Kidneys
BED (Gy2.5)
Total amount (nmol)
Red marrow
BED (Gy15)
Total amount (nmol)
Optimal combination tumor
BED kidney 20 Gy
BED red marrow 1 Gy
Kidney and RM over dose
Kidney over dose
Reduced tumor dose
Activity (GBq)
Total amount (nmol)

Figure 9

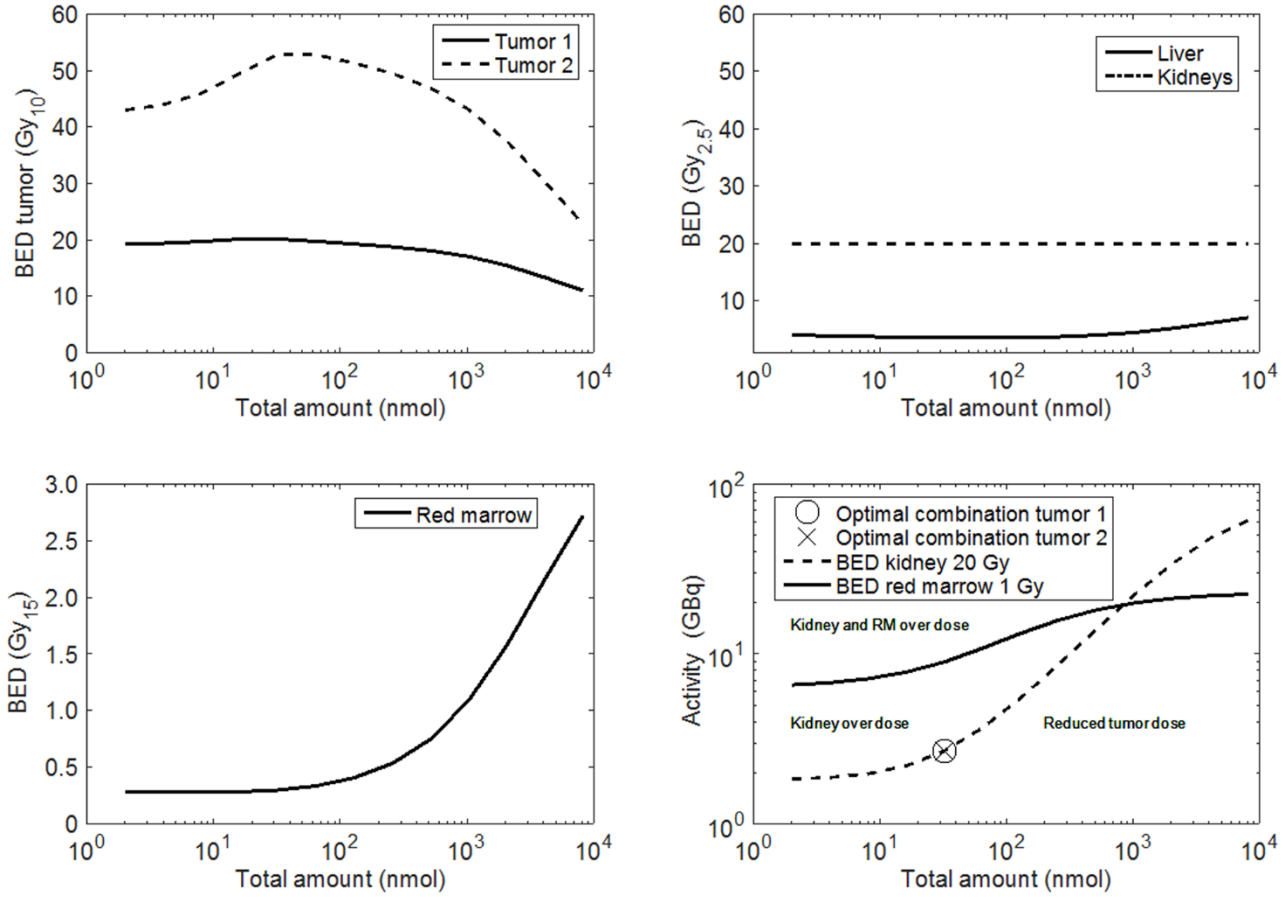
Tumor 1
Tumor 2
BED tumor (Gy10)
Total amount (nmol)
Liver
Kidneys
BED (Gy2.5)
Red marrow
BED (Gy15)
Optimal combination tumor 1
Optimal combination tumor 2
BED kidney 20 Gy
BED red marrow 1 Gy
Kidney and RM over dose
Kidney over dose
Reduced tumor dose
Activity (GBq)

Figure 10

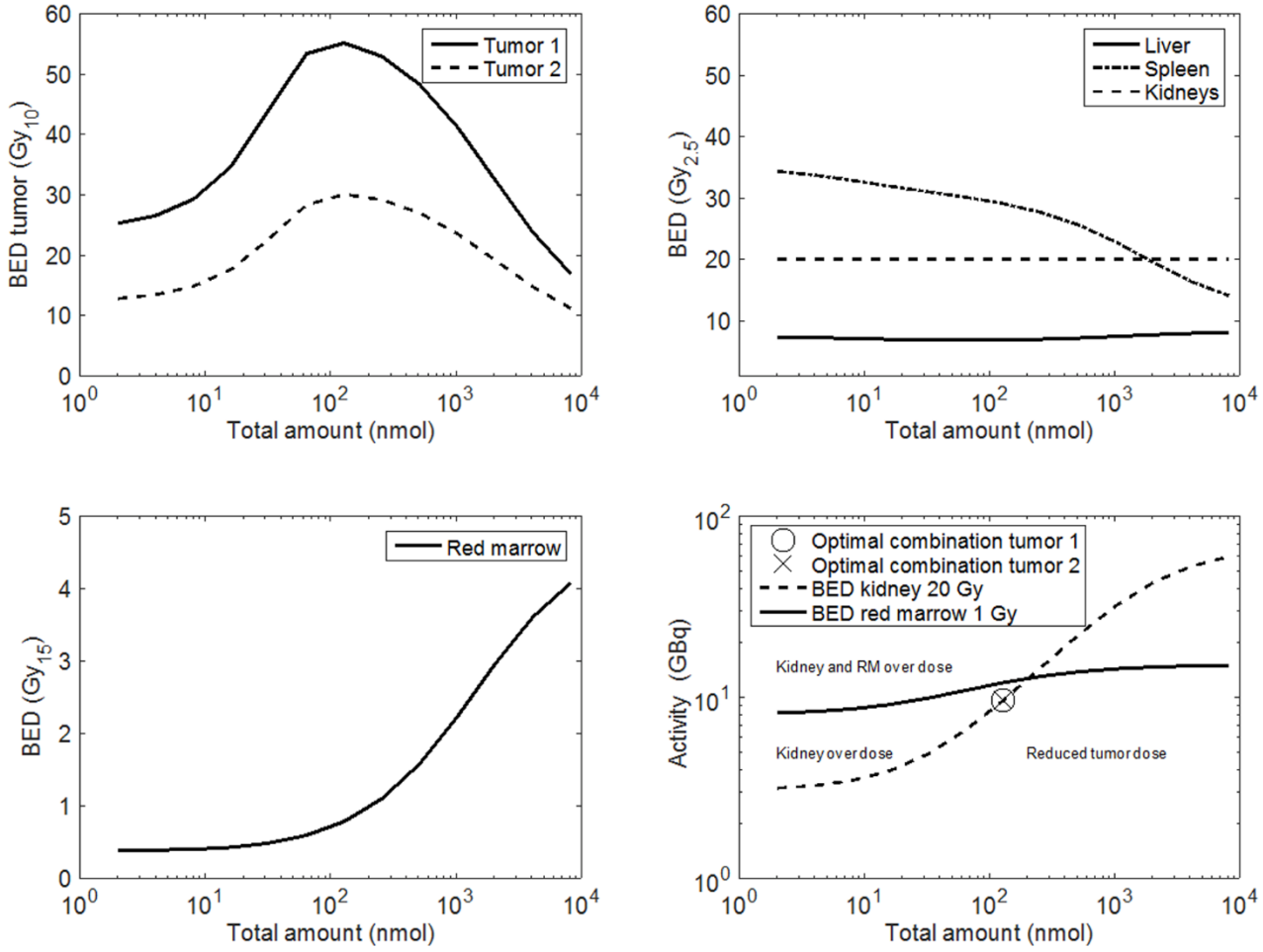
Tumor 1
Tumor 2
BED tumor (Gy10)
Total amount (nmol)
Liver
Spleen
Kidneys
BED (Gy2.5)
Total amount (nmol)
Red marrow
BED (Gy15)
Total amount (nmol)
Optimal combination tumor 1
Optimal combination tumor 2
BED kidney 20 Gy
BED red marrow 1 Gy
Kidney and RM over dose
Kidney over dose
Reduced tumor dose
Activity (GBq)
Total amount (nmol)

Figure 11

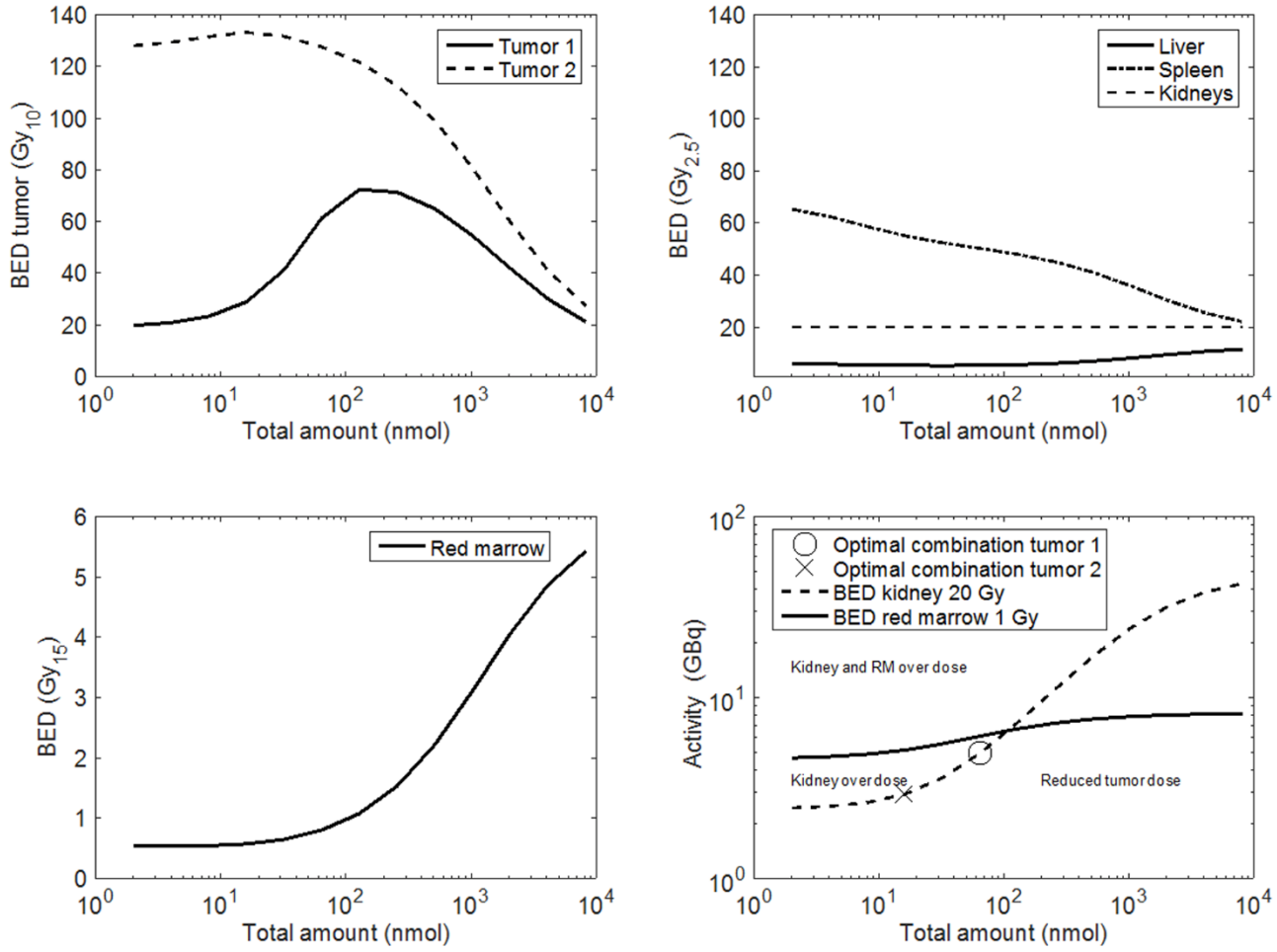
Tumor 1
Tumor 2
BED tumor (Gy10)
Total amount (nmol)
Liver
Spleen
Kidneys
BED (Gy2.5)
Total amount (nmol)
Red marrow
BED (Gy15)
Total amount (nmol)
Optimal combination tumor 1
Optimal combination tumor 2
BED kidney 20 Gy
BED red marrow 1 Gy
Kidney and RM over dose
Kidney over dose
Reduced tumor dose
Activity (GBq)
Total amount (nmol)

Figure 12

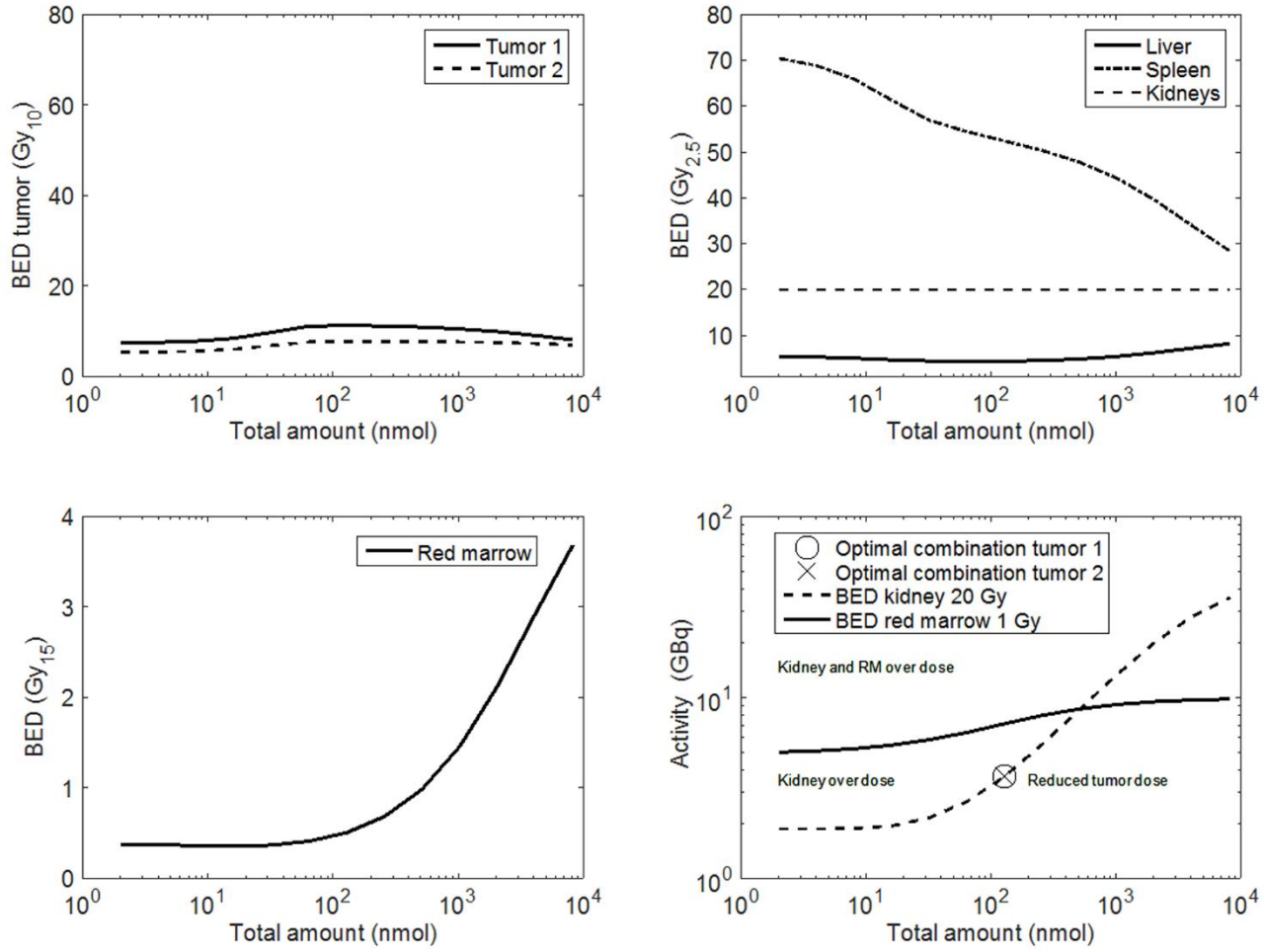
Tumor 1
Tumor 2
BED tumor (Gy10)
Total amount (nmol)
Liver
Spleen
Kidneys
BED (Gy2.5)
Total amount (nmol)
Red marrow
BED (Gy15)
Total amount (nmol)
Optimal combination tumor 1
Optimal combination tumor 2
BED kidney 20 Gy
BED red marrow 1 Gy
Kidney and RM over dose
Kidney over dose
Reduced tumor dose
Activity (GBq)
Total amount (nmol)

Supplemental Data

internalization rate sensitivity analysis

Figure 1

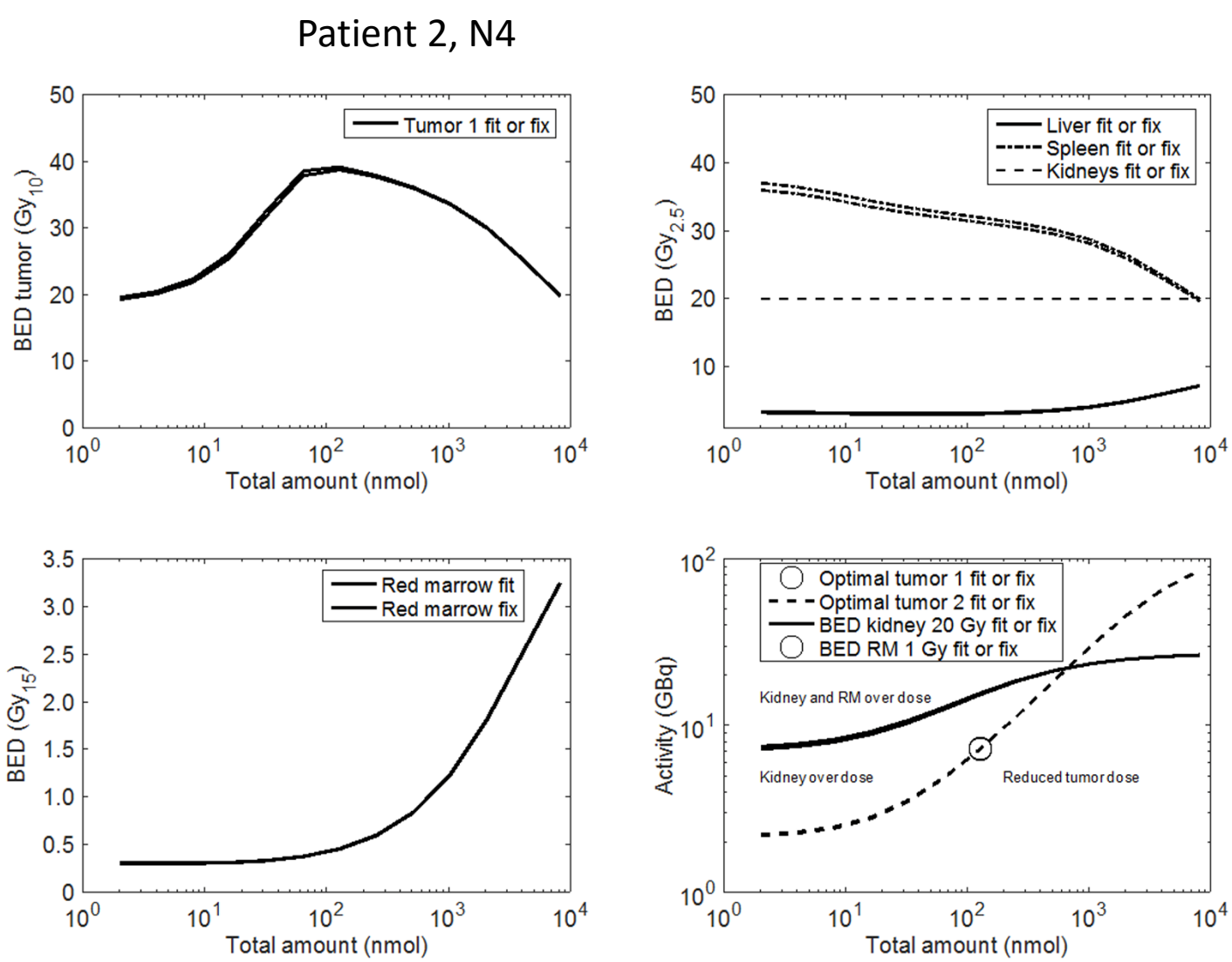

The internalisation rate was fixed due to high correlation. However, for the sensitivity analysis the internalisation rate was also fitted to the data. The fitted parameters of both cases were used for the simulations. The curves are very similar, as the assumed internalisation rate (0.0017 min^{-1}), is similar to the fitted (0.0023 min^{-1}) and small changes are compensated by changes in the receptor densities during the fitting process. If considerably larger or smaller internalisation rates are assumed and fixed, the model can not be adequately fitted (bad fits). Therefore, the assumption is reasonable and can be used for modelling and simulation.

Figure 2

Patient 7, N10

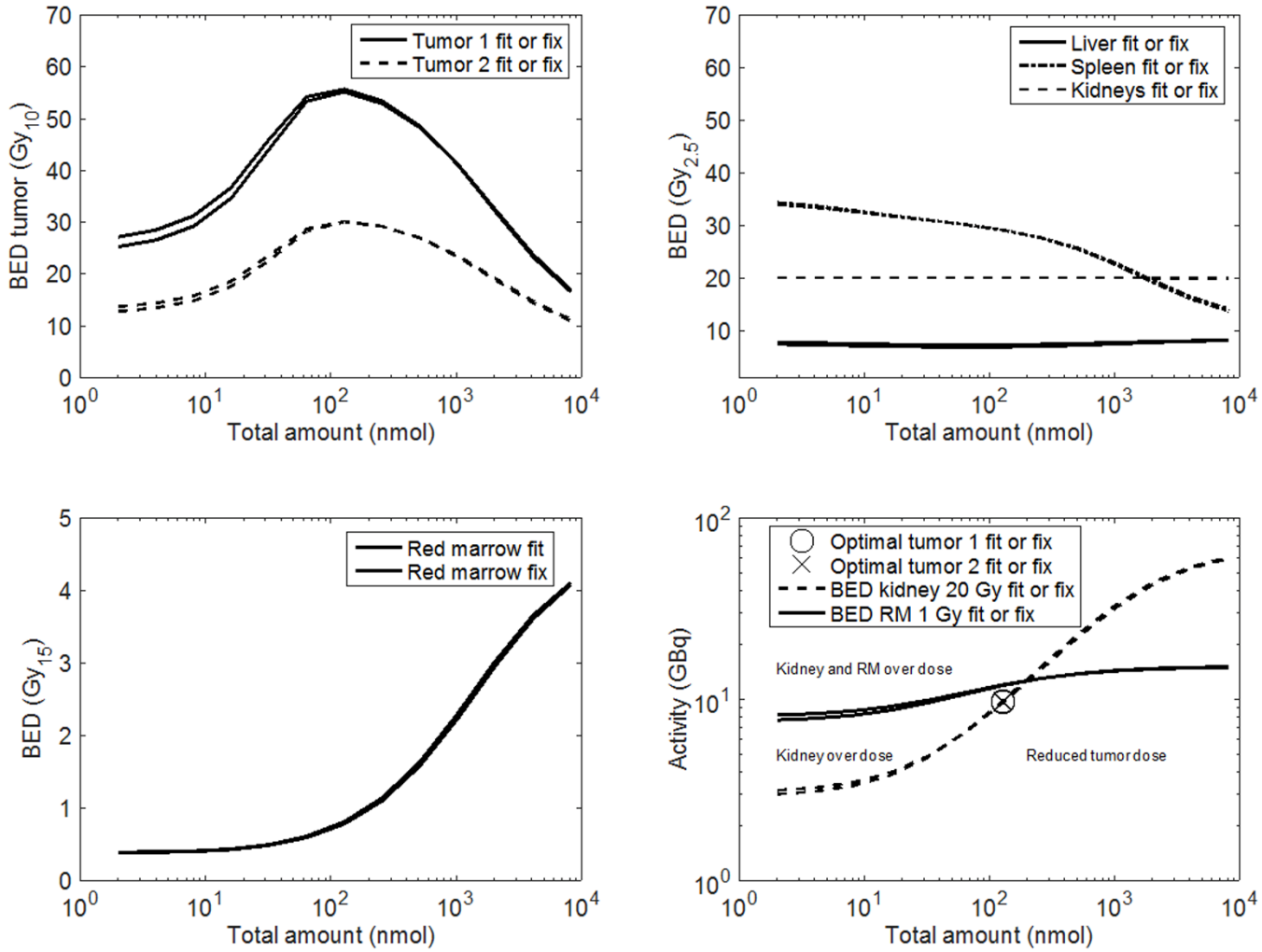

The internalisation rate was fixed due to high correlation. However, for the sensitivity analysis the internalisation rate was also fitted to the data. The fitted parameters of both cases were used for the simulations. The curves are very similar, as the assumed internalisation rate (0.0017 min^{-1}), is similar to the fitted (0.001 min^{-1}) and small changes are compensated by changes in the receptor densities during the fitting process. If considerably larger or smaller internalisation rates are assumed and fixed, the model can not be adequately fitted (bad fits). Therefore, the assumption is reasonable and can be used for modelling and simulation.